THESIS FOR THE DEGREE OF DOCTOR OF PHILOSOPHY

IN

PRODUCT AND PRODUCTION DEVELOPMENT

OPTIMIZATION OF COMPRESSIVE CRUSHING

ELISABETH LEE

DEPARTMENT OF PRODUCT AND PRODUCTION DEVELOPMENT
CHALMERS UNIVERSITY OF TECHNOLOGY

GÖTEBORG, SWEDEN

MAY 2012

Optimization of Compressive Crushing

Elisabeth Lee

ISBN 978-91-7385-714-7

Doktorsavhandlingar vid Chalmers tekniska högskola

Ny serie nr 3395

ISSN: 0346-718X

Published and distributed by
Chalmers University of Technology
Product and Production Development
SE-412 96 Göteborg

Printed in Sweden by
Chalmers Reproservice
Göteborg 2012

To my family

ABSTRACT

With almost all infrastructures being dependent on the supply of crushed rock materials, minerals, and ores, it is fair to say that the foundation of modern society is literally built upon these materials. As society continues to develop and standards of living progressively increase, the subsequent growing demand for crushed rock materials, minerals, and ores will result in a need for improving the performance and efficiency of rock crushing equipment.

The main hypothesis of this research is that better crushing machines can be achieved by first optimizing a given crushing process theoretically, and then designing the actual crusher. The conducted research can therefore be divided into five main stages, namely rock material characterization, modeling, optimization, evaluation, and implementation

In this thesis, the complex compressive breakage behaviors of four different rock materials (i.e. gneiss, diabase, marble, and quartzite) and two different iron ores were experimentally studied and mathematically modeled. A genetic algorithm was also applied to theoretically optimize the compressive crushing of these rock materials and ores. The obtained results indicated that optimal compressive crushing differs depending on the application and optimization objective. Different types of crushing applications, such aggregate and mining, should therefore not be operated in the same way. Similarly, crushing applications with different optimization objectives, e.g. the same type of application but different production situations, should not be run identically.

Analyses also showed that existing cone crushers and crushing applications are not operating optimally. In fact, defined theoretical performance efficiencies of 30-40 % were calculated for studied aggregate applications. These numbers indicate great improvement potential despite possible mechanical and practical restraints. More specifically, comparison between existing cone crushers and theoretical crushing concepts showed that the implementation of optimization results can be more or less difficult depending on the type of crusher.

For aggregate applications, the optimization results particularly suggested that rock materials are currently being over-crushed, and that the size reduction process should be separated from the process of particle shaping. In comparison, the results for mining applications indicated that a larger amount of size reduction should be performed by single particle crushing, if the overall size reduction of the process is to be maximized and the energy consumption is to be kept to a minimum. These optimization results for both aggregate and mining applications were implemented in prototypes, which were then tested in full scale experiments. The subsequent analysis of the results indicated that the performance of cone crushers can be improved in terms of product yield as well as reduction ratio.

In conclusion, considering the variety of applications as well as rock materials, minerals and ores, a truly optimal performance of a crushing application must be based on an optimized crusher design as well as a continuously optimized crusher operation.

Key words: compressive crushing, modeling, optimization, cone crusher, implementation

PUBLICATIONS

This thesis contains the following papers.

Paper A: Lee, E. and Evertsson, C. M., *Yield and Energy Optimizations of Compressive Crushing*, Proceedings of the XXIV International Mineral Processing Congress (partly peer reviewed), Volume 1, pp 316-324, ISBN: 978-7-03-022711-9, Beijing, China, 24-30 September 2008.

Paper B: Lee, E. and Evertsson, C. M., *Optimized Compressive Crushing with Respect to Energy Consumption, Pressure and Multiple Product Yield,* Proceedings of the European Symposium on Comminution and Classification 2009 (partly peer reviewed), Espoo, Finland, 15-18 September 2009.

Paper C: Lee, E., Svedensten, P., and Evertsson, C. M., *Validation and Simulation of Optimised Compressive Crushing,* Proceedings of XXV International Mineral Processing Congress (peer reviewed), pp. 943-956. ISBN: 978-1-921522-28-4, Brisbane, Australia, 6-10 September 2010.

Paper D: Lee, E. and Evertsson, C. M., *A Comparative Study between Cone Crushers and Theoretically Optimal Crushing Sequences*, Minerals Engineering (Journal), 2011, Volume 24, pp 188-194.

Paper E: Lee, E. and Evertsson, C. M., *Evaluating Cone Crusher Applications with Respect to Theoretically Optimal Crushing Sequences*, Submitted to Minerals Engineering (Journal), Under review, May 2012.

Paper F: Lee, E. and Evertsson, M., *Optimizing and Evaluating Theoretical Concepts of Compressive Crushing*, Submitted to the XXVI International Mineral Processing Congress, Under review, May 2012.

Paper G: Lee, E. and Evertsson, M., *Implementation of Optimized Compressive Crushing in Full Scale Experiments*, Proceedings of Comminution '12 (partly peer reviewed), Cape Town, South Africa, 17-20 April 2012. Also submitted for publication in Minerals Engineering (Journal), May 2012.

CONTRIBUTIONS TO CO-AUTHORED PAPERS

In all the papers A-G, Lee and Evertsson initiated the idea.

Papers A-B & F-G: Implementation was carried out by Lee. Lee wrote the papers with Evertsson as a reviewer.

Paper C: Implementation was conducted by Lee and Evertsson. Svedensten provided crushing plant expertise. Lee wrote the paper with Svedensten and Evertsson as reviewers.

Papers D-E: Implementation was performed by Lee and Evertsson. Lee wrote the papers with Evertsson as reviewer.

CONTENTS

Appendix

Paper A: Yield and Energy Optimizations of Compressive Crushing

Paper B: Compressive Crushing with Respect to Energy Consumption, Pressure and Multiple Product Yield

Paper C: Validation and Simulation of Optimised Compressive Crushing

Paper D: A Comparative Study between Cone Crushers and Theoretically Optimal Crushing Sequences

Paper E: Evaluating Cone Crusher Applications with Respect to Theoretically Optimal Crushing Sequences

Paper F: Optimizing and Evaluating Theoretical Concepts of Compressive Crushing

Paper G: Implementation of Optimized Compressive Crushing in Full Scale Experiments

ACKNOWLEDGEMENTS

There are so many people to whom I owe my gratitude for helping me coming this close to finally crossing the finish line of this PhD marathon. For in all fairness, although it technically only takes one person to write a thesis, figuratively it takes a village…

So, I would like to start by thanking my supervisor, Professor Magnus Evertsson, who gave me the opportunity of conducting this research and enrolling in this PhD marathon. Thank you, Magnus, for your constructive guidance, support and dedication!

Being further fortunate to work in a fun and stimulating research environment, I would like to acknowledge all my past and present colleagues at Chalmers Rock Processing Research (CRPR) and the department of Product and Production Development. A special thanks goes to Dr. Per Svedensten (Sandvik, formerly at CRPR) for believing in me and for helping me to implement my research into full scale prototypes, and Dr Erik Hulthén for all his good advice. I wish the best of luck to Johannes Quist and the PhD students Robert Johansson and Gauti Asbjörnsson.

I would also like to thank my sponsors Sandvik, the Swedish Mineral Processing Research Association (MinFo), the Ellen, Walter and Lennart Hesselman's Foundation for Scientific Research, and the Knutberg Foundation for their financial support of this project. Each member of the technical reference group formed by representatives of these organizations are gratefully acknowledged as well (here in alphabetical order, both past and present members); Richard Bern (Sandvik), Jan Bida (MinFo), Torbjörn Nilsson-Wulff (Sandvik), Niklas Skoog (Sand och Grus AB Jehander), Lars Sunnebo (formerly at Nordkalk), Per Svedensten (Sandvik), Kent Tano (LKAB), Marianne Thomaeus (formerly at MinFo), and Urban Åkesson (the Swedish Transportation Administration, formerly at SP Technical Research of Institute of Sweden). Jan Bida, Marianne Thomaeus, and Kurt Beckius are specially recognized for all their help regarding the funding of this project.

I am truly grateful to all of you who have in some way helped or contributed to this research. Please know that your support has been appreciated.

Now to all my friends and family, without your encouragement, love and support, this PhD marathon would have been much, much harder to partake in. You should know that only through your continuous cheering from the side line, have I been able to pull this off with a smile on my face. Thank you for everything and a special thanks to those of you, who have graciously helped me to proof read this thesis!

Finally, I would like to personally acknowledge my sister, Christina Lee Fältman. Thank you for always being there for me, supporting me and cheering me up with your wonderful personality! There are really no words for expressing the feeling, which I have, of knowing that I am always welcome to your loving home. I am truly fortunate to have you as a sister!

Elisabeth Lee

Göteborg, May 2012

NOTATION

AG	Autogenous Grinding	
CSS	Closed Side Setting	[mm]
EA	Evolutionary Algorithm	
GA	Genetic Algorithm	
HPGR	High Pressure Grinding Roll	
IP	Integer Programming	
IPB	Interparticle breakage	
MLS	Multi-start Local Search	
SA	Simulated Annealing	
SAG	Semi-Autogenous Grinding	
SPB	Single particle breakage	
VSI	Vertical Shaft Impactor	
TA	Tabu Search	
A	Cross sectional surface area perpendicular to a compressed volume of particles	[m^2]
B_{Inter}	Breakage function for interparticle breakage	[-]
B_{Single}	Breakage function for single particle breakage	[-]
C	Capacity of a crushing process	[-]
C_{Bond}	Material constant in Bond's law	[kWh·m$^{1/2}$/ton]
C_{Kick}	Material constant in Kick's law	[kWh/ton]
$C_{\text{Rittinger}}$	Material constant in Rittinger's law	[kWh·m/ton]
E_{Bond}	Energy input described in Bond's law	[kWh/ton]
$E_{\text{Rittinger}}$	Energy input described in Rittinger's law	[kWh/ton]
E_{Kick}	Energy input described in Kick's law	[kWh/ton]
F_{Single}	Force response in single particle breakage	[N]
N	Number of generations in optimization	[-]
P_{Inter}	Pressure response in interparticle breakage	[Pa]
S	Selection function for interparticle breakage	[-]
W_{Inter}	Energy of an interparticle compression	[J/mass unit]
W_j	Energy consumption of compression j	[J/mass unit]

W_{Single}	Energy of a single particle compression	[J/mass unit]
W_{Total}	Energy consumption for a crushing sequence	[J/mass unit]
W_{I}	Work index of a material used in Bond's law	[kWh·µm$^{1/2}$/ton]
a_i , $i=1:9$	Fitted selection function constants	[-]
b	Bed height	[mm]
c_i , $i=1:3$	Fitted force response constants	Constant dependent
d_i , $i=1:6$	Fitted pressure response constants	Constant dependent
f	Feed size distribution	[-]
f_{80}	Particle size which 80 % of the feed passes	[mm]
n	Number of individuals in optimization	[-]
$p_j^{'}$	Product from compression j	[-]
p_1	Relative amount of by-product	[-]
p_m	Circulating load of a crushing unit	[-]
p_{80}	Particle size which 80 % of the product passes	[mm]
s	Stroke	[mm]
$s_{\aleph}$	Dimensionless compression ratio	[-]
$s_{\aleph,\mathrm{max}}$	Maximum theoretical compression ratio	[-]
v_i	Value of product p_i	[-]
x	Particle size	[mm]
x_0	Initial particle size	[mm]
x_{min}	Reference particle size	[mm]
$x_{\aleph}$	Dimensionless relative particle size	[-]
α_i	Fitted breakage function constants $i=1:4$ for IPB and $i=1:5$ for SPB	[-]
φ	Fitness function of an optimization	Function dependent
$\eta_{\mathrm{real/theory}}$	Theoretical performance efficiency	[-]
ρ	Bulk density	[kg/m^3]
$\rho_{\aleph}$	Normalized density	[-]
ρ_{s}	Solid density	[kg/m^3]
$\sigma_{\aleph}$	Normalized standard deviation	[-]

1 INTRODUCTION

The aim of this chapter is to:

- *Introduce crushed rock materials as the important base product it is in modern society*
- *Briefly describe the physical properties of minerals and rock materials*
- *Provide an overview of rock crushing equipment, cone crushers in particular*
- *Present the challenges facing the rock processing industry*

The foundation of modern society is literally built upon crushed rock materials, minerals and ores. Infrastructure such as roads, railways, airports, bridges, water systems, and buildings all depend on the supply of these materials [1]. Without them, society as we know it would not be the same, let alone current standards of living. The supply of crushed rock materials, minerals and ores is thus crucial for the continuous development and upkeep of modern society. However, despite the importance of these materials, most people are actually not aware of them or their wide use. Instead, the access to metals and construction materials is more or less taken for granted and little attention is paid to their production, unless it directly impinges on one's everyday life. With a growing demand and an increasing concern for sustainability, the need for improving the performance and efficiency of rock crushing equipment is nevertheless becoming increasingly important.

1.1 MINERALS AND ROCK MATERIALS

Most rock materials are coherent, naturally occurring solid aggregates of minerals [2],[3]. As such, rock materials are inherently heterogeneous in chemical as well as physical composition, as opposed to minerals which by definition are homogeneous, generally inorganic, with definable chemical compositions [2],[3]. In comparison, ores are simply rock materials with significant economical worth; e.g. native metals such as copper, silver and gold, or rock materials with high concentrations of ore minerals (i.e. minerals containing large amounts of metal).

Most minerals, and consequently rock materials, are crystalline materials. This means that atoms are positioned in three-dimensional patterns commonly referred to as crystal lattices [4]. When a sample of mineral or rock material is externally loaded, stress arises internally within the sample on the inter-atomic bonds in the crystal lattice. Assuming that most minerals and rock materials are brittle [4],[5], this transformation of potential energy to elastic energy takes place up to the point, when a critical level of stress is reached somewhere in the sample. A crack will then start propagating and will, like any preexisting crack or flaw, act as a site for stress concentration. As the crack propagates, new surfaces will be created with surface energy transformed from the elastically stored energy [5],[6]. Unless hindered, the crack propagation will result in a macroscopic fracture of the sample at which the sample relaxes and the rest of the elastic energy dissipates.

1.2 ROCK CRUSHING EQUIPMENT

Minerals and rock materials are usually first drilled and blasted, and then crushed, sometimes several times, before a final product or a product ready for the next stage of the process emerges. The purpose of comminution is thus to reduce the particle size of rock materials (like in the aggregate industry), or to liberate valuable minerals from ores (as in the mining industry) [4]. Depending on the type of application, different comminution devices are applied. For instance, in the aggregate industry where the product size is in the millimeter range, gyratory, jaw, cone and Vertical Shaft Impact (VSI) crushers are often used (see Figure 1). This can be compared to the mining industry, where size reduction occurs down to the micrometer range. To achieve this, devices such as gyratory and cone crushers, High Pressure Grinding Rolls (HPGRs), Autogenous Grinding (AG) mills, Semi-Autogenous Grinding (SAG) mills, and ball mills are used. Rock crushers are in other words used in both the aggregate and mining industry.

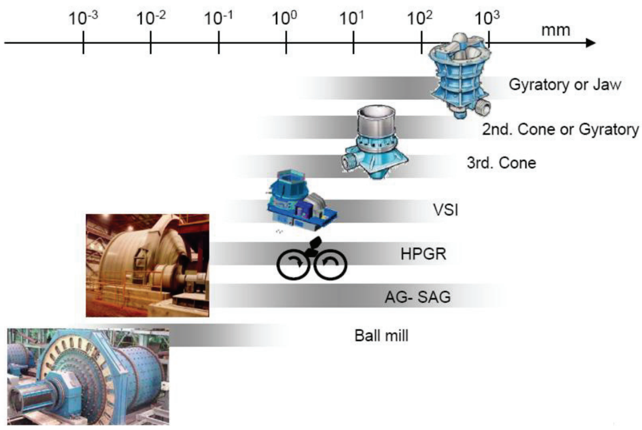

Figure 1. Illustration of the operating size range of common comminution device by M. Lindqvist.

Crushing can normally be divided into two different categories; energy conditioned or form conditioned [4]. As an impact crusher, VSI crushers (see Figure 2) apply impact or energy conditioned crushing. This type of crushing is enabled by the transfer of kinetic energy to particles, upon which the particles are released against a solid (metallic) wall or a bed of particles. This means that in energy conditioned crushing, the amount of size reduction is controlled by the energy transmitted to and absorbed by the particles.

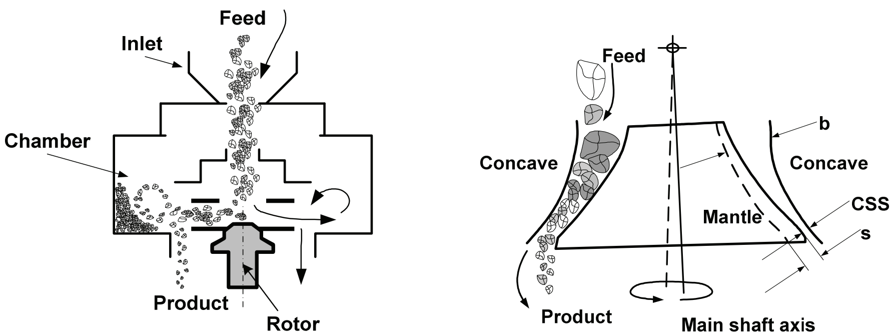

Figure 2. Schematic illustration of a VSI crusher to the left [7] and a cone crusher to the right [4].

In comparison, form conditioned crushing occurs when particles are compressed to a given degree or a given displacement between two or more surfaces. Consequently, form conditioned crushing is also called compressive crushing in which the size reduction can be controlled by controlling the degree of compression. This means that the energy input and the resulting force are secondary effects in compressive crushing as opposed to energy conditioned crushing. Cone crushers (see Figure 2), gyratory crushers (essentially similar to cone crushers) and jaw crushers (see Figure 3) are three types of crushers, which apply compressive crushing.

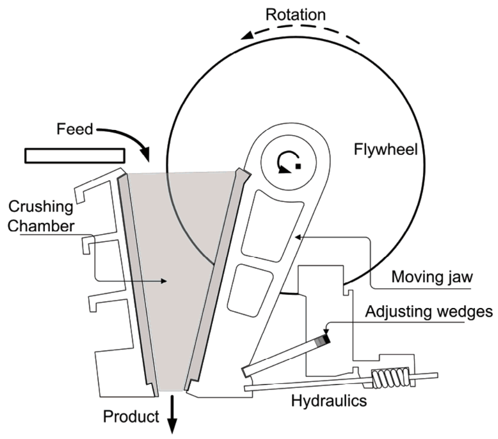

Figure 3. Schematic illustration of a jaw crusher by J. Quist.

All of the presented compression crushers operate cyclically; jaw crushers on half-cycles due to their flywheels and gyratory and cone crushers on full cycles due to an eccentric gyratory movement of the main shaft axis. Particles entering the crushing chambers of these compression crushers are repeatedly nipped and crushed as they pass through the cavity [4],[8],[9]. This can be compared to HPGRs and roll crushers (essentially similar to HPGRs but operated at lower pressures, higher roll speeds, and lower feed rates [10]) in which compression is applied only once [8].

In jaw, gyratory and cone crushers, the crushing process is highly affected by the geometry of the crushing chamber. As illustrated in Figure 4, the three commonly used cone crusher chamber geometries *fine*, *medium* and *coarse* result in different crushing. This is because of the different way and position in which larger particles are crushed [7]. In the *fine* crushing chamber, where particle beds cannot be formed due to chamber geometry, larger particles are crushed individually in the upper part of the chamber. In the *medium* and *coarse* crushing chambers, on the other hand, particles are crushed in particle beds down to a so called choke level after which the particles are believed to be crushed individually [4]. The choke level, which is defined as the smallest cross sectional area in a crushing chamber, is located in different positions depending on the chamber geometry. As shown in the figure, the cross sectional area of a crushing chamber varies throughout the chamber. Its gradual decrease down to the choke level allows particle beds to be formed as the volume of material arriving at a particular cross section is larger than that leaving. Similarly, its gradual increase after the choke level indicates that particle beds cannot easily be formed, since the volume of incoming material to a particular cross section is smaller than the area it is distributed over.

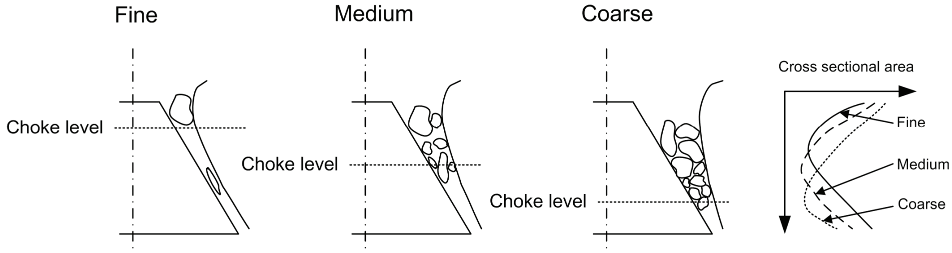

Figure 4. Depiction of three commonly used chamber geometries of cone crushers; fine (to the left), medium (in the middle), and coarse (to the right) [7].

Other variables affecting the crushing process in cone crushers include operating parameters such as the eccentric speed, the Closed Side Setting (CSS), and the stroke s (also known as the eccentric throw). As illustrated in Figure 2, the CSS is defined as the smallest distance between the mantle and the concave during crusher operation. This can be compared to the stroke, which can be regarded as a measure of normal mantle movement as the mantle shifts from its opened to closed position.

1.3 CHALLENGES OF THE ROCK PROCESSING INDUSTRY

In Sweden, natural gravel has traditionally been one of the main ingredients in making concrete. However, due to the uprising shortage of the material in many parts of the country over the last years, measures are being taken to limit the use of natural gravel to the protection of ground water. As a consequence, the use of crushed rock material as a replacement for natural gravel has increased. According to the Geological Survey of Sweden (SGU), the annual Swedish production of aggregates was roughly 101 million tons in 2008, before dropping to 84 million tons in 2009 following the global economic crisis [11]. In comparison, the European aggregate production was 3.25 billion tons in 2009 (corresponding to 5.5 tons per capita) [12]. It was predicted to have declined to around 3 billion tons in 2010, but is expected to return to growth in 2012 as hopefully the economy recovers. As the latter comes about, an increase will undoubtedly follow as a result of expansions of infrastructures, new construction projects, and improved standards of living.

In terms of minerals and ores, roughly 8.8 million tons of industrial mineral and 61.5 million tons of ore (an all time high at that time) were mined in Sweden in 2010 [13]. This recovery in the mining industry seems to be globally widespread as both metal prices and investment costs increased during that same year. In fact, during 2010, the global production of iron ore increased to 1.8 billion tons, which corresponded to a growth of 15.4 % in comparison to 2009 [13]. According to Raw Materials Group, the production forecast for 2011 was 1.9 billion tons.

Considering the rapid growth of the world population as well as the globally increasing urbanization, the demand for aggregate and ores seems to be non-ceasing and steadily growing as the economy recovers. Apart from the challenge of living up to this rising product demand, the rock processing industry, like many other industries, is confronted with additional demands of energy savings as well as considerations of sustainability and environment. Thus, in order to successfully face the challenges ahead, efforts must be focused towards improving the performance and efficiency of existing crushers and crushing processes. This entails striving towards improving process and production efficiency, as well as lowering energy consumption.

Compression crushers have been used for size reduction of rock materials ever since their arrival on the market over a hundred years ago. Changes and adjustments have since then been made to the machines alongside their development over time. This value development within a product by incremental improvements over time was described by Lindstedt and Burenius [14]. According to them, this value development follows the shape of an S-curve and can be divided into four different stages, i.e. infancy, growth, maturity, and retirement. By their definition, the cone crusher could be argued to be in the maturity phase of the S-curve. This means that the value development of cone crushers has reached stagnation, and that new strategies must be taken in order to enable leaps to a new S-curve. However, in order to do so and to successfully improve existing crushers, the knowledge gap of extended basic knowledge about the crushing process must be filled. This knowledge gap is thus the starting point of this thesis.

2 OBJECTIVES

The aim of this chapter is to:

- *Describe the aim and objective of this research*
- *State research questions*
- *Clarify the delimitations of the research undertaken*

2.1 RESEARCH OUTLINE

The purpose of this research is to understand how different rock materials should be crushed compressively and to develop knowledge to optimize existing compression crushers such as cone crushers. Consequently, the main hypothesis of this research is simply that better crushing machines can be achieved by first optimizing a given crushing process theoretically, and then designing the actual crusher. Such a process is visualized in Figure 5. It is, in other words, believed that the outcome of a crushing unit can be affected by changing different parameters (e.g. design and operational parameters such as chamber geometry and eccentric speed in a cone crusher). It is also believed that different rock materials should be crushed differently depending on material characteristics, conditions of the crushing application as well as requirements of the end product. These hypotheses form the basis of this research in which the objective is to:

- Develop the existing knowledge and approaches on fragmentation of rock materials using compressive crushing
- Examine how compressive crushing should be performed in different crushing applications
- Evaluate the performance of existing cone crushers
- Give advice for crusher selection and design

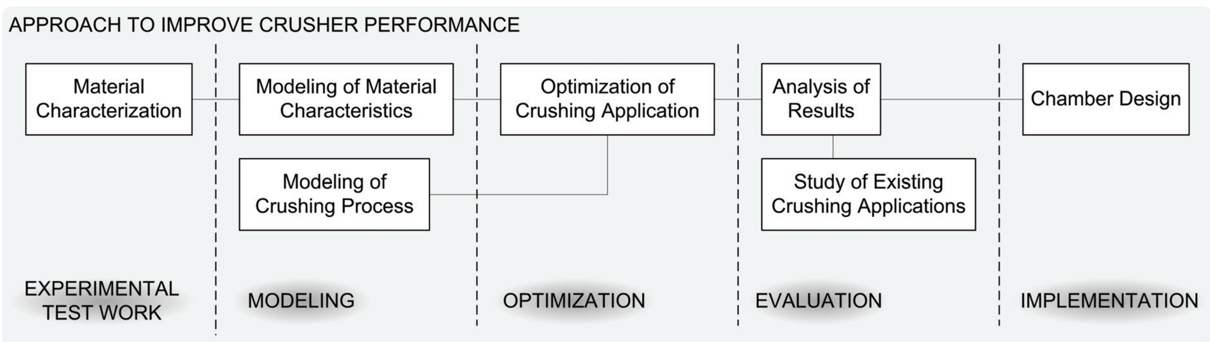

Figure 5. Suggested process to improve crusher performance.

2.2 RESEARCH QUESTIONS

The scope of this research can be described by the following research questions:

RQ1: How can the compressive breakage behavior of a given rock material be modeled?

RQ2: How can the compressive crushing of a given rock material be optimized?

RQ3: How should the outcome from optimizations of compressive crushing be evaluated?

RQ4: How should a given rock material be crushed by means of compressive crushing if e.g. product yield or energy consumption is to be theoretically optimized?

RQ5: What are the main differences between current cone crushers and comparable theoretically optimal crushing units?

RQ6: How much can the performance of today's cone crushers be improved by practically implementing research results from this project?

These research questions will be addressed throughout this thesis and will be answered in the final chapter of Conclusions. Figure 6 shows the disposition of this thesis in relation to the stated research questions. The figure also illustrates how the appended papers relate to the different chapters as well as to the research questions posed.

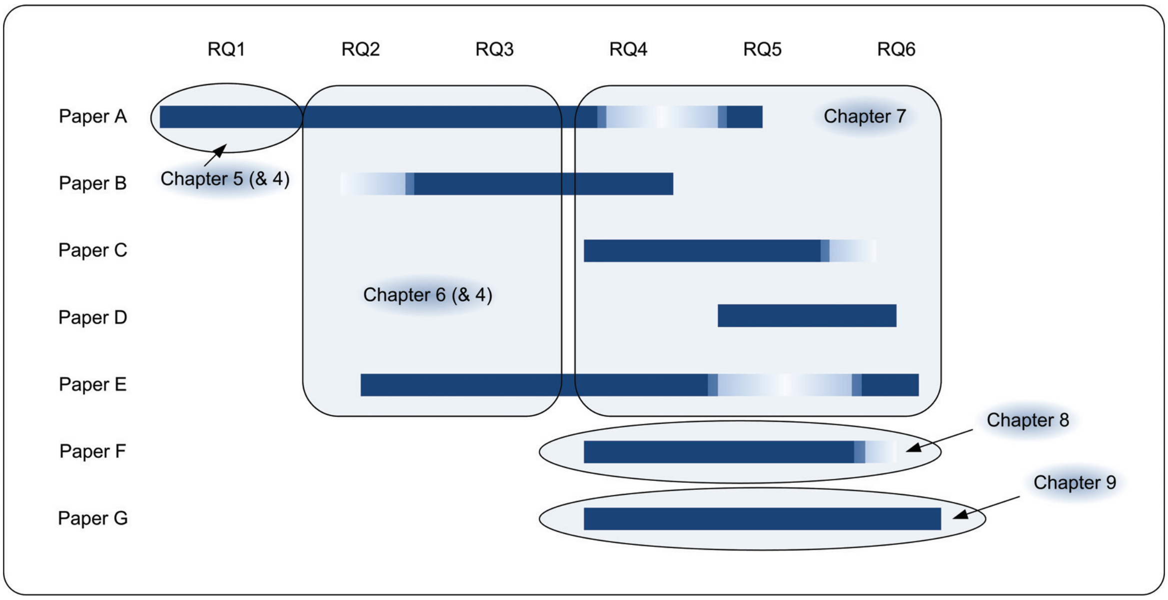

Figure 6. The disposition of the thesis relative to the stated research questions as well as the appended papers.

2.3 DELIMITATIONS

The presented research is performed from a macroscopic perspective as viewed from a mechanical machine such as a rock crusher. No in-depth aspects of mineralogy, petrology or any other microscopic rock texture or crack propagation are thus considered. Laboratory experiments and full-scale tests are consequently analyzed and evaluated through the size distributions of both the feed and the product, along with mechanical and physical parameters, such as compression ratio, pressure or energy. Moreover, focusing on compressive crushing, the scope of this research does not include the analysis of impact crushing or any other form of comminution.

3 RESEARCH APPROACH

The aim of this chapter is to:
- *Describe the applied mindset regarding research and knowledge*
- *Present the applied research model*
- *Introduce the methodology used in this research*

The research in this thesis was carried out at Chalmers Rock Processing Research (CRPR), which is part of the Machine Elements Group at the Department of Product and Production Development at Chalmers University of Technology. In particular, CRPR has been active within the research area of equipment [4],[7],[15],[16] and processes [17],[18] for the production of crushed rock material since 1993.

3.1 GENERAL MINDSET

According to Evertsson [4] and Allwood and Eriksson [19], research is defined as the activities, which are undertaken in order to create new knowledge or to reduce an existing knowledge gap. Knowledge is, in turn, often defined as "*justified true belief*"[1], meaning that knowledge is something that is believed to be true and that can be argued to be true with reasonable arguments [19]. What is considered to be true depends, however, on the definition of truth. In *epistemology* (i.e. the study of knowledge), three main definitions are commonly viewed upon; the correspondence theory of truth, the coherence theory of truth, and the pragmatic theory of truth. While the correspondence theory of truth regards something as true if it exists in reality, the coherence theory of truth equates truth to consistency with other known truths [19]. This can be compared to the pragmatic theory of truth in which something is viewed as true if it leads to usefulness, and if it works in practice, etc. The latter perspective is thus in close proximity to what is considered as central in engineering reasoning and problem solving, as well as in industrial collaborations. It is therefore the main conception of truth in this research, although the coherence theory of truth has been practiced as well.

In terms of view of knowledge, an empirical outlook has been applied in this research. Specifically, empiricism asserts that knowledge comes from experiences and what is observable, whereas rationalism (an alternative view) argues that knowledge comes from the interpretations made by the observer [19]. Empiricism is also closely linked to positivism (or logical empiricism), which is a philosophy of science characterized by an empirical outlook and an aim to generalize and to understand cause and effect relationships [19]. The performed research can thus be categorized as positivistic, which further implies a realistic ontological[2] approach, meaning that the existence of an outer world is assumed and that knowledge about it can be obtained [21].

[1] Plato (424/423 BC -348/347 BC [20])
[2] From ontology, which is the study of the nature of reality

3.2 RESEARCH MODELS

In order to understand and to evaluate research in a specific field today, it is crucial not only to clarify the general mindset of the performed research, but also the research model to which the research in question is attributed. Only by relating the research to its right framework, can the motive for different choices and approaches be understood and assessed. Putting research into an inappropriate context, on the other hand, risks causing misunderstanding as well as devaluation of research results. This section is consequently dedicated to describing the main differences between two principal research models.

Research, which has traditionally been a predominantly academic activity, has with time become more multifaceted and found a wider market for development as alternative research sites, such as company or corporate R&D departments; consulting companies; R&D centers; special interest organizations; and research institutes etc, have emerged (Svensson et al. [22], Jacob et al. [23]). As a consequence, new models of research have also come forward. For instance, in the work of Svensson et al. [22] two alternative research models are described; *discipline oriented research* and *multidisciplinary research*. A brief description of these models is given in Table 1. As can be seen, traditional academic research with its distanced approach; aim and objective of theoretical knowledge; and close relation to a specific academic discipline falls under the category of discipline oriented research. Multidisciplinary research, on the other hand, is typically interactive with a focus on generating applicable and useful knowledge for those involved (i.e. researchers as well as practitioners). Moreover, the knowledge, usually generated by a problem-oriented approach, is contextual rather than general and is often validated by the application of research results in real life situations.

Research undertaken according to the two different models clearly differentiates from one another in both views and objectives. For example, when traditional academic research (i.e. discipline oriented research) is reviewed by practitioners, it is often considered as inaccessible and far too general to be of any "real" use. Conversely, many traditional researchers regard multidisciplinary research as being too contextual and not general enough in order to draw any "valid" conclusions or formulate any "valid" theories. However, despite the different approaches and views applied, both research models share a common overall purpose of creating new knowledge or reducing an existing knowledge gap. It is therefore important to stress that both discipline oriented research and multidisciplinary research are needed as they complement one another.

Table 1. Two research and knowledge enhancement models as described by Svensson et al. [22], here translated as by Almefelt [24] but simplified to provide an overview.

	Model 1 – Discipline oriented	**Model 2 – Multidisciplinary**
Orientation	The academic field	Problem-oriented
Aim	Theoretical understanding	Applicability
Form	Institutionalized	Flexible
Time perspective	Long-term	Short-term
Approach	Distanced	Interactive
Players	Researchers	Researchers – practitioners
Kind of knowledge	General	Specific, contextual
Focus	Theory	Development, usage

3.3 APPLIED RESEARCH MODEL AND METHODOLOGY

The research described in this thesis was conducted in collaboration with a crushing equipment manufacturer as well as aggregate producers. It was undertaken using a problem-oriented research methodology[3] (described below), which has a long history of implementation within the area of Machine Elements with its focus on machine components and machines. More specifically, it was first adopted in 1950 by Jakobsson (Swedish full Professor with a PhD in Machine Elements), who introduced a new systematic and analytical approach to the subject [25]. Naturally, adopting this over-half-a-century-long tradition of interactive research, as well as the overall aim of the research group to generate contextual and useful knowledge, implies that the conducted research can be categorized as multidisciplinary.

As described by Evertsson [4], in problem-oriented research the choice of method for solving the problem or question of interest is based on the nature of the problem itself. In other words, the problem itself is in focus rather than the method or tool for solving it. The starting point of the adopted research process, depicted in Figure 7, is thus always a question or a problem, often arising from a need to improve or increase the performance of a process, machine or component. The first step, according to the methodology, is then to identify the nature of the problem through observations such as literature reviews, data acquisition, guiding experiments etc. Once identified, the nature of the problem determines the choice of method – a selection made based on the performed observations as to which method would be best equipped to solve the problem at hand. This is often an iterative process, which will repeat itself until a method determined to be acceptable is found. The obtained model is then verified through both simulations and experiments validating results generated using the model.

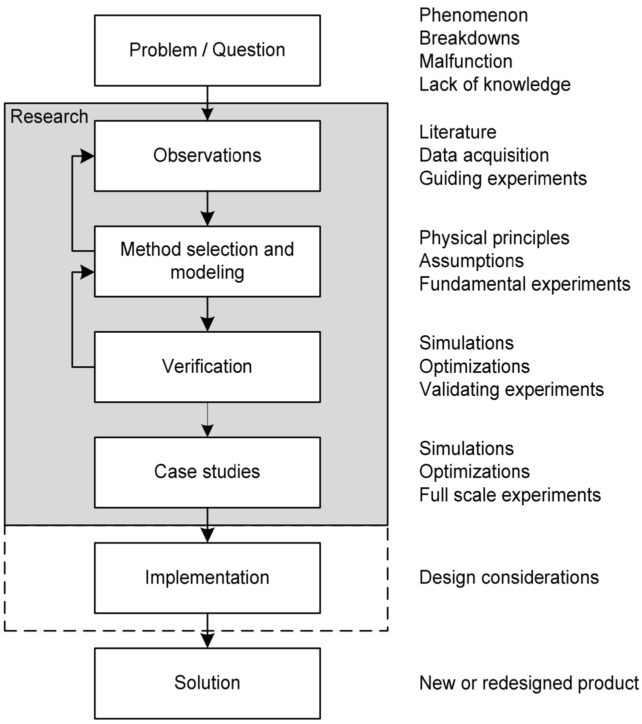

Figure 7. The applied problem-oriented research process (cf. Evertsson [4] and Svedensten [17], as well as Popper's view on the evolution of science as described by Allwood and Eriksson [19]).

[3] "A *methodology* can be defined, in a general sense, as a situation-adapted system of methods solving a complex problem (Metaphor: A cookery-book). By the corresponding definition, a *method* supports the management of a certain class of problems." (Almefelt [17])

After verifying the model and validating obtained results, case studies are conducted, preferably in cooperation with the industry. Simulations, optimizations as well as full scale experiments can be performed in order to draw conclusions regarding important effects and possible improvement potentials. This newly gained knowledge can then be formulated in so-called design considerations, which can in turn be implemented through improvements of the original product or through a complete redesign of the product [4].

The benefit of a problem-oriented approach is that the outcome from the research is often directly implementable and can be applied directly to solve the original problem. The result is thus a tailor-made solution more or less ready for use, as opposed to findings generated by a non problem-oriented research approach which are often more general and have to be adapted before being applicable to a specific problem [22].

To summarize, the research performed in this project can be categorized as multidisciplinary, as well as positivistic, and has been carried out using a problem-oriented research methodology. In practice, this research has been conducted in collaboration with the industry with the objective to produce knowledge and results, which can be practically implemented for use in the foreseeable future. Moreover, with the applied pragmatic approach to truth, the accuracy of applied models has been considered in relation to their levels of complexity. A model, which works and which shows good agreement with empirical data considering its level of complexity, can in other words be accepted, even though better agreement can possibly be achieved by increasing its complexity. The same reasoning has also been applied to optimizations in which e.g. the gain of an improved convergence through an increased number of iterations is weighted against the conveyed increase of computational time.

In terms of generalization of results, one can argue that by studying the compressive crushing of several rock materials for different crushing applications, the obtained results can be generalized for each studied crushing application. Similarly, the results obtained for a given rock material in different crushing applications may also be possible to generalize with respect to the rock material.

4 LITERATURE REVIEW

The aim of this chapter is to:

- *Explain the traditional focus of comminution research on grinding processes*
- *Introduce the classical comminution theories*
- *Describe some of the most common test methods in rock breakage characterization*
- *Present a selection of different optimization methods*

Despite having been introduced to the market over a hundred years ago, research regarding compression crushers and their applied mode of crushing, i.e. compressive crushing, hav been relatively limited. Instead, the main focus has been on grinding equipment operating further down in the size reduction process of minerals and ores. The explanation to this lies partly in the fact that mining companies are usually larger with more resources available for research and development than companies within the aggregate industry. Also, since aggregates have traditionally been considered as an inexpensive product, research within the aggregate industry has not been prioritized in the same way as in the mining industry. The larger focus on grinding processes than on crushing processes is further explained by the perception that the lion's share of comminution work is performed by grinding.

4.1 COMMINUTION THEORY

The aim of classical comminution theory is to describe the relationship between the energy consumed and the amount of size reduction brought about by the energy consumption. There are three classical comminution theories in all of which rock materials are assumed to be brittle. The first of these theories was proposed in 1867 by Rittinger, who suggested that the surface area produced by comminution is directly proportional to the energy consumed [26],[27]:

$$E_{\text{Rittinger}} = C_{\text{Rittinger}}\left(\frac{1}{p_{80}} - \frac{1}{f_{80}}\right) \tag{1}$$

where $E_{\text{Rittinger}}$ is the energy input, $C_{\text{Rittinger}}$ is a material constant, p_{80} is the size which 80 % of the product passes, and f_{80} is the size which 80 % of the feed passes. However, since an infinite number of different size distributions pass the single points of p_{80} and f_{80}, neither of the parameters can satisfactorily characterize a size distribution [27].

The second classical comminution theory was introduced by Kick in 1883. He stated that the energy required for breakage is proportional to the reduction in volume of the broken particles [5], [27]. This can be formulated as in Eq.(2)

$$E_{\text{Kick}} = C_{\text{Kick}} \ln\left(\frac{f_{80}}{p_{80}}\right) \tag{2}$$

where E_{Kick} is the energy input and C_{Kick} is a material constant. Unfortunately, similar to Rittinger's law, Kick's law lacks precision in describing the shape of a size distribution curve as only a single point is used [27].

The third and final classical relationship was proposed by Bond in 1952. According to his theory, the energy input is proportional to the length of the produced crack tip and is equal to the difference in energy represented by the product and the feed [4],[5]. This can be written as in Eq.(3), since the crack length l in a unit cube L^3 is considered to be proportional to one side of the surface area of that unit cube (i.e. $l \sim L$). As the surface area of the unit cube for particles of similar shape is inversely proportional to the particle diameter (i.e. $6L^2 \sim 1/d$), the crack length is inversely proportional to the square root of the particle diameter (i.e. $l \sim 1/\sqrt{d}$).

$$E_{\text{Bond}} = C_{\text{Bond}}\left(\frac{1}{\sqrt{p_{80}}} - \frac{1}{\sqrt{f_{80}}}\right) = W_{\text{I}}\left(\frac{10}{\sqrt{p_{80}}} - \frac{10}{\sqrt{f_{80}}}\right), \qquad \text{where } p_{80} \text{ and } f_{80} \text{ are in microns.} \tag{3}$$

Bond called the material constant in the formula the *work index* W_{I}. The work index was defined as the amount of energy required to reduce a short ton of material from infinite feed size to 80 % passing 100 microns [27]. It expresses the resistance of a material to crushing or grinding, and is often used by machine manufacturers to estimate the amount of energy required for a given crushing or grinding task. However, due to the varying ability between different machines in utilizing energy for breakage, the work index will be dependent on the efficiency of a given machine [27].

The presented classical laws of comminution were surrounded by much controversy during a long period of time, as published results would many times satisfy only one of the relationships [26]. Finally, in 1975 Hukki suggested that all three relationships were in fact applicable but in different and relatively narrow size ranges [5],[28]. Based on Hukki's work, Morrell [28] later successfully proposed a modification of Bond's equation. Unfortunately, as pointed out by Lindqvist [29], Morrell's modified energy model still lacks precision due to the sole use of f_{80} and p_{80}. An alternative approach to calculate the energy cost to produce a given product size distribution from a given feed size distribution was therefore suggested by Lindqvist [29]. Although it is conceivable that the relationship could be used to predict the resulting particle size distribution of a crushed feed sample, the fact that the main focus of this research concerns form conditioned and not energy conditioned crushing, still remains. The same reasoning is thus applied with respect to the models put forward by e.g. Schönert and coworkers [30],[31],[32] , and Vogel and Peukert [33],[34]. These models can be compared to the form conditioned crushing model proposed by Evertsson [4] to describe the compressive breakage behavior of different rock materials.

4.2 TESTS METHODS AND EXPERIMENTAL WORK

Test methods to characterize the breakage behavior of different rock materials can generally be divided into fundamental *rock mechanics tests* and *rock aggregate tests* (often referred to as comminution tests). The focus of rock mechanics tests lies mainly in determining the mechanical properties of a given rock material, whereas the aim of rock aggregate tests is to determine the comminution behavior of the material.

ROCK MECHANICS TESTS

The *Uniaxial Compressive test*, the *Hopkinson Pressure Bar test*, and the *Bond Work Index* test are three examples of commonly used fundamental rock mechanics tests. In the Uniaxial Compressive test, drill core samples with well-defined dimensions are loaded axially in compression until they fail [35]. This allows the strength of the rock to be determined as well as Young's modulus and Poisson's ratio. In comparison, the Hopkinson Pressure Bar test is used to measure the force and energy required to initiate catastrophic failure in rock specimens [36]. The test consists of attaching a rock sample to one end of a suspended steel bar (Hopkinson Bar) and releasing a colliding seconding steel bar (impact bar) from known levels of energy until catastrophic failure occurs.

As previously mentioned, the Bond Work Index is a measure of the resistance of a rock material to crushing or grinding. In terms of crushing, the parameter is related to the average energy required to break 10-15 individual rock particles of approximately 75 mm by 50 mm in size using a twin pendulum device [9]. Specifically, the rock sample is mounted between two hammer shaped pendulums, which are then used to strike the particle simultaneously as well as repeatedly (but with an incrementally increased energy) until rock breakage occurs.

ROCK AGGREGATE TESTS

Due to the traditional focus on grinding processes, most rock aggregate tests concern comminution by energy conditioned crushing. Two well-known examples of such tests are the *Twin Pendulum Test*, and the *Drop Weight Test* (DWT). In the Twin Pendulum Test, single particles are crushed between an input pendulum, which is released from a known height, and a rebound pendulum to which the particle is attached [37]. This can be compared to the Drop Weight Test, which has come to replace the Twin Pendulum Test and where single particles are instead placed on a hard surface and struck by a falling steel weight [36]. By varying the mass of the falling weight and the height from which it is released, the amount of applied energy can be varied. In characterization tests for particle breakage concerning crushers, three different particle sizes representative of the size range of interest are tested; with each test containing 20-50 particles of the tested particle size [38]. The t_{10} parameter of the material is then the percentage of particles passing $1/10^{th}$ of the initial feed size. The t_{10} is often used within the mining industry to quantify the breakage behavior of an ore.

Apart from being energy conditioned, the described comminution tests so far are all conducted for single particles. As compression crushers apply form conditioned and not energy conditioned crushing, it would seem that form conditioned compression tests would be more appropriate. Also, as indicated by Figure 4, particles in cone crushers can be crushed both individually and in particle beds. Thus, in order to describe the crushing process in compression crushers, the breakage behavior of different rock materials when compressed in particle beds must also be characterized. A form conditioned comminution test was therefore developed by Evertsson [4]. The main principle of this test was to compress rock particles contained in a cylindrical steel vessel using piston and die equipment. Contrary to the energy conditioned Dutch Static Compression test [39], the samples are compressed to different compression ratios (i.e. the ratio between the stroke s and the initial bed height b) according to a defined test plan [4]. This form conditioned rock aggregate test was later adapted by Bengtsson et al. [40] to study the compressive breakage behavior of single particles.

In terms of experimental work, extensive studies using piston and die equipment have been carried out by several authors such as Schönert et al. [30],[31],[41],[42], Fuerstenau et al. [43],[44], Benzer et al. [45], Unland and Szcelina [46], Tondo [47], and Daniel [10]. Unfortunately, most of this work has been performed with an energy conditioned perspective.

4.3 OPTIMIZATION METHODS

In its broadest context, optimization refers to choosing the best element from a set of alternatives. However, in mathematics, optimization is referred to as the technique to seek local and global maxima of a function in its defined variable and parameter space. This can be performed using a variety of different methods depending on the type of problem. More specifically, an optimization problem can be categorized as *continuous* or *discrete* based on whether the variables can assume real values or not. If real values can be assumed, the problem is continuous and can be solved by e.g. linear programming or nonlinear programming [48]. Conversely, if only discrete values are allowed, the problem is discrete and can be solved by either integer programming or combinatorial programming.

INTEGER PROGRAMMING AND COMBINATORIAL PROGRAMMING

In *Integer Programming (IP)*, the ground set of variables is binary or consists of a set of integers. This can be compared to *Combinatorial Programming*, which deals with finding the best combination of variables subject to given constraints [49]. Both IP and combinatorial programming, which for some instances can be considered as a special class of IP, are NP-hard (i.e. non-deterministic polynomial-time hard) [48]. A problem, which is NP-hard, has no efficient algorithm for finding the solution. Metaheuristic solution methods, which generate good (but not guaranteed optimal) solutions within limited amounts of time, are therefore commonly used to solve IP and combinatorial problems [49]. Examples of metaheuristics are multi-start local search, simulated annealing, tabu search, and genetic algorithms.

METAHEURISTIC SOLUTION METHODS

Multi-start Local Search (MLS) [17],[50] is an optimization method, which uses a number of initial local searches with hill climbing routines. In these searches, the solution is repeatedly replaced by a better solution until a better solution cannot be found. The best solution during the entire search is then the output.

In *Simulated Annealing (SA)*, which has taken inspiration from the physical annealing process [17],[50] , test solutions are randomly generated from an allowed set of solutions. Each test solution is assigned a probability, whose value depends on whether or not the test solution is better than the previous test solution. If the new test solution is better, the probability of choosing it is 1. Otherwise, the probability is between 0 and 1. This means that the search is allowed to move towards a worse solution, which in turn enables a possible escape from poor locally optimal solutions. This strategy of allowing moves to worse solutions is also applied in *Tabu Search (TS)* [49]. However, an additional feature in TS is that a move to a new solution is always executed, even if the current solution is better or equally good [50]. This makes the algorithm more efficient than SA since it is more likely to move towards a worse solution, i.e. escape from poor locally optimal solutions.

In comparison, *Genetic Algorithms (GAs)* is a class of Evolutionary Algorithms (EAs), which are inspired by the evolutionary process. Like the evolution, a GA seeks to gradually improve the generated solutions through processes such as combination and mutation of candidate solutions (i.e. slight modifications of the solutions) [50],[51].

In terms of comminution related research, Svedensten [17] used a GA for crushing plant optimization, whereas Hulthén et al. [52] initiated the idea of using GAs to optimize compressive crushing. While et al. [53] also used an EA for optimizing crusher design and process parameters, but did not mention the crusher model applied or the rock material assumed. Other GA applications can be further found in several manufacturing industries, where tolerance allocation is optimized to minimize cost and to improve production [54]. GAs have also been used to optimize filter implementation in morphological image processors [55], and to optimize the design of composite laminates in the aerospace industry [56].

4.4 CRUSHER GEOMETRY OPTIMIZATIONS

Optimizations of crushing chamber geometry have been attempted by Gang et al. [57],[58], Huang et al. [59], and as previously mentioned While et al. [53]. The common denominator of the works of these authors seems to be an approach, which is based on the optimization of operational and design parameters of existing cone crushers. The approach thus implies a presumption that the optimized machine design is and should be similar to the existing cone crusher design. This can be compared to a more general approach in which none or only a few assumptions regarding the design of the crushing machine are predetermined.

In terms of the applied comminution models in the described optimizations, Gang, Huang and coworkers [57],[58],[59] have endeavored to apply the flow and compressive interparticle breakage models by Evertsson [4], whereas While et al. [53] did unfortunately not specify the applied crusher model. With respect to optimization specifics, While et al. applied an EA as opposed to Huang et al. who used non-linear sequential quadratic programming. Gang et al. [57],[58], on the other hand, failed to specify the applied optimization method.

Though it is commendable that the works of Gang, Huang and coworkers [57],[58],[59] have resulted in manufactured prototypes, which seem to have been successfully tested in full scale, there remain yet several question marks regarding their work. For instance, the fact that only interparticle crushing has been considered is questionable considering that research by e.g. Evertsson [4] and Eloranta [60] clearly state that existing cone crushers normally apply both interparticle and single particle crushing. Also, in terms of the applied models, there seem to be some uncertainties regarding their correct use as well as their correct calibrations with respect to the studied rock materials.

Moreover, although not clearly stated, the mathematically formulated optimization objectives in the works of Gang, Huang and coworkers [57],[58],[59] suggest that the optimized crushing chambers are to be used in mining applications. As particle shape is of most concern for the aggregate industry, this thus raises the question of the relevance of including flakiness in the optimizations of Gang et al. [57],[58]. What is more, it is also unclear as to which rock material that has been studied [58] and for which feed size distributions the optimizations have been performed [57],[58]. One could further argue that since the optimizations have been conducted with user-defined numerical constraints on e.g. the capacity, the percentage passing the CSS, and the product flakiness [57],[58],[59], the risk of sub-optimization is at hand.

5 MODELING

The aim of this chapter is to:

- *Describe the crushing process in a cone crusher*
- *Introduce the applied model of the crushing process in a cone crusher*
- *Describe the fundamental experiments conducted in order to characterize the compressive breakage behavior of a given rock material*
- *Present the mathematical models describing the compressive breakage behavior of a given rock material*

In order to theoretically optimize compressive crushing, models describing the compressive breakage behavior of different rock materials are needed. Similarly, in order to theoretically optimize the crushing process in a cone crusher, a model of the size reduction process is required. Combined together, these different models provide a description of how different rock materials are fragmented in cone crushers.

5.1 CRUSHING PROCESS IN A CONE CRUSHER

The crushing process in a cone crusher can be described by dividing the crushing chamber into a number of different crushing zones [4],[60]. This means that the crushing process is discretized, as shown in Figure 8, where each crushing zone corresponds to a crushing event performed by a compression that is defined by the ratio of the stroke s and the bed height b. The crushing process in a cone crusher can in other words be modeled as a series of consecutive compressions, where the outgoing material from one compression serves as the ingoing feed to the next compression. This approximation can be visualized as in Figure 9.

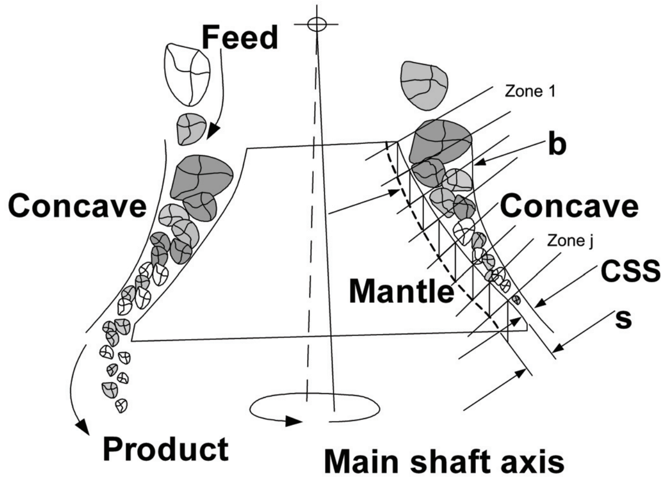

Figure 8. Schematic illustration of the crushing zones in a cone crusher (cf. Evertsson [4]).

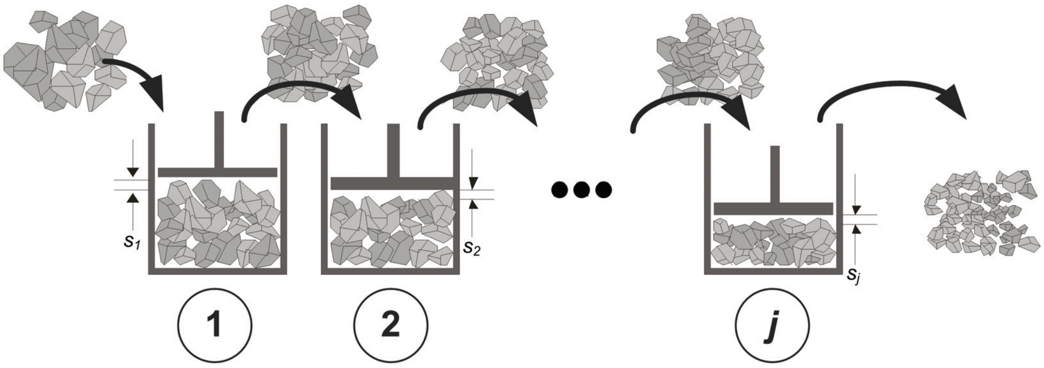

Figure 9. Approximation of a compressive crusher with a series of consecutive compressions (cf. Hulthén [52]).

According to Evertsson [4], a particle subjected to compression inside a cone crusher can be broken through either interparticle breakage (also known as bed breakage) or single particle breakage. The mode of breakage generally depends on the stress state (i.e. loading conditions) which the particle is subjected to at the time of compression. More specifically, it is believed that interparticle breakage (IPB) can only occur above the choke level of the crushing chamber, whereas single particle breakage (SPB) commonly occurs below the choke level. This means that crushing chambers with choke levels far up in the chamber will nominally have less interparticle crushing than crushing chambers with choke levels positioned further down in the chamber [7].

The difference between interparticle and single particle breakage is illustrated in Figure 10. As can be seen, rock particles in interparticle breakage have several contact points to other surrounding particles, whereas rock particles in single particle breakage only have two contact points by definition. Also shown in the figure is the definition of compression ratio $s_{\aleph}$.

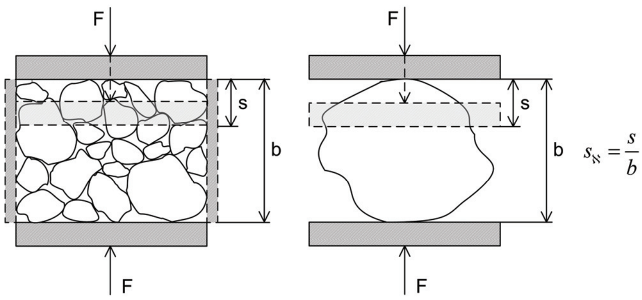

Figure 10. Schematic illustration of interparticle breakage (left) and single particle breakage (right) along with the definition of the compression ratio $s_{\aleph}$ in each breakage mode.

Assuming that interparticle crushing normally precedes single particle crushing in a cone crusher, the crushing process can be modeled as in Figure 11. It is also assumed that the compressive breakage behavior of a rock material can be described by a breakage function B and a selection function S [4],[30],[31]. The breakage function describes *how* different particles will break (i.e. the resulting particle size distribution), whereas the selection function describes *which* particles that will break (i.e. the breakage probability). Depending on the breakage mode, different breakage functions will apply. This can be compared to the selection function, which only appears to be active for interparticle breakage. This is because the breakage probability of single particle breakage is assumed to always be 1, when a particle is subjected to a single particle compression. In a real cone crusher, however, not all particles in a single particle crushing zone are crushed. Particles with particle sizes smaller than the local gap between the closing mantle and the concave will slip through single particle crushing zones without being broken. This type of event, which can be visualized as in Figure 12, is described by the classification function C in the model. Particles, which are larger than the local gap and which will be crushed in single particle breakage, will thus have a value of 1 in this classification function, whereas particles too small to be broken will have a value of 0.

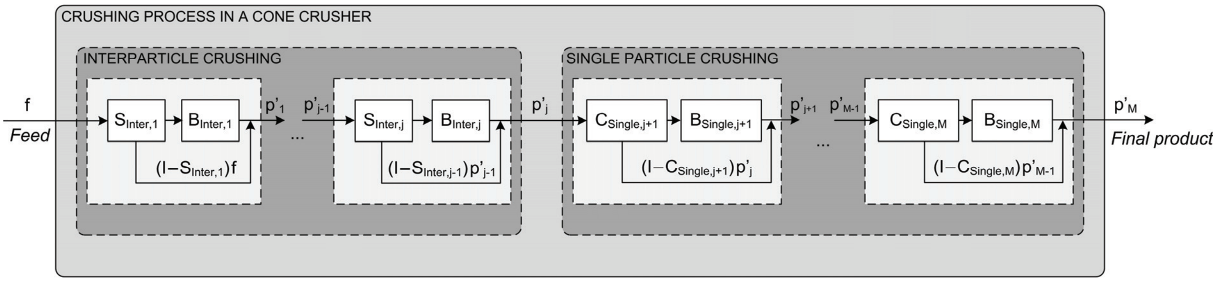

Figure 11. Applied process model of a cone crusher in which S corresponds to the selection function, B the breakage function, and C the classification function. A feed f will thus result in a product p'_M through a series of j interparticle crushing events and M-j single particle crushing events.

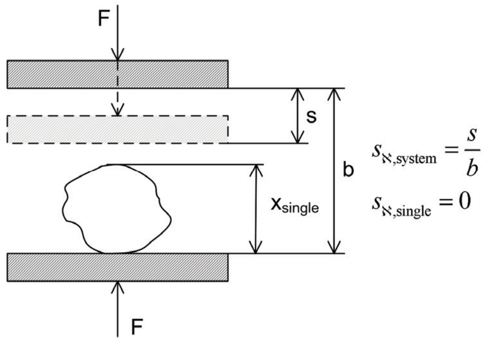

Figure 12. Particle not subjected to single particle breakage due to its particle size x_{single} being smaller than the remaining gap, i.e. the bed height b minus the stroke s.

5.2 MATERIAL CHARACTERIZING CRUSHING TESTS

The compressive breakage behavior of a given rock material can be characterized by form conditioned piston and die tests. A method for characterizing for interparticle breakage was developed by Evertsson [4], who used monosized fractions of 16-19 mm particles. Bengtsson et al. [40] later adapted this method for the characterization of single particle breakage.

The characterization method for interparticle breakage as described by Evertsson [4] was initially used in this study. However, following results suggesting a need for an increased statistical significance of the measurements, the method was modified into using monosized 8-11.2 mm particles instead. This change of test fractions resulted in a sevenfold increase in particle count, thereby implying an increase in the statistical significance of the measurements.

In contrast, the test method, described by Bengtsson et al [40], for characterizing single particle breakage was applied without any alterations. Characterizations of single particle breakage were therefore performed using 16-19 mm particles, whereas 8-11.2 mm particles were used for the characterizations of interparticle breakage.

In this study, four different rock materials and two different iron ores were tested. The studied materials include *gneiss* (from Dalby in Southern Sweden), *diabase* (from Billingsryd in Southern Sweden), crystalline limestone, which is also called *marble* (from Forsby in Middle Sweden), *quartzite* (from Södra Sandby from Southern Sweden), and *iron ore* (from Donganshan and Dagushan in China). Table 2 shows the applied test plans during the characterization testing of both breakage modes. As can be seen, series of compressions were undertaken at different compression ratios. In single particle breakage, rock particles were compressed separately so that each individually tested particle would experience the actual single particle compression ratio as specified in the table. This can be compared to the testing of interparticle breakage in which each batch of test samples is contained in a cylindrical steel container. The applied compression ratio in interparticle breakage is thus the external compression ratio as viewed from the system of the cylindrical container.

In practice, the material samples for single particle breakage were collected after testing and sieve analyzed to determine the resulting size distributions. For interparticle breakage, on the other hand, the material of each test series was taken out after each compression, sieve analyzed, remixed and then recompressed. This was applied to all interparticle tests except for test number 10, which used the outgoing material from test number 20 as feed material. The reason for this was to study the material's breakage behavior when samples of wide size fractions were compressed with small compressions.

Table 2. Test plans for the material characterizing crushing tests for interparticle and single particle breakage.

Interparticle breakage

Test no	Test material	$s_{\aleph}$
1	350 particles of 8-11.2 mm	0.10
2	from no 1	0.10
3	from no 2	0.10
4	from no 3	0.10
5	from no 4	0.10
6	350 particles of 8-11.2 mm	0.15
7	from no 6	0.15
8	from no 7	0.15
9	from no 8	0.15
10	from no 20	0.15
11	350 particles of 8-11.2 mm	0.20
12	from no 11	0.20
13	from no 12	0.20
14	from no 13	0.20
15	350 particles of 8-11.2 mm	0.25
16	from no 15	0.25
17	from no 16	0,25
18	from no 17	0.25
19	350 particles of 8-11.2 mm	0.30
20	from no 19	0.30
21	350 particles of 8-11.2 mm	0.35
22	from no 21	0.35

Single particle breakage

Test no	Test material	$s_{\aleph}$
1	30 particles of 16-19 mm	0.10
2	30 particles of 16-19 mm	0.15
3	30 particles of 16-19 mm	0.20
4	40 particles of 16-19 mm	0.25
5	60 particles of 16-19 mm	0.30

5.3 COMPRESSIVE BREAKAGE BEHAVIOR

Mathematical models describing the compressive breakage behaviors of different rock materials were developed by Evertsson [4] and Bengtsson et al. [40]. These models were essentially population balance models and were developed along with the previously described characterization methods. Empirical data from the experiments such as measured size distributions, and pressure and force responses are thus required for these models.

BREAKAGE FUNCTION

The breakage function of a rock material mathematically describes how a compressed particle of a given particle size breaks into smaller fragments. In other words, the output of the function is the resulting particle size distribution, which is expressed cumulatively. Specifically, the relative breakage of particles is assumed to be only dependent on the applied compression ratio $s_\aleph$ [4],[40]. For interparticle breakage, this implies that only the first compression of each compression series in the characterization tests needs to be considered when calibrating the function. According to Evertsson [4], the breakage function for *interparticle breakage* can be expressed as

$$B_{\text{Inter}}\left(x_\aleph, s_\aleph\right) = \left(1-\left(\alpha_3+\alpha_4 s_\aleph\right)\right)\cdot x_\aleph^{\alpha_1+\alpha_2 s_\aleph} + \left(\alpha_3+\alpha_4 s_\aleph\right)\cdot x_\aleph \tag{4}$$

where $x_\aleph$ is a vector of particle sizes relative to the initial particle size x_0 and $\alpha_i,\ i=1,...,4$, are fitted constants. The vector of relative particle size $x_\aleph$ is defined in Eq.(5), where $x_{\min}$ is a small reference particle size (of pure numerical reasons, $x_{\min}$ is set to 0.008 mm).

$$x_\aleph = \frac{\log_2\left(x/x_{\min}\right)}{\log_2\left(x_0/x_{\min}\right)} \tag{5}$$

The corresponding expression for *single particle breakage* is obtained by adding another exponential term α_5 [40]:

$$B_{\text{Single}}\left(x_\aleph, s_\aleph\right) = \left(1-\left(\alpha_3+\alpha_4 s_\aleph\right)\right)\cdot x_\aleph^{\alpha_1+\alpha_2 s_\aleph+\alpha_5 s_\aleph^2} + \left(\alpha_3+\alpha_4 s_\aleph\right)\cdot x_\aleph \tag{6}$$

where $\alpha_i,\ i=1,...,5$, are fitted constants specific for single particle breakage.

Figure 13 shows the predicted, as well as the measured, normalized particle size distributions for the examined gneiss during the material characterizing crushing tests. The agreement between the simulations and the measured data indicates that the model works well for one compression. The fitted breakage function constants used in the predictions are presented in Table 3.

Table 3. Breakage function constants for the examined gneiss.

Breakage mode	α_1	α_2	α_3	α_4	α_5
Interparticle	23.58	-45.86	0.03614	0.5374	-
Single particle	20.72	-12.19	-0.001184	0.4326	-60.43

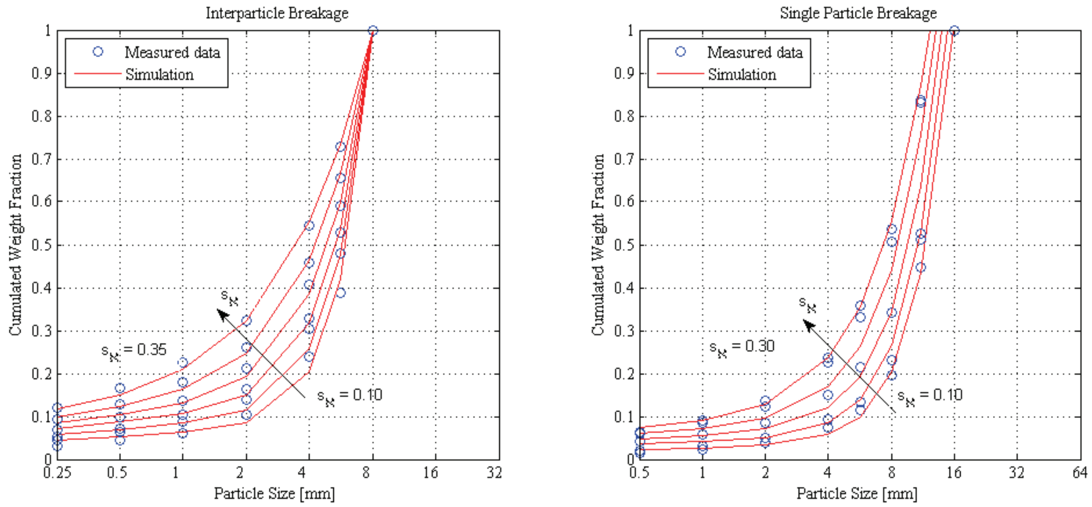

Figure 13. Normalized breakage behavior of the examined gneiss with interparticle breakage depicted to the left and single particle breakage illustrated to the right.

SELECTION FUNCTION

When a bed of particles is subjected to compression, only a fraction of those particles will be reduced in size. This is due to the distribution of forces [41] and can be formulated in terms of breakage probability, which is described by the selection function. For single particle breakage, however, the corresponding selection is as mentioned always equal to 1.

The breakage probability, or selection, of a given material is assumed to be equivalent for all particles in a sample regardless of particle size. This is a crucial assumption and is the same as assuming that a comparable relative amount of particles is broken regardless of the initial particle size [32]. It implies that selection will only be dependent on the compression ratio $s_ℵ$ and the feed size distribution measured in terms of the standard deviation of particle size $\sigma_ℵ$.

The mathematical expression for selection is put together by two separate functions; one describing the dependency of the compression ratio and the other describing the relationship to the feed fraction width [4]. The combination of these functions gives that the selection S, i.e. the breakage probability, increases with the compression ratio $s_ℵ$ and decreases for a growing feed fraction width $\sigma_ℵ$. This is intuitively correct as a wider feed size distribution implies a smaller breakage probability, whereas a larger compression increases the probability of breakage. These dependencies are also mentioned in the work of Liu and Schönert [31]. The resulting selection function can thus be represented as follows

$$S(s_ℵ,\sigma_ℵ) = a_1 s_ℵ^2 \sigma_ℵ^2 + a_2 s_ℵ^2 \sigma_ℵ + a_3 s_ℵ^2 + a_4 s_ℵ \sigma_ℵ^2 + a_5 s_ℵ \sigma_ℵ + a_6 s_ℵ + a_7 \sigma_ℵ^2 + a_8 \sigma_ℵ + a_9 \qquad (7)$$

where a_i are fitted constants. Figure 14 shows the selection function for the examined gneiss for which the following selection function constants were determined.

$$\begin{array}{lll} a_1 = -10.40 & a_4 = 3.385 & a_7 = -0.05121 \\ a_2 = 3.956 & a_5 = -1.292 & a_8 = -0.2732 \\ a_3 = -1.585 & a_6 = 3.118 & a_9 = -0.1632 \end{array}$$

The limit of the different selection function curves, as seen in the figure, is set by the theoretically maximum values of compression ratio $s_{ℵ,\max}$, which are in turn governed by the relation between the uncompressed bulk density of the material ρ and its solid density ρ_s:

$$s_{\aleph,\max} = 1 - \frac{\rho}{\rho_s} = 1 - \rho_{\aleph} \tag{8}$$

where $\rho_{\aleph}$, representing the normalized density of the material, is dependent on the fraction width $\sigma_{\aleph}$ of the material [4]. In other words, a bed of particles can only be compressed as long as there is air inside the bed. Once all air has been pushed out or evacuated, the density of the particle bed will be comparable with that of the solid material, thereby implying that the maximum compression has been reached.

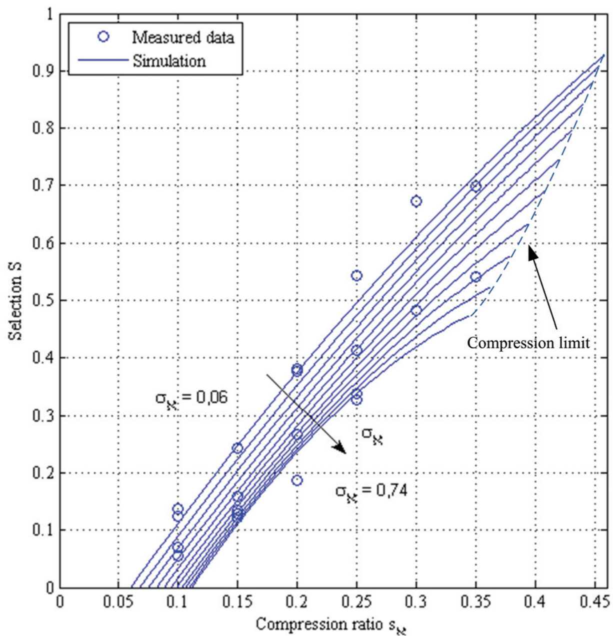

Figure 14. Two-variable selection function fitted to experimental data (gneiss).

PRESSURE AND FORCE RESPONSES

The pressure or force required to compress a particle bed or a single particle to a given compression ratio can be equated with the pressure or force response arising in the piston following particle breakage. These responses, which were recorded at the characterization tests, were used for modeling the mechanical behavior of the studied materials.

According to Bengtsson et al. [40], the pressure P_{Inter} required for compressing a particle bed is related to the compression ratio $s_{\aleph}$ and the feed fraction width $\sigma_{\aleph}$:

$$P_{\text{Inter}} = s_{\aleph}^2\sigma_{\aleph}^2 d_1 + s_{\aleph}^2\sigma_{\aleph} d_2 + s_{\aleph}^2 d_3 + s_{\aleph}\sigma_{\aleph}^2 d_4 + s_{\aleph}\sigma_{\aleph} d_5 + s_{\aleph} d_6 \tag{9}$$

For *single particle breakage*, the force F_{Single} required for crushing a single particle can be expressed as a function of the particle size x and the single particle compression ratio (s/x), i.e. the compression ratio experienced by the single particle:

$$F_{\text{Single}} = x^2 \cdot \left(c_1 \cdot \frac{s}{x} + c_2 \cdot \left(\frac{s}{x}\right)^{c_3} \right) \tag{10}$$

The model constants $d_i\left(i=1,..,6\right)$ and $c_i\left(i=1,2,3\right)$ of Eq.(9) and (10) can be determined by fitting the models to the experimental data from the characterization tests. Table 4 shows the corresponding constants for the examined gneiss, whereas a comparison between the response models and the experimental data can be seen in Figure 15.

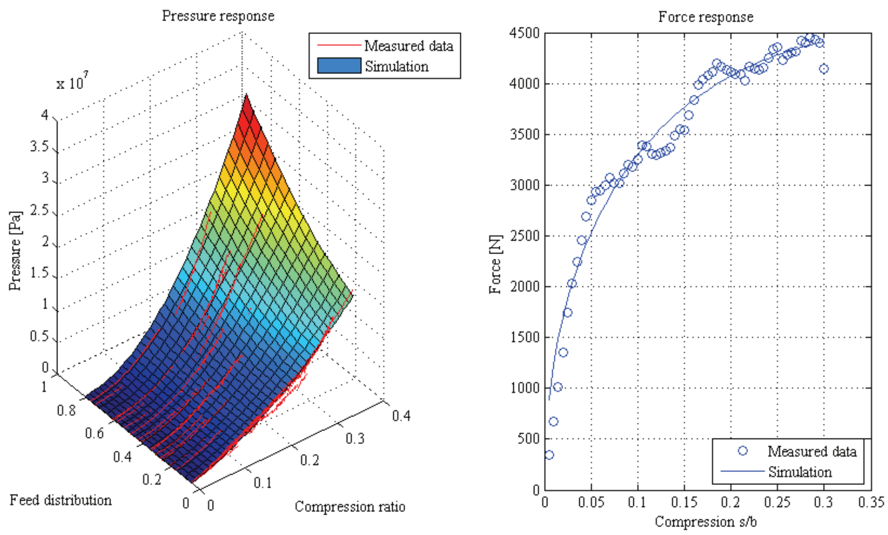

Figure 15. Pressure (interparticle breakage) and force (single particle breakage) responses for the tested gneiss.

Table 4. Pressure and force response constants for the examined gneiss.

Breakage mode	**Response constants**		
Interparticle	$d_1 = 0.2615\cdot10^8$	$d_2 = 2.057\cdot10^8$	$d_3 = 0.7695\cdot10^8$
	$d_4 = 0.3145\cdot10^8$	$d_5 = -0.3864\cdot10^8$	$d_6 = 0.2042\cdot10^8$
Single particle	$c_1 = -53.62$	$c_2 = 68.39$	$c_3 = 0.5189$

In terms of energy consumption, the required energy W_{Inter} for compressing a particle bed is obtained by integrating the pressure response P_{Inter} over the volumetric displacement s, and multiplying the cross sectional surface area A perpendicular to the compressed volume:

$$W_{\text{Inter}} = A\cdot\int P_{\text{Inter}}\left(s_{\aleph},\sigma_{\aleph}\right)\ \mathrm{d}s \tag{11}$$

Similarly, the required energy W_{single} for crushing a given single particle is obtained by integrating the force response F_{single} over the volumetric displacement, or stroke s:

$$W_{\text{Single}} = \int F_{\text{Single}}\left(x,s\right)\ \mathrm{d}s \tag{12}$$

The energy consumption for a crushing sequence, expressed as energy per mass unit material, can thus be calculated by summarizing the energy consumptions for each compression. For a crushing process with both interparticle (*j* events) and single particle breakage (*M-j* events), the total energy consumption would be:

$$W_{\text{Total}} = \sum_{j'=1}^{j} W_{\text{Inter}}^{j'} + \sum_{k'=1}^{M-j} W_{\text{Single}}^{k'} \tag{13}$$

This expression can in other words be used for the crushing process shown in Figure 11.

6 OPTIMIZATION

The aim of this chapter is to:
- *Describe the applied optimization algorithm*
- *Motivate the choice of optimization method*
- *Clarify how a fitness function is defined and the importance of it*
- *Define a selection of the applied fitness functions*

The compressive crushing process of a given rock material can be optimized with regards to different situations and different applications. By allowing the optimization to be performed on an ideal crushing stage, free from any mechanical limitations and decoupled from existing machine parameters, the actual crushing process can be studied and new unbiased crusher concepts can be developed. Thus, in the interest of innovative machine design, the knowledge of how different rock materials should optimally be crushed should be related to general and non-machine specific parameters. Examples of such parameters are e.g. the number of compressions and the corresponding compression ratios.

6.1 SELECTION OF OPTIMIZATION METHOD

As described in Chapter 4, optimization can be performed using a variety of different methods. One means of optimization is the use of genetic algorithms (GA), which were selected in this work. This choice of optimization method was motivated by the previous use of GAs in comminution related research, the complex non-linear functions involved, as well as the discrete variables at hand. Specifically, according to Svedensten [17], optimization of discrete parameters can only be conducted by using discrete methods, such as e.g. GAs. Wahde [51] further stated that GAs do not require the function being optimized to be differentiable or even continuous. GAs thus seem qualified for the optimization task in this work. Also, since GAs are initialized at random, they present a smaller risk of not finding a solution close to the global optimum as opposed to optimization methods relying on initial user estimates in which only local optima might be identified. Finally, yet another advantage of GAs is their robustness [50]. Their performance will in many cases almost remain the same even if the problem structure and/or the parameters of the algorithm are changed.

6.2 APPLIED GENETIC ALGORITHM

An optimization routine based on a genetic algorithm was applied to theoretically optimize the compressive crushing of different rock materials in this thesis. Used at first to optimize the compressive crushing of the different breakage modes separately, the optimization routine was then adapted for the optimization of crushing sequences of both interparticle and single particle compressions. Figure 16 illustrates the structure of this adapted optimization routine, which is initiated by the random generation of n crushing sequences (i.e. a population of 200 crushing sequences, which are also called individuals). These crushing sequences contain j

interparticle compressions with random interparticle compression ratios, $s_{\aleph,j}$, and k single particle compressions with random single particle compression ratios, $s_{\aleph,k}$. These parameters are generated within limits generally defined as $0 \le j+k \le 10$, $2 \le j,k \le 8$, $0 \le s_{\aleph,j} \le 0.35$ and $0.05 \le s_{\aleph,k} \le 0.45$. The motivation for some of these limits will be discussed in later chapters. In comparison, the applied limit for the number of compressions in the optimizations of a single breakage mode was $0 \le j+k \le 20$ for $j=0$ or $k=0$.

The initial generation of crushing sequences is followed by the simulation of the sequences using models describing the compressive breakage behavior of the material. These simulations take place for one crushing sequence at a time during which the sequence is simulated compression by compression. This means that the outgoing material from one compression serves as the ingoing feed to the next compression. Upon completing the simulation of an entire crushing sequence, a so called user-defined fitness function (see the following subchapter) evaluates the simulated crushing sequence and assigns a fitness value to it. The fitness value allows the routine to rank the crushing sequences according to their results once all sequences have been simulated. Similar to the evolution, the best crushing sequences will then give rise to the next set, or generation, of crushing sequences through processes such as crossover, mutation, and elitism (explained further down in this text). This procedure of generation, simulation, and evaluation will then repeat itself in an iterative way for a defined number of generations *N*. In optimizations of one breakage mode, this corresponds to 500-1500 iterations. This can be compared to the 4000-8000 iterations applied in optimizations containing both breakage modes. The idea is that the crushing sequences will then gradually improve along the course of generations, eventually leading to an optimal crushing sequence, which fulfills the set demands.

Table 5 shows the optimization parameters of the applied genetic algorithm. As indicated, the selection process of the algorithm is performed using a roulette wheel selection. In roulette wheel selections, two individuals (i.e. crushing sequences) are selected from the population using an imaginative roulette wheel [51]. Each individual of the population is assigned a slice of the roulette wheel based on its fitness value – the larger the fitness value; the larger the slice of the roulette wheel obtained. An individual with high fitness value is therefore more likely to be selected than an individual with low fitness value. When these parenting individuals have been selected, two new individuals are generated through the processes of crossover and mutation. This procedure of selection, crossover, and mutation is repeated until an entire population of *n* newly generated individuals is obtained.

The crossover process can be compared to the reproduction process in biology. Features of the selected parenting individuals are combined into new individuals at a probability of 0.3. This means that there is a probability of 0.7 that the offspring, sent to the mutation process, are unaltered copies of the selected parenting individuals. In other words, a larger probability of crossover implies a quicker introduction of new solutions into the population. However, as the probability of crossover increases, so does the risk of solutions being disrupted before being properly exploited by selection [61]. Consequently, due to the amount of variables as well as the complex non-linear functions involved, a more conservative crossover probability of 0.3 [52] is chosen as opposed to the otherwise typical values of 0.5 -1.0 [61].

After crossover, the individuals are modified with a probability of 0.03 in the mutation process. Mutation is used to prevent inbreeding and premature convergence of the GA to suboptimal solutions [51],[61]; with a larger probability of mutation allowing for a larger diversity in the solutions. Typical values are in the range of 0.005-0.05 [61], as a too large mutation probability renders the GA into a purely random search algorithm. In this study, the applied mutation scheme, operated with a probability of 0.03, is called bit flip, since each individual is described by a set of genes which forms a binary chromosome.

As mentioned earlier, the process of elitism is also applied. Elitism is used in order to ensure that the best individual in each generation is not lost. This is accomplished by simply making copies of the best individual and planting them in the next generation.

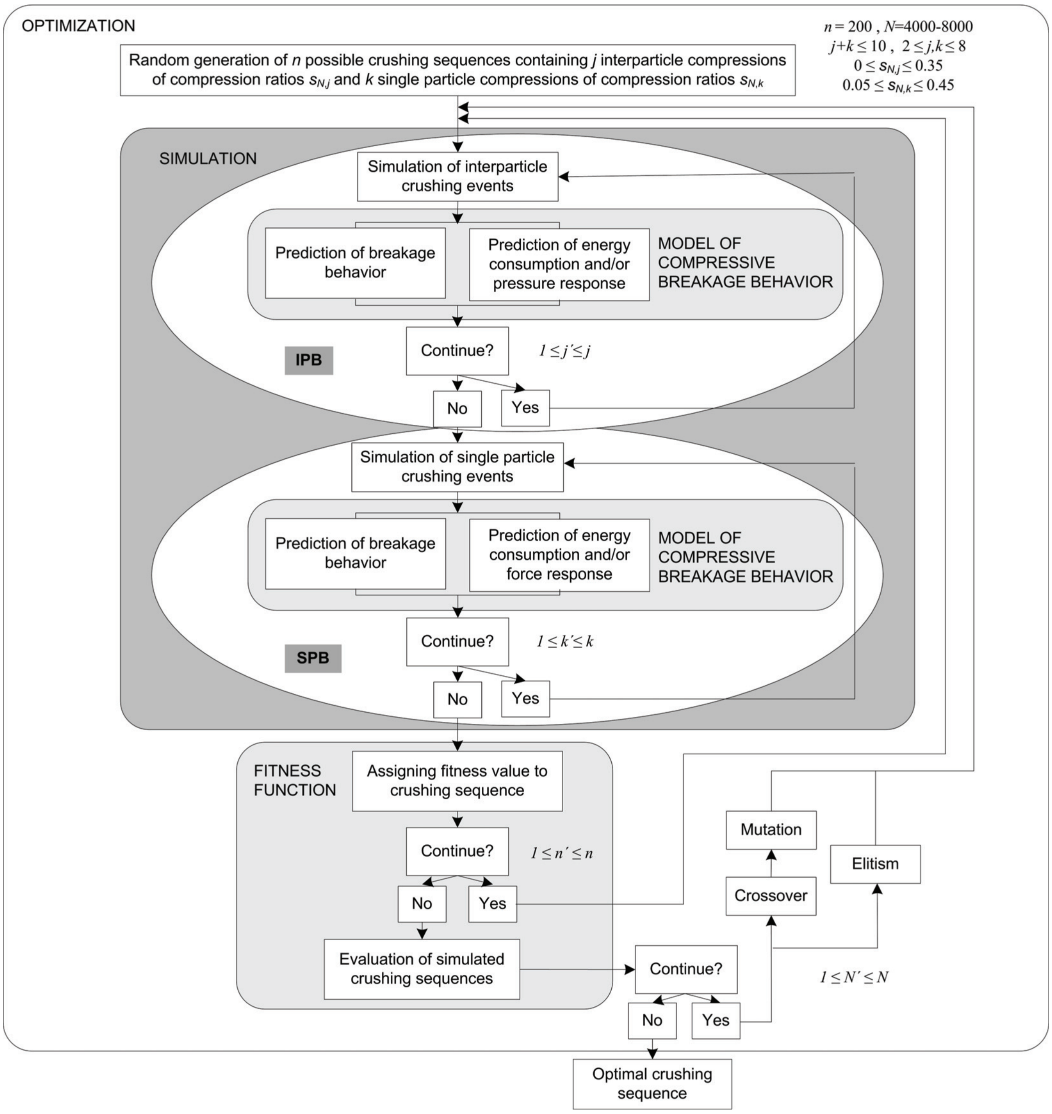

Figure 16. Schematic layout of the applied optimization routine based on a genetic algorithm.

Table 5. Optimization parameters for the applied genetic algorithm.

Parameter	**Value**
Number of individuals, n	100, 150 or 200
Number of generations, N	500 - 1500 (one breakage mode), 4000 - 8000 (both breakage modes)
Probability for mutation of a gene	0.03
Probability for crossover between two individuals	0.3
Mutation type	Bit flip
Selection ranking	Roulette wheel

In the simulation routine, the compression ratio for single particle breakage is calibrated after the largest particle in the feed. This means that differently sized particles experience different single particle compression ratios. The reason for this is that in real applications, the actual stroke exerted on a single particle differs depending on the particle size (see Figure 12). In other words, the single particle compression ratio experienced by a particle is dependent on its particle size in two different ways; the actual stroke and the particle bed height. Each particle in single particle breakage can thus be considered to have its own reference system in terms of compression. This can be compared to interparticle breakage, where the particles are considered as a unit volume and are therefore subjected to the same compression ratio.

6.3 FITNESS FUNCTIONS

A fitness function is a user-defined evaluation function, which depending on the application can have several different names such as cost function, objective function, target function etc. The purpose of the fitness function is to evaluate and assign performance values, or fitness values, to examined solutions (i.e. crushing sequences here). The assigned fitness value should reflect how well a given solution matches the applied optimization objective. Thus, depending on the formulation of the fitness function, the optimization can be steered in completely different directions. This means that in order to achieve a given optimization objective, the applied fitness function must be correctly formulated to reflect that objective.

The formulation of a fitness function is not always straight-forward as the function needs to be formulated mathematically in order to enable its computer-assisted application. Different applications as well as different situations often require a “unique” fitness function of their own. What might be optimal in one case might not necessarily be optimal in another. It is thus crucial to keep in mind that an optimal solution obtained from a given fitness function is only true for that specific application or situation described by the applied fitness function.

Different fitness functions have been formulated and applied during the course of this project. Although simplified, they all originate from real situations or issues in real industrial applications. Table 6 presents a selection of the applied fitness functions for which the variables capacity, product, and by-product can be visualized as in Figure 17 and Figure 18. As can be seen, the definition of what is considered to be product widely differs depending on the type of application, i.e. aggregate or mining. As a result, different issues will be encountered depending on the application. This is reflected in the different types of fitness functions presented, as well as the slight variation of fitness function in terms of energy consumption for the different applications.

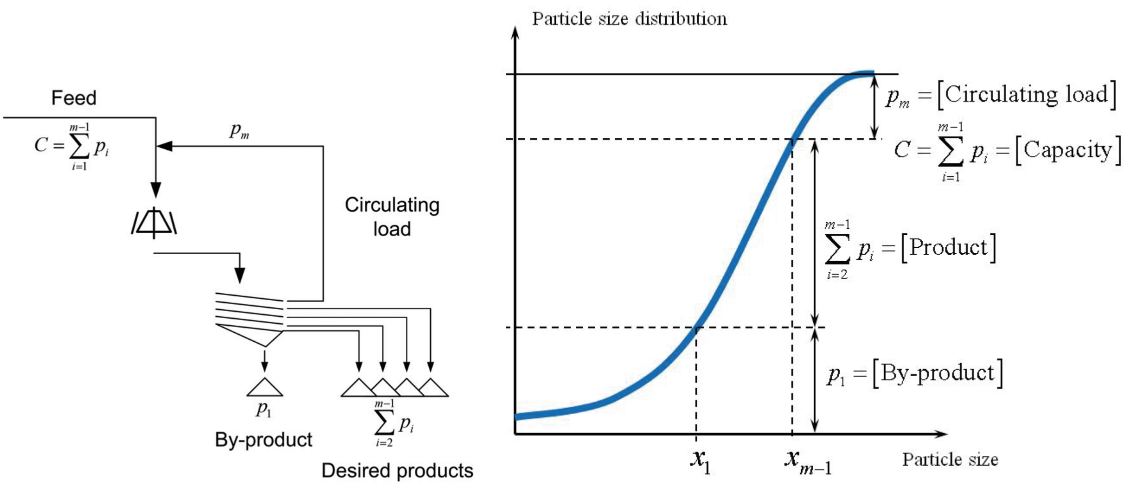

Figure 17. Schematic illustration of capacity, product and by-product in aggregate optimizations.

Table 6. Examples of fitness functions in the aggregate and mining industries.

Optimization objective	**Fitness function**
Maximize *product yield*	$\varphi_{\text{Yield}} = \dfrac{C \cdot \sum_{i=2}^{m-1} p_i}{p_1} = \dfrac{[\text{Capacity}] \times [\text{Product}]}{[\text{By-product}]}$
Maximize *balanced product yield*	$\varphi_{\substack{\text{Balanced}\\\text{yield}}} = \dfrac{C \cdot \sum_{i=2}^{m-1} \frac{v_i}{v_1} \cdot p_i}{p_1} = \dfrac{[\text{Capacity}] \times [\text{Relative values} \times \text{desired products}]}{[\text{By-product}]}$
Minimize *energy consumption*	$\varphi_{\text{Energy}} = \dfrac{C \cdot \sum_{i=2}^{m-1} p_i}{\sum_{j=1}^{M} W_j} = \dfrac{[\text{Capacity}] \times [\text{Product}]}{[\text{Energy}]}$ $\varphi_{\text{Energy\_mining}} = \dfrac{C \cdot \sum_{i=1}^{m-1} p_i}{\sum_{j=1}^{M} W_j} = \dfrac{[\text{Capacity}] \times [\text{Product}]}{[\text{Energy}]}$
Maximize *product*	$\varphi_{\text{Product}} = \sum_{i=1}^{m-1} p_i = [\text{Product}]$

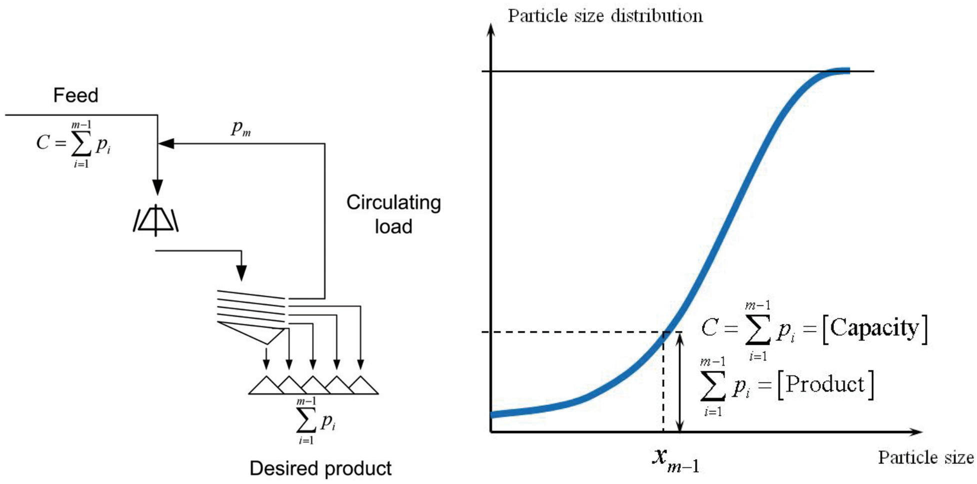

Figure 18. Schematic illustration of capacity, product and by-product in mining optimizations.

The presented fitness function of *product yield* addresses a common issue of interest within the aggregate industry; to maximize the production of a certain product as well as the throughput of the process, while reducing the amount of by-product. The challenge of finding the best approach to this comes from the different interrelated and counteractive objectives, which makes manual optimization not only difficult but also inefficient. Another level of complexity is further added as most crushing plants within the aggregate industry produce several selling products p_i with different economical values v_i. This issue is addressed by adjusting the fitness function to a *balanced product yield*, which in the presented form assumes a by-product p_1 with an economical value v_1. This balanced product yield can be considered as a measure for the total value of the desired products as well as capacity per value of generated by-product.

An issue of interest shared by both the aggregate and mining industry is that of reducing the energy consumption in production. The predominant question of how to attain as much production and process capacity as possible, while minimizing the energy required for operation is addressed by the fitness function of *energy consumption*. As seen in Table 6, the function varies slightly depending on the application. This is as mentioned, due to the different definitions of product in the aggregate and mining industries.

To achieve as much size reduction as possible is generally the main focus of the mining industry. This can be quantified into the objective to maximize the production of material smaller than a given particle size. In other words, this corresponds to the fitness function of *product* shown in Table 6.

7 EVALUATION OF REAL APPLICATIONS

The aim of this chapter is to:

- *Determine the performances of existing cone crusher applications*
- *Study how crusher performance can be improved by means of operational parameters*
- *Evaluate the performances of real applications relative to what is theoretically optimal*
- *Define performance efficiency*

The performance of a crusher application can be measured in a variety of different ways depending on the type of application and the focus of the evaluation. For instance, common on-line measures of performance involve capacity (i.e. tons per hour) and power draw. However, while these measures are simple and straight-forward regarding the throughput of the process and the amount of work performed, they do not address the actual output of the application. In other words, they do not measure the size reduction performed by the application, how well the application produces certain desired products, or how well it manages to limit the production of undesired by-products. To address issues like these, measures based on the actual crusher output should instead be used. In mining applications, an example of such measure would be the p_{80}, or perhaps the generated relative amount of material below a certain particle size. These measures can also be compared to the concept of product yield, which would be more appropriate for aggregate applications.

Apart from the advantage of measuring performance directly related to crusher output, measures such as the p_{80} and product yield can also be applied to theoretical crushing sequences. As the aim of this chapter is to evaluate real applications in comparison to their theoretically optimal crushing sequences, measures directly related to the crusher output seem appropriate. The performances of the existing applications described in this thesis will thus be determined based on these measures.

7.1 INTERPARTICLE CRUSHING IN CONE CRUSHERS

As described in Chapter 5, the crushing process in existing cone crushers consists of both interparticle and single particle crushing. It is believed that interparticle crushing can only occur above the choke level of a crushing chamber, whereas single particle crushing generally takes places below the choke level [4]. Thus, in order to better understand the initial crushing process in real cone crushers, both theoretical and experimental studies of interparticle crushing were conducted.

According to Evertsson [4], and Onnela and Eloranta [62], the compression ratio in a cone crusher increases from the crushing chamber inlet to the crushing chamber outlet, where the utilized interparticle compression ratio is believed to be around 0.3-0.4. This means that for a cone crusher, the interparticle compression ratio increases along the crushing chamber, which in the applied cone crusher model would translate into a series of gradually increasing interparticle compressions.

GENERAL COMPARISON BETWEEN OPTIMAL CRUSHING SEQUENCES AND CONE CRUSHERS

Optimization of interparticle crushing has been conducted for a variety of different fitness functions (i.e. optimization objectives). Figure 19 presents the optimization results for four different materials for which the product yield of the theoretical size fraction of 2-5 mm material has been optimized from a monosized fraction of 8-11.2 mm material (see Eq.(14)). As can be seen, the optimal crushing sequences for the different rock materials differ from one another. These dissimilarities are explained by the different compressive breakage behaviors of the materials. For instance, the results show that marble, which is more brittle than the other rock materials, should be crushed with fewer and larger compressions. This is consistent with prior practical experiences with the material in which the material has been perceived as more easily crushed while generating a finer product. Likewise, the longer crushing sequence indicated for quartzite seems plausible as the rock material is perceived as harder than the other studied materials. For gneiss and diabase, on the other hand, the perceived similarities through practical experiences would probably explain the similarities between the crushing sequences. In the same way, the larger toughness perceived in diabase might explain its larger final compression. It should be noted, however, that these optimal crushing sequences would change, should the feed size distributions greatly change.

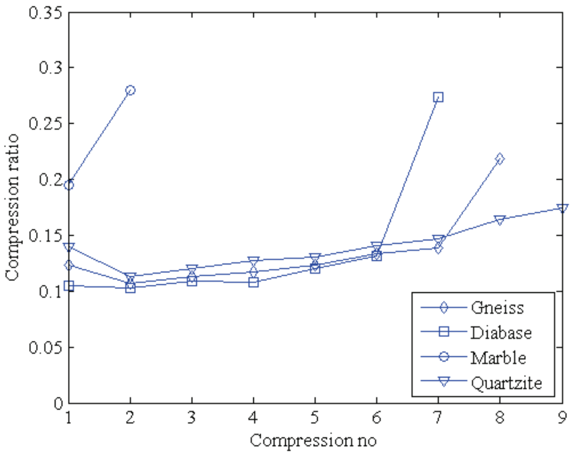

Figure 19. Optimal crushing sequences for the 2-5 mm product yield for gneiss, diabase, marble, and quartzite.

$$\varphi_{\text{Yield}} = \frac{[\text{Capacity, i.e. rel. amount of 0-5 mm}]\times[\text{Rel. amount of 2-5 mm}]}{[\text{Rel. amount 0-2 mm}]} \qquad (14)$$

As shown in Figure 19, with the exception of the initial compressions of the crushing sequences for gneiss and quartzite, the compression ratio increases along the crushing sequence. This gradual increase of compression ratio is explained by the breakage probability of the materials (i.e. the selection value), which generally decreases with a growing fraction width but increases with an increasing compression ratio. As the fraction width of a sample generally increases along a crushing sequence, a gradually increasing compression ratio is required in order to maintain a given breakage probability.

In contrast, the slightly larger initial compressions of gneiss and quartzite are probably needed to generate wider size distributions, which enable more diverse size reduction processes. This can be compared to the significantly larger final compressions of gneiss, diabase and marble, which can be applied as the amount of by-product will not increase by further compressions.

Comparison with the described crushing process of a cone crusher shows that the general trend of gradually increasing compressions is shared by the theoretically optimal crushing sequences as well as the real crushing process. Further comparison also shows that larger compression ratios are applied in modern cone crushers than in the optimal crushing sequences. This means that, in terms of the studied aspects, smaller compressions should be applied in order to increase product yield. Slightly larger initial compressions and considerably larger final compressions are also indicated for some materials. However, due to current design, these features cannot easily be achieved in existing cone crushers.

To validate the presented optimization results, laboratory crushing tests were conducted. Testing was performed using material from the same batch of 8-11.2 mm particles used for the material characterization of interparticle breakage. Similar to during the characterization testing, samples were compressed, sieved, remixed, and recompressed according to predefined crushing sequences. The results from these crushing tests are shown in Figure 20. Both theoretically calculated and experimental data are shown in the figure for comparison.

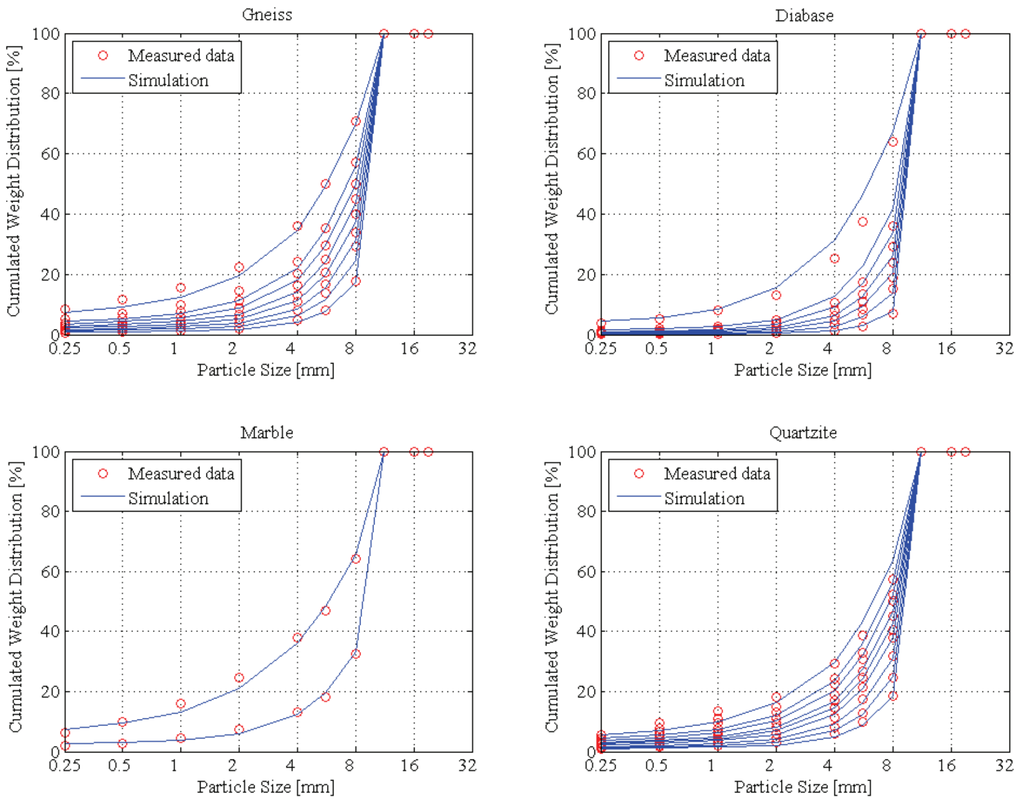

Figure 20.Simulated model predictions and measured data from validating laboratory crushing tests.

As can be seen, the measured data generally agree with the simulated model predictions. The minor discrepancies, which can be found in the smaller particle sizes for gneiss, are believed to be caused by the material's breakage function. This can be compared with the deviations found in the coarser particle sizes for diabase, which are believed to be caused by the material's selection function. For quartzite, on the other hand, the cause of discrepancy is probably a combined effect of the material's breakage and selection functions. In addition, it is also likely that some discrepancies are caused by the flakiness of the crushed particles. Since flaky particles tend to appear as larger during sieving than during simulation and optimization [4], the presence of flaky particles will probably give rise to deviations between measurements and simulations. Nevertheless, the correlation between the measurements and their model predictions validates the presented optimal crushing sequences for product yield.

Optimizations have also been carried out for minimizing energy consumption. Figure 21 shows the results of these optimizations, where the energy consumption was optimized against the amount of product (i.e. the 2-5 mm material) as well as the process capacity (i.e. the amount of 0-5 mm material). As can be seen, marble should preferably be crushed by a single large compression much like the crushing process in e.g. HPGRs, whereas the rest of the materials (i.e. gneiss, diabase, and quartzite) should be crushed by six to nine significantly smaller compressions. More specifically, the compression series for gneiss and quartzite both contain gradually increasing compressions, whereas the crushing sequence for diabase consists of slightly decreasing compressions. The results thus indicate that not all materials should be crushed by crushing sequences with gradually increasing compressions as applied in existing cone crushers. Similar to the optimization results of product yield, the study shows that larger compression ratios are applied in modern cone crushers than in the optimal crushing sequences for gneiss, diabase, and quartzite.

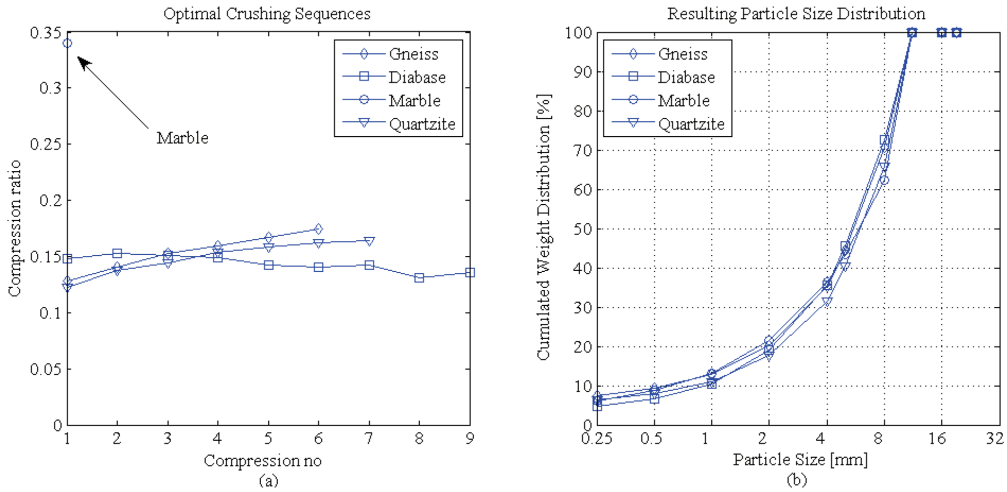

Figure 21(a). Optimal crushing sequences with respect to optimized energy consumption for the studied gneiss, diabase, marble, and quartzite (b). Resulting particle size distributions from the different crushing sequences.

PERFORMANCE OF THE INTERPARTICLE CRUSHING ZONE IN CONE CRUSHERS

To evaluate the performance of the interparticle crushing zone in cone crushers, the effects of the normally subsequent single particle compressions must be either identified or eliminated. One way of accomplishing this is to modify a cone crusher by e.g. shortening the crushing chamber, so that the size reduction is almost exclusively attributed to interparticle breakage. By using measured data from such a cone crusher, a direct comparison can be made between measured crusher output and simulated output from a theoretically optimal crushing sequence.

Figure 22 shows the measured output from an interparticle cone crusher and the simulated output from the optimized crushing sequence of 2-5.6 mm product yield (for definition, see Eq.(15)). Also shown in the figure is the measured feed size distribution, which was fed to the real application and applied in the performed optimizations. The results of these optimizations, which were carried out for the same gneiss as in the real application, are presented in Table 7 along with the crusher output. As can be seen, the relative amount of the 0-2 mm by-product is significantly larger in the theoretically optimized output. This is due to the definition of product yield as fitness function, as differences in economical value between the different size fractions have not been taken into account. The results also show a considerably larger relative amount of the desired 2-5.6 mm product in the theoretically optimized output. This combined with a larger relative amount of 0-5.6 mm material, which can be considered as a measure of capacity, results in a product yield almost threefold that of the real crusher. The results thus indicate that the interparticle crushing in the studied cone crusher is not optimal in terms of the studied aspect. Instead, the optimal crushing sequence consisting of a single compression at roughly 0.35 in compression ratio suggests that given the feed size distribution width and the desired reduction ratio, crushing should either be performed using both breakage modes or by applying a single large interparticle compression.

$$\varphi_{\text{Yield}} = \frac{\left[\text{Capacity, i.e. rel. amount of 0-5.6 mm}\right]\times\left[\text{Rel. amount of 2-5.6 mm}\right]}{\left[\text{Rel. amount 0-2 mm}\right]} \tag{15}$$

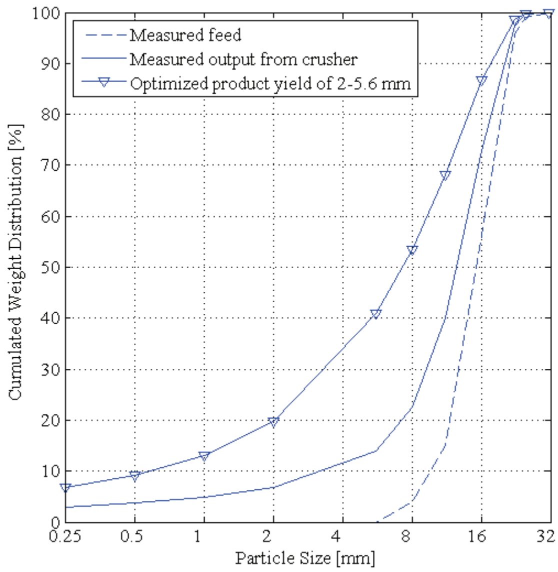

Figure 22. Comparison between the measured output from an interparticle cone crusher and the simulated output from the optimized crushing sequence with respect to 2-5.6 mm product yield.

Table 7. Values of the different outputs in Figure 22.

	Relative amount of by-product 0-2 mm [%]	**Relative amount of 2-5.6 mm [%]**	**Capacity, i.e. relative amount of 0-5.6 mm [%]**	**Product yield of 2-5.6 mm (Eq.(15))**
Real crusher	6.80	7.10	13.9	14.5
Optimized product yield of 2-5.6 mm	19.9	21.1	41.0	43.6

7.2 CRUSHING PROCESSES IN REAL APPLICATIONS

Having showed that the interparticle crushing in modern cone crushers is not optimal, the crushing process in real cone crushers consisting of both interparticle and single particle crushing is studied. Full scale experiments as well as theoretical optimizations and simulations of model predictions are performed in order to gain knowledge and insight into the crushing process of a real cone crusher.

PARAMETER STUDY OF A CONE CRUSHER APPLICATION

A set of full scale experiments was conducted on a Sandvik CH430 cone crusher, which was equipped with a modified crushing chamber. A parameter study of the eccentric speed, Closed Side Setting (CSS) and stroke was carried out during which a 10-50 mm size fraction of gneiss from Southern Sweden was used. Feed samples as well as belt cuts of test samples were periodically taken throughout testing.

The test results obtained for different CSS at the eccentric speed of 288 rpm and 36 mm stroke are shown in Figure 23. As can be seen, the results clearly indicate that different distribution curves are obtained for different CSS values. The distribution curves shift towards larger particle sizes as the CSS increases. This well-known effect [18] is partly due to the increase of top size following an increased CSS, and partly due to the overall smaller size reduction which an increased CSS entails.

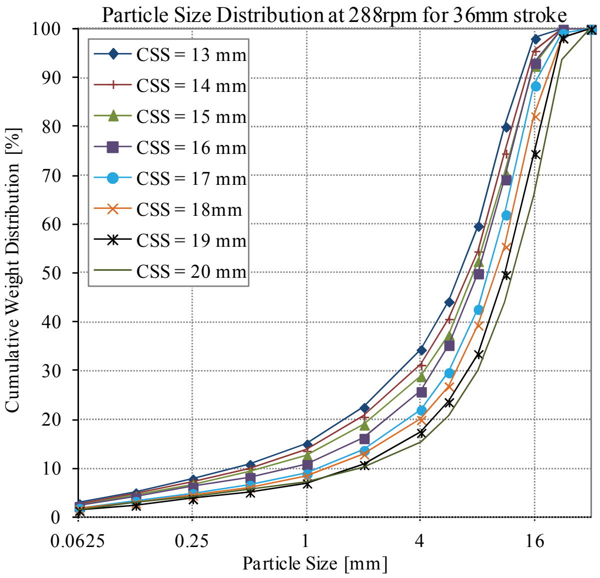

Figure 23. Crusher output for different CSS at 288 rpm and 36 mm stroke.

Figure 24 presents the results obtained for different eccentric speeds and CSS at 36 mm stroke. As shown, the amount of size reduction decreases as the CSS increases. This is seen for all size fractions and can be compared to that of an increasing eccentric speed. According to Evertsson [4], the general increase of size reduction at the increase of eccentric speed can be correlated to the number of crushing zones in the cone crusher. The results thus indicate that the number of crushing zones in a cone crusher increases with the eccentric speed.

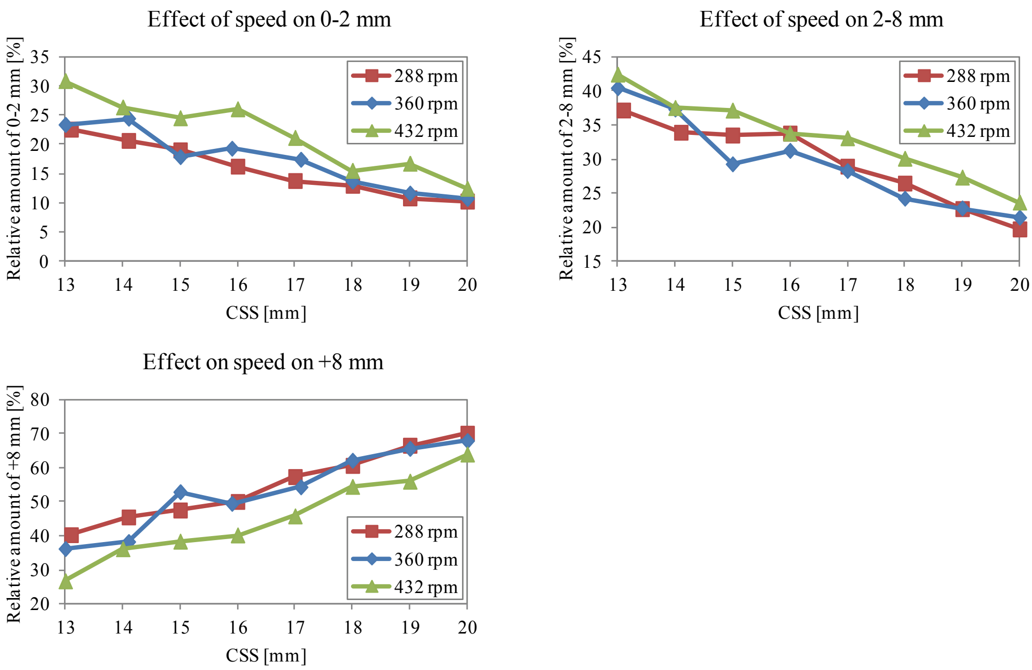

Figure 24. Test results illustrating the effects of eccentric speed on crusher output at 36 mm stroke.

Figure 25 shows the effects of eccentric speed on the product yields of the 2-8 mm and the 2-16 mm products respectively. Comparisons between the product yields of the same product show that, within the studied range of the CSS, the 2-16 mm product yield generally benefits from a reduced eccentric speed, whereas the 2-8 mm product yield does not. This suggests that, in terms of the studied 2-16 mm product yield, fewer compressions should be used than those applied at the standard eccentric speed of 360 rpm. Moreover, although the 2-16 mm product yield seems to have an optimal CSS, which depends on the eccentric speed, a general increase can be observed at increasing CSS within the studied range. In comparison, a negative trend can be seen for the 2-8 mm product yield. This indicates that a reduced eccentric speed and an increased CSS are generally favorable in the studied aspect of the 2-16 mm product yield, but not in the studied aspect of the 2-8 mm product yield.

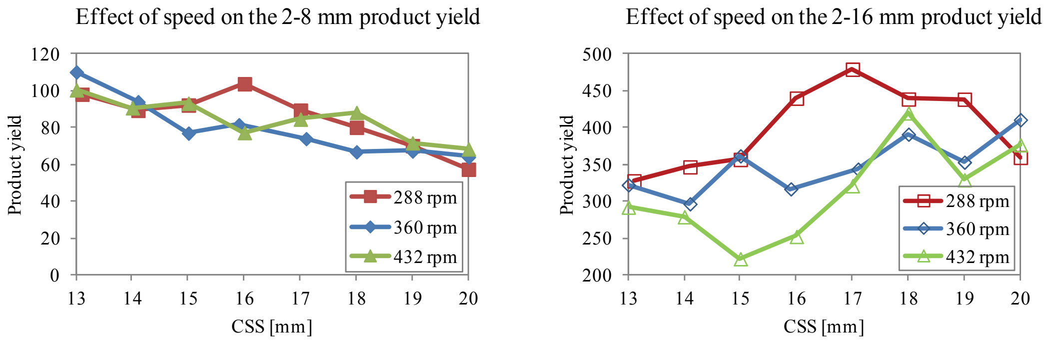

Figure 25. Effects of eccentric speed on the product yields obtained for the studied application at 36 mm stroke.

The effects of stroke on crusher output and performance are shown in Figure 26. As can be seen, the difference in stroke at the eccentric speed of 288 rpm seems to mainly affect the relative amount of 0-2 mm material, which increases as the stroke decreases. This increase also seems to decline with an increasing CSS, which suggests that the effect of stroke decreases for larger CSS. Further comparisons between the different 2-8 mm product yields indicate that the larger stroke is favorable in terms of the studied aspects and application. This is mainly due to the smaller relative amounts of the 0-2 mm material generated by the larger stroke. This, combined with the larger relative amounts of oversized +8 mm material at certain CSS, suggests that the actual size reduction of the larger stroke is smaller in this case than that of the smaller stroke. In other words, it would seem that the intuitive knowledge that a larger stroke implies an increased compression ratio as well as size reduction is not always valid. In fact, it is believed that the parameter stroke affects crusher dynamics, thereby making the effects of an altered stroke more difficult to predict. These dynamical effects might also explain why different eccentric speeds seem optimal depending on the CSS.

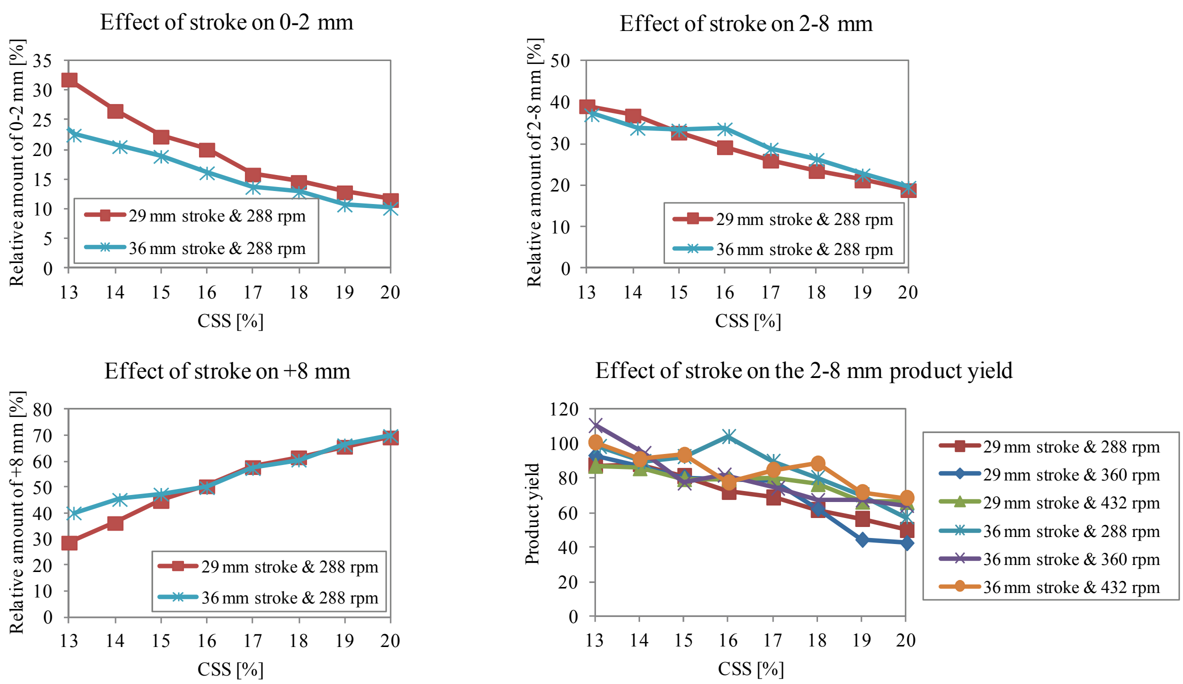

Figure 26. Test results illustrating the effects of stroke on crusher output and performance.

PERFORMANCE OF REAL APPLICATIONS

The performances of two existing applications have been studied. These include the application examined by Evertsson [4] in his full scale experiments (henceforth referred to as *application I*), and an aggregate application run outside Gothenburg in Sweden (henceforth referred to as *application II*). Both applications were assumed to be fed with gneissic rock materials, which at the time of the study happened to have different feed size distributions of 10-45 mm particles.

Table 8 and Figure 27 present the measured data from *application I*. As can be seen, the largest relative amounts of both 2-8 mm and 0-8 mm material can be found in the samples with the smaller CSS. In fact, the largest relative amounts of both size fractions can be found in sample 5, i.e. the measurement with the highest eccentric speed and the smallest CSS. Further comparison also shows that the same sample, with a value of 163, has the largest 2-8 mm product yield despite its larger relative amount of 0-2 mm material.

Table 8. Specifics from application I [4].

	Sample 1	**Sample 2**	**Sample 3**	**Sample 4**	**Sample 5**	**Sample 6**
Speed [rpm]	269	269	360	360	429	429
CSS [mm]	8	12	8	12	8	12

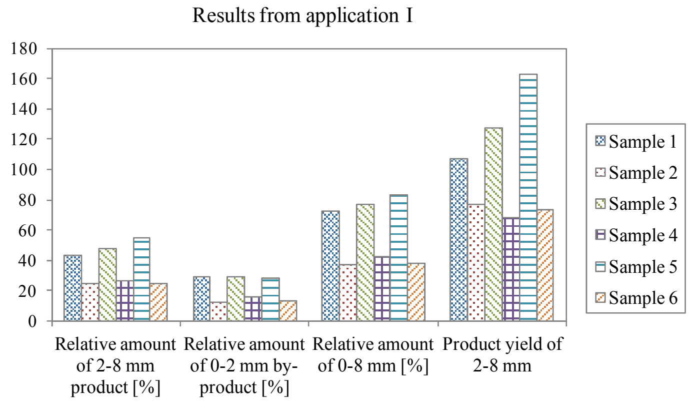

Figure 27. Data and results from application I [4].

Presented in Figure 28 is a typical product size distribution of *application II*, which has the task of producing several products sorted by particle size. The assumed market situation in Table 9 implies that everything produced (even the 0-2 mm size fraction commonly referred to as the by-product) can be sold, but to different economical values. Thus, in order to fairly determine the performance of the application, the product yield is balanced with regards to the different product values. This balanced product yield can be considered as a measure for the relative value of the desired products and capacity per generated unit of by-product (see expression in Table 6). For *application II*, this balanced product yield amounts to 3989, which can be compared to a corresponding value of 659 for the best sample (i.e. sample 5) in *application I.* The large difference in value can be explained by the significantly larger amount of 0-2 mm material, which is more than four times larger in the sample of *application I* than in *application II*.

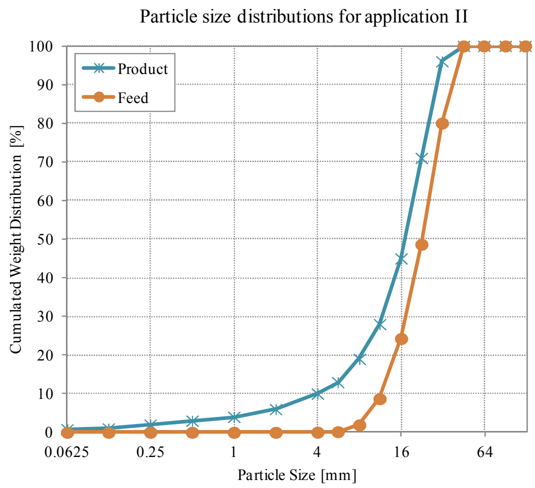

Figure 28. Particle size distributions for application II describing the production at the time of the study.

Table 9. Assumed market situation for application II.

Product	Assumed market value v_i
16- 31.5 mm	70 SEK/unit
11.2- 16 mm	90 SEK/unit
8-11.2 mm	90 SEK/unit
5.6-8 mm	110 SEK/unit
2-5.6 mm	130 SEK/unit
0-2 mm	30 SEK/unit

THEORETICAL OPTIMIZATIONS OF REAL APPLICATIONS

Theoretical optimizations of the previously described *applications I* and *II* have been performed. More specifically, crushing sequences consisting of both interparticle and single particle compressions have been optimized with respect to product yield. Similar to a real crushing process, the optimized crushing sequences begin with interparticle crushing before transitioning to single particle crushing. Table 10 shows the predetermined proportions of breakage modes, which have been applied along with an assumed sequence length of 10 compressions[4] in order to limit the computational time (typically a couple of days instead of weeks).

Table 10. Number of interparticle and single particle compressions in the different optimizations.

	Case I	Case II	Case III	Case IV
#IP compressions	2	4	6	8
#SP compressions	8	6	4	2

As can be seen in Figure 29, the optimization results for both applications differ depending on the proportion of breakage modes. It should, however, be noted that the optimization results for *application II* were obtained for a balanced product yield in which the product of 16-31.5 mm material (as in the real application) was replaced by the product of 16-22.4 mm. The switch of products was motivated by the large inherent amount of 16-31.5 mm material in the feed material. With more than half of the feed material consisting of a desired product, only a very small amount of crushing would be feasible. Thus, in order to allow for a slightly larger size reduction and crushing efficiency, the product of 16-31.5 mm material was replaced by the product of 16-22.4 mm particles. However, an evaluation directly based on this adjusted balanced product yield would not be fair due to the larger top size permitted in the real process. Therefore, in order to allow for a more just evaluation, the comparison between theory and reality was conducted by defining 16-22.4 mm material as the largest sized product in the optimizations, and 16-31.5 mm particles as the largest desired size fraction in the real application.

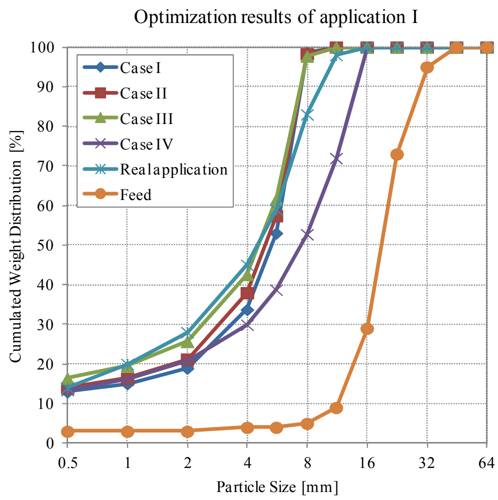

(a)

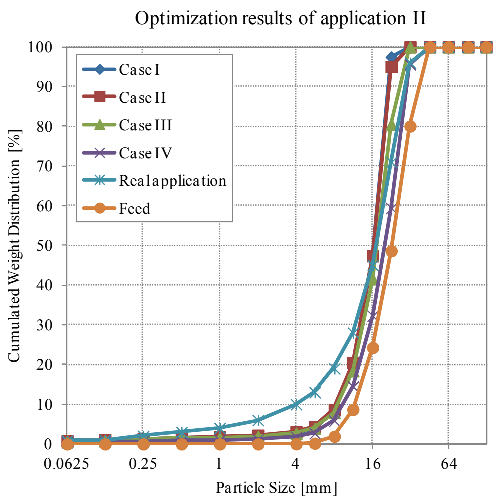

(b)

Figure 29(a). Optimization results of application I shown together with sample 5 of the real application. (b). Optimization results of application II shown together with real measured data.

[4] According to Evertsson [4], the number of compressions in a cone crusher is approximately 10 at the standard eccentric speed of 360 rpm.

The comparison of product yields in Figure 30 shows that, with the exception of case IV in *application I*, the performance of the real applications are outdone by those of the theoretically optimal crushing sequences. For *application I*, this superiority of the theoretical crushing sequences is explained by smaller relative amounts of the 0-2 mm by-product and larger relative amounts of 0-8 mm material (considered as capacity) as well as the 2-8 mm product. Similarly, the low product yield of case IV is shown to be caused by smaller relative amounts of 0-8 mm material and the 2-8 mm product. For *application II*, on the other hand, the explanation for the larger balanced product yields is foremost due to the significantly smaller amounts of the 0-2 mm by-product shown in Figure 31a. With the exception of case IV in this application (see Figure 31b-c), the optimized crushing sequences are all superior to the real application in every aspect regarding the balanced product yield.

Figure 30 also shows that the product yield in both applications decreases as the proportion of interparticle compressions increases. The results thus indicate that interparticle crushing should be kept to a minimum if product yield is to be solely considered. In fact, further analysis of the theoretically optimal crushing sequences reveals that the interparticle crushing in a majority of the sequences has extremely low efficiency and is almost negligible. This is due to the low interparticle compression ratios generated by the optimization routine as the most optimal in the studied aspects. Considering that these small interparticle compressions all have compression ratios close to the smallest permitted value in the optimizations further indicates that interparticle crushing should be kept to a minimum in the studied applications.

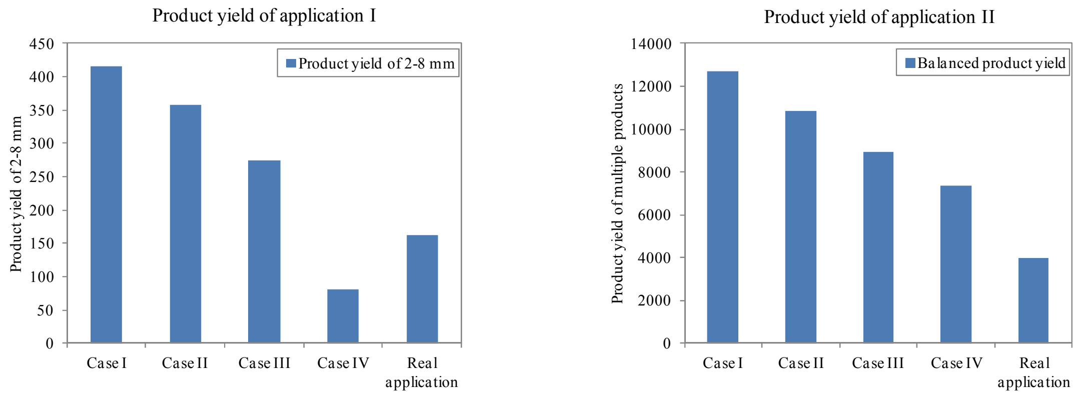

Figure 30. Product yields of the theoretically optimal crushing sequences and the real applications in applications I and II.

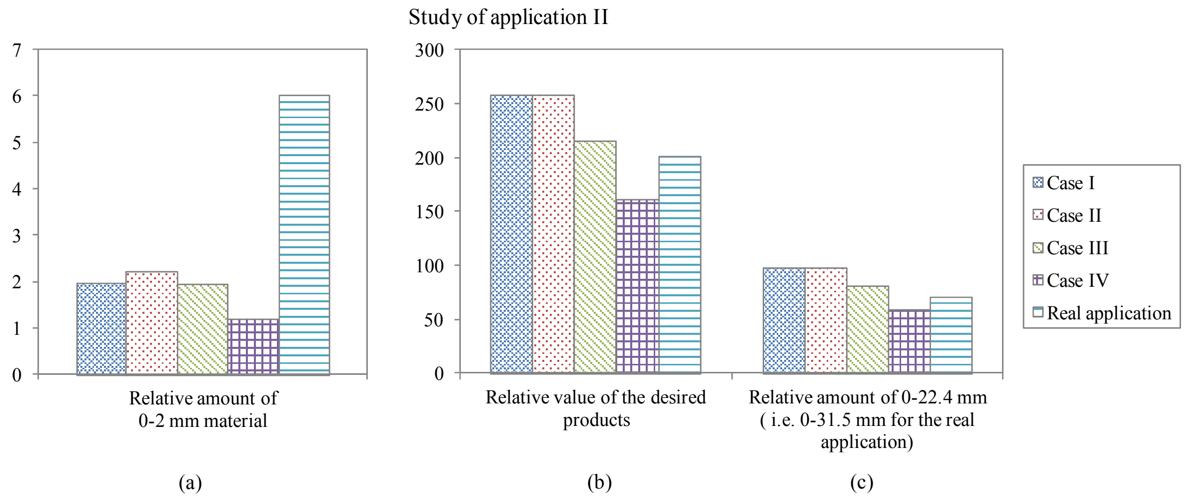

Figure 31. Results of the theoretically optimal crushing sequences in application II compared to corresponding data of the real application.

PERFORMANCE EFFICIENCIES OF REAL APPLICATIONS

While the performance of a real application can be measured in terms of its p_{80} or product yield, these measure do not reveal how well the application operates in relation to what is theoretically optimal. In order to obtain such a measure, the performances of the real application and its theoretically optimal counterpart must be compared to one another. One way of going about this is to determine a so called performance efficiency. By determining the ratio of the performance of the real application and its theoretically optimal counterpart, the so called theoretical performance efficiency of the application $\eta_{\text{real/theory}}$ can be determined.

The evaluation of *application I* in terms of its theoretical performance efficiency for product yield is shown in Eq.(16), where the values of optimization case I (see Figure 30a) has been used as reference.

$$\eta^{\text{I}}_{\text{real/theory}} = \frac{\varphi_{\text{real}}}{\varphi_{\text{theory}}} = \frac{163}{416} \approx 0.40 \tag{16}$$

As can be seen, the evaluation indicates that the theoretical performance efficiency of *application I* only amounts to ~40 %. The product yield of *application I* can, in other words, in theory be more than doubled. Visually, in terms of the particle size distribution, this means a steeper distribution curve with a smaller top size.

Eq.(17) shows the corresponding theoretical performance efficiency $\eta^{\text{II}}_{\text{real/theory}}$ of *application II* (see Figure 30b for the theoretical reference value). This evaluation, using the results of optimization case I as reference, clearly shows that the real application is not optimal in terms of the studied aspects of balanced product yield. In fact, it indicates that the real application achieves less than half of the balanced product yield of the theoretically optimal crushing sequence. In terms of particle size distributions, this means that the distribution curve of the application can in theory be slightly rotated to increase the steepness of the curve.

$$\eta^{\text{II}}_{\text{real/theory}} = \frac{\varphi_{\text{real}}}{\varphi_{\text{theory}}} = \frac{3989}{12721} \approx 0.31 \tag{17}$$

With theoretical performance efficiencies of 40 % and 31 % respectively, great improvement potential is indicated in both applications I and II. However, it is also conceivable that technical and mechanical restraints might prevent practical implementations from gaining such large improvements. In such situations, a so called mechanical performance efficiency can instead be considered. This mechanical performance efficiency would provide a measure of the mechanical performance of existing equipment in relation to what is theoretically optimal. In other words, one would consider the extent to which existing equipment can be altered in order to mimic a theoretically optimal crushing sequence. This can be compared to a practical performance efficiency, which would regard the practical restraints of existing equipment compared to the present mechanical restraints.

8 CRUSHING CONCEPTS

The aim of this chapter is to:

- *Present different concepts of how to apply compressive crushing*
- *Investigate how compressive crushing should optimally be performed in the studied crushing concepts*
- *Evaluate the different crushing concepts*

In the applied model of compressive crushing, the crushing process is described by a series of consecutive compressions. So far, theoretical optimizations have been conducted without any considerations to crushing chamber geometry, or how the compressions should be carried out. The reason for this was to allow for an unbiased and machine independent development of fundamental knowledge. However, as the objective is to develop approaches to compressive crushing, different concepts of how to apply compressive crushing will now be examined. An overview of the proposed possible crushing concepts is presented in Table 11. As can be seen, different sets of parameters such as the number of compressions, the system stroke, the (system) bed height, and the system compression ratio are optimized in each concept. It should be noted that the system stroke and system bed height correspond to a stroke and a bed height in an imagined crushing chamber. They should therefore not be confused with the stroke experienced by an individual particle, nor with the bed height of the particle (see Figure 12). Similarly, the system compression ratio (i.e. the interparticle compression ratio) is not identical to the single particle compression ratio experienced by an individual particle.

Table 11. Overview of the examined crushing concepts.

Crushing concept	System stroke	Bed height	System compression ratio	Number of compressions	Corresponds to
I	Constant	Constant	Constant	To be optimized	Plane parallel crushing chamber with constant system stroke
II	Constant	To be optimized *(indirectly through system compression ratio)*	To be optimized	Constant	Crushing chamber with constant system stroke
III	To be optimized *(indirectly through system compression ratio)*	Constant	To be optimized	Constant	Crushing chamber with constant bed height
IV	To be optimized	To be optimized *(indirectly through system compression ratio and system stroke)*	To be optimized	Constant	Crushing chamber with varying system stroke and bed height

Table 11 presents four different possible crushing concepts of compressive crushing. One could also easily consider yet another crushing concept, where all of the parameters are optimized. However, since such an optimization would require an extensive increase of computational time, the concept has not been included in this study.

8.1 CONCEPT I – CONSTANT SYSTEM STROKE AND BED HEIGHT

In *crushing concept I*, a constant system stroke, a constant bed height, and a constant system compression ratio are applied, thereby leaving the number of compressions (with allowed values of 0-20) as the parameter to be optimized. As indicated in Table 11, the concept can be visualized as a plane parallel crushing chamber with a constant system stroke. This implies that only effective interparticle compressions can be obtained as it is assumed that interparticle crushing precedes single particle crushing. All compressions were therefore allowed to be interparticle.

Optimizations were performed for a balanced product yield of 2-5.6 mm material (as specified in Eq.(18)) from a monosized feed fraction of 8-11.2 mm material. The results of these optimizations in Figure 32 show that the optimal number of compressions decreases with an increasing constant compression ratio. Figure 32a shows the results for gneiss compared with the corresponding optimization results when the compression ratio is allowed to vary freely. The results are compared in order to examine the possibility of replacing the more-difficult-to-implement crushing sequence containing free compression ratio with a crushing sequence containing constant compression ratio. The small difference in fitness value (i.e. less than 2 % of the balanced product yield) indicates that such a replacement can be made without significant deterioration. This is a good fact from an implementation point of view. Similar results are also found for the studied diabase, marble, and quartzite, as well as for the corresponding optimizations for energy consumption (see Table 6).

$$\varphi_{\text{Balanced\_yield}} = \frac{\left[\text{Capacity, i.e. rel. amount of 0-5.6 mm}\right] \times \left[\text{Rel. value } \times \text{rel. amount of 2-5.6 mm}\right]}{\left[\text{Rel. amount 0-2 mm}\right]} \tag{18}$$

Note: the assumed relative market value for 2-5.6 mm is 70/30 $\approx$ 2.33

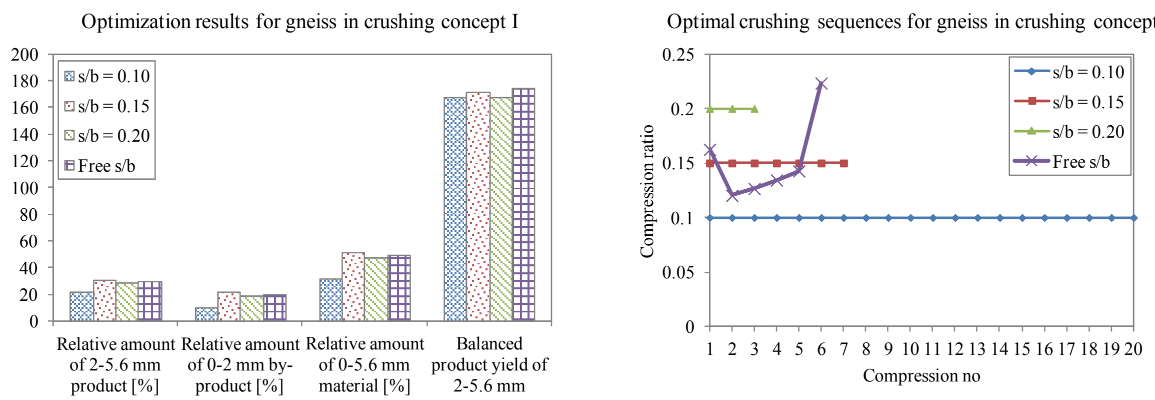

(a) (b)

Figure 32(a). Optimization results for the studied gneiss in crushing concept I together with the corresponding optimization results for varying compression ratios. (b). Corresponding crushing sequences to the results in (a).

8.2 CONCEPT II – CONSTANT SYSTEM STROKE

Crushing concept II, which can be visualized as a crushing chamber with constant system stroke, has a constant number of compressions (set to 10) and a constant system stroke. This means that the parameters to be optimized in this concept are the system compression ratio and (indirectly) the bed height. As the bed height is allowed to vary, effective interparticle as well as single compressions can be obtained as opposed to the optimizations of *crushing concept I*. Each simulated crushing sequence was therefore assumed to have four interparticle and six single particle compressions. This roughly corresponds to the proportions of breakage modes determined by Evertsson [4] at different crusher settings.

Prompted by initial optimization results, which indicated that interparticle crushing should be kept constant at its smallest permitted compression ratio of 0.10, constant 0.10 interparticle compressions were assumed. The limited interparticle crushing is believed to be caused by the optimization objective to reduce fines. Figure 33 shows the results obtained for the studied gneiss at two different constant system strokes in terms of a balanced product yield.

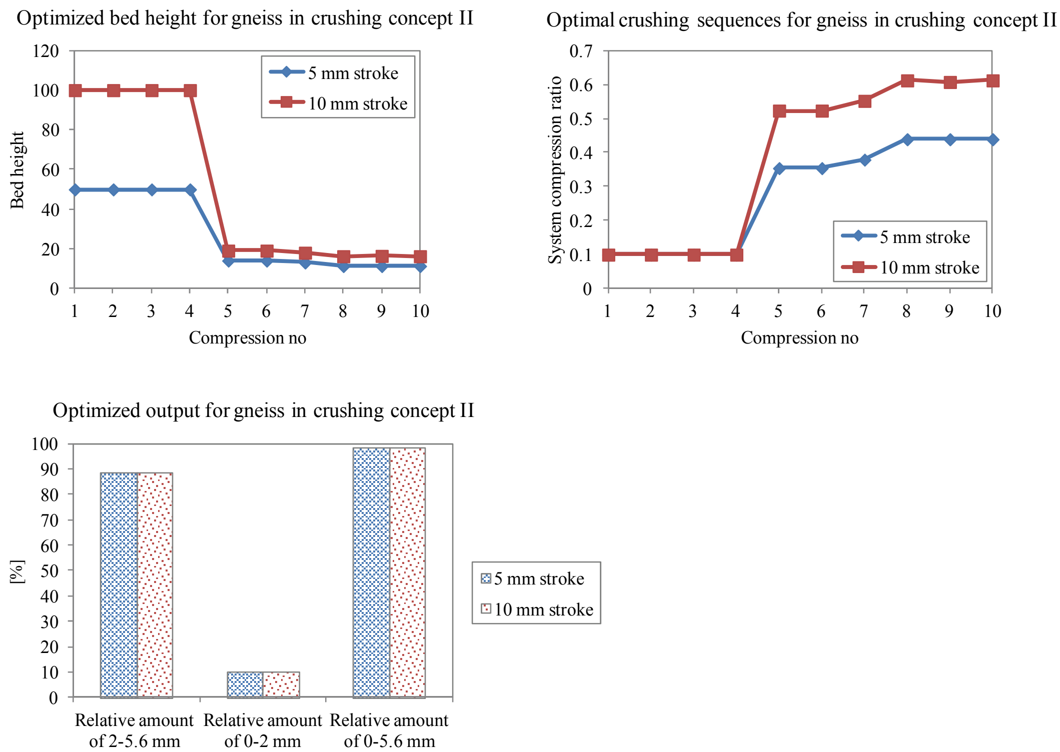

Figure 33. Optimization results for the studied gneiss in crushing concept II with respect to a balanced product yield for the constant system strokes of 5 mm and 10 mm respectively.

As can be seen, the bed height is drastically reduced at the transition of interparticle to single particle crushing, after which it continues to gradually decrease. Conversely, the system compression ratio is significantly increased after the first four interparticle compressions, and continues to generally increase throughout the remaining crushing sequence. Although, the developments of bed height and system compression ratio differ depending on the applied system stroke, analyses show that roughly the same single particle compressions are applied. As a consequence, less than 0.2 % difference can be found between the outputs as well as the balanced product yields of the different optimizations. This implies that the crushing sequences with different constant system strokes are comparable. Similar results, although with slight variations, are obtained for the studied diabase, marble, and quartzite.

8.3 CONCEPT III – CONSTANT BED HEIGHT

Balanced product yield optimizations were also performed for *crushing concept III* in which the bed height and the number of compressions are kept constant, while the system compression ratio and (indirectly) the system stroke are optimized. The results of these optimizations are shown in Figure 34. Similar to the results of *crushing concept II*, constant interparticle crushing at its smallest permitted compression ratio of 0.10 is applied. The system compression ratio is then significantly increased at the transition to single particle crushing, and continues to gradually increase throughout the remaining crushing sequence. A similar trend can be seen in the system stroke.

Moreover, comparison of the optimizations with different constant bed heights shows less than 4 % difference in output and balanced product yield. This suggests that comparable results can be achieved by crushing sequences with different bed heights. Similar results, although with slight variations, are obtained for the studied diabase, marble, and quartzite.

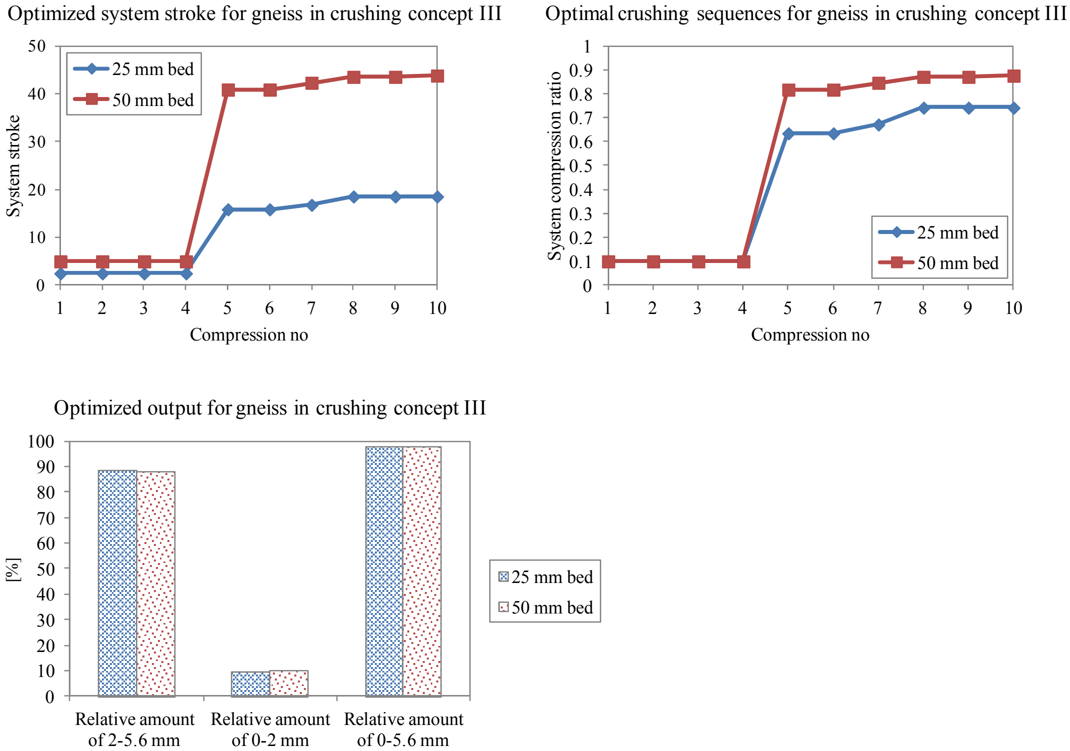

Figure 34. Optimization results for the studied gneiss in crushing concept III with respect to a balanced product yield at the constant bed heights of 25 mm and 50 mm respectively.

8.4 CONCEPT IV – VARYING SYSTEM STROKE AND BED HEIGHT

Contrary to *crushing concepts II* and *III*, the system stroke, the system compression ratio and (indirectly) the bed height are all optimized in *crushing concept IV*. The concept can thus be visualized as a crushing chamber with varying system stroke as well as bed height. Optimizations of both balanced product yield and energy optimization were carried out for the concept. The results for gneiss in Figure 35 reveal that while the interparticle compressions are kept constant at their minimum in terms of a balanced product yield, the final interparticle compression obtained for the energy optimizations is slightly larger (0.12) than the initial constant compressions (0.10). This slightly larger final interparticle compression is also found for the studied diabase, marble, and quartzite.

The small interparticle compressions in the energy optimal crushing sequences are believed to be prompted by an energy consumption, which increases with the size distribution width of the material due to an increasing pressure response. Thus, in order to minimize the energy consumption, interparticle compressions followed by further interparticle compressions should be kept to a minimum. In contrast, the final interparticle compression can be allowed to be slightly larger, since the size distribution width does not affect the energy consumption of single particle crushing. This is why the system compression ratio of the subsequent single particle compressions can be allowed to increase throughout the crushing sequence.

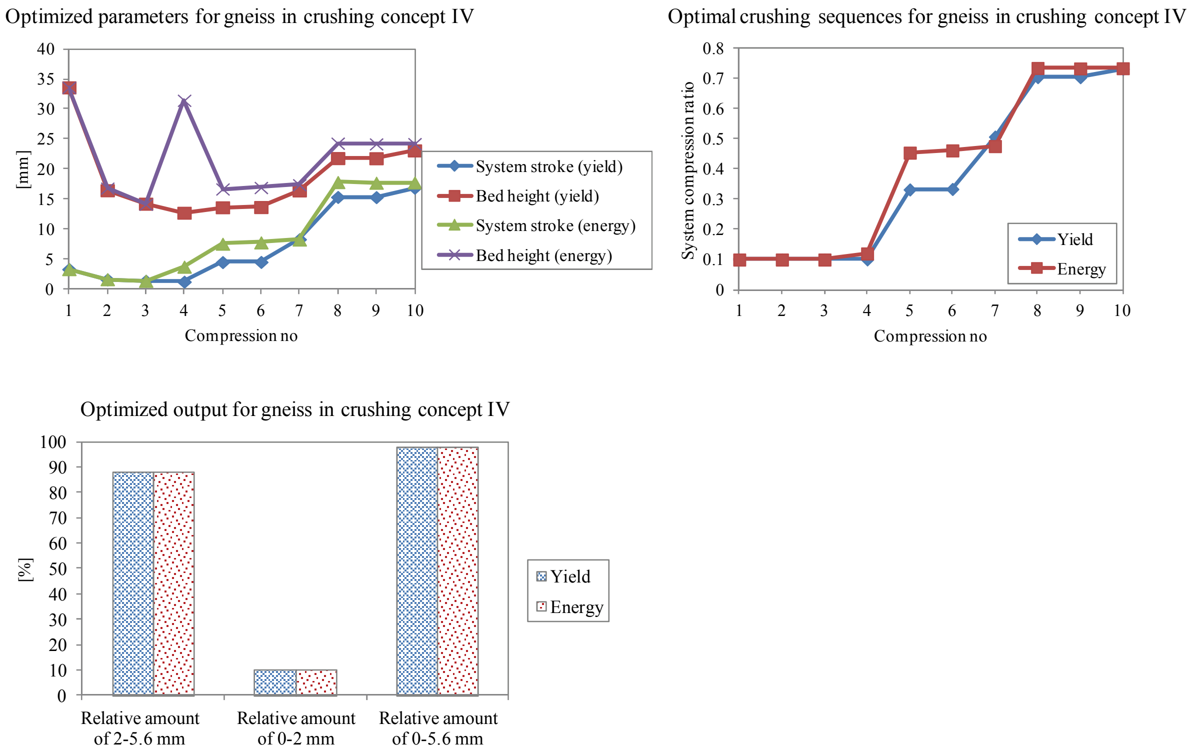

Figure 35. Optimization results for the studied gneiss in crushing concept IV.

The varying bed height and system stroke of the constant interparticle compressions of both optimizations clearly show that in interparticle crushing, only the compression ratio is considered. This means that regardless of the bed height and system stroke, the same interparticle crushing can be achieved as long as the applied compression ratio remains identical. Analysis also shows that despite the larger system compression ratio in the energy optimal crushing sequence, the applied single particle compressions in both sequences are comparable. This is confirmed by the similar outputs generated by the different sequences.

Figure 36 presents the corresponding results for the studied iron ores for which the production of 0-4 mm material has been maximized (see Table 6). Clearly, a considerable larger bed height should be applied for the interparticle compressions than for the subsequent single particle compressions. For the Donganshan iron ore, the bed height then slightly decreases for the remaining series. This can be compared to the Dagushan iron ore for which two different levels of bed height can be observed. These trends are mirrored in the system strokes of the single particle crushing for both materials. As a result, the system compression ratios of both materials generally increase throughout each crushing sequence. Comparison with the results in Figure 35 indicates that larger system compression ratios are applied in these product optimal crushing sequences, and that a larger amount of interparticle crushing is used.

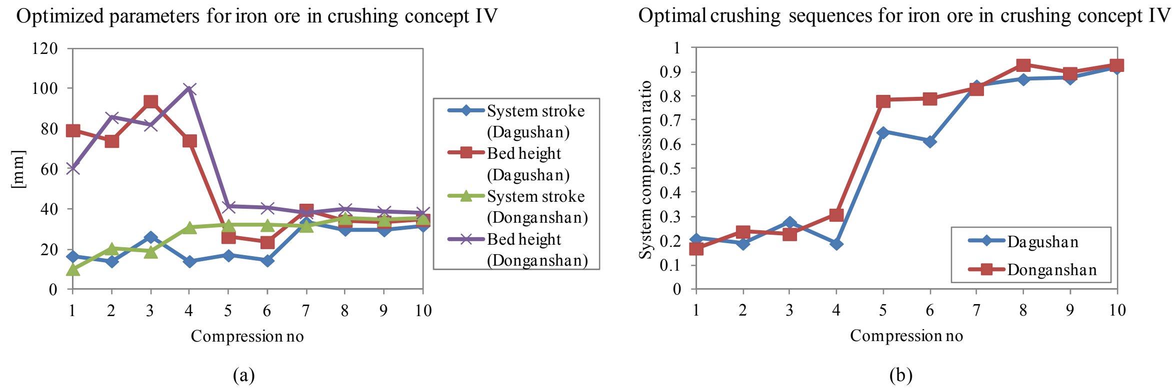

Figure 36. Optimization results for the studied iron ores in terms of a maximized production of 0-4 mm material.

8.5 EVALUATION OF CRUSHING CONCEPTS

Comparisons between *crushing concept I* and *crushing concept II-IV* indicate that significantly larger fitness values (approximately factor 10 in difference) are obtained when both breakage modes are used. In terms of product yield optimizations, this is probably due to the larger efficiency of single particle crushing in reducing top size and the smaller amounts of fines generated by the breakage mode. For energy optimizations, the presumed explanation lies in single particle crushing being more efficient in reducing top size, as well as it being more energy efficient than interparticle crushing [63]. Conversely, the downside of pure single particle crushing is likely a worse particle shape [63] and a lower process capacity [4].

Analysis of *crushing concepts II-IV* shows that less than 4 % difference in fitness value can be found for the different crushing concepts. This suggests that different approaches to compressive crushing can achieve the same results, and that the concepts are comparable.

With respect to existing cone crushers, the system stroke as well as system compression ratio (also referred to as nominal stroke [4],[60] and nominal compression ratio [4]) generally increase from crushing chamber inlet to crushing chamber outlet [4]. The increasing system stroke is due to the gyratory movement of the mantle. The amount of increase is dependent on the position of the pivot point of the movement; with a lower positioned pivot point conveying a larger increase. In crushers with suspended top bearing (like Hydrocone-type crushers), the pivot point of the gyratory movement coincides with the suspended top bearing. This can be compared to crushers without suspended top bearing (like Symons-type crushers) in which the pivot point is an imaginary point in line with the center of the main shaft above the crushing chamber. It should also be noted that when the mantle is solely supported from below (like Symons-type crushers), the forces arising from rock crushing must be mechanically dealt with in a different way than if the mantle has suspended top bearing. It is thus clear that these two different types of crushers each have their own mechanical advantages and disadvantages depending on the applied perspective.

In terms of implementation, it is evident that the results of *crushing concept II* cannot easily be implemented in Hydrocone-type crushers due to the concept's constant system stroke. However, it is conceivable that the results may be achieved in crushers without suspended top bearing. In comparison, the results of *crushing concept III* can be achieved in Hydrocone-type crushers, if one disregards the constant bed height in the interparticle crushing zone and only considers achieving the optimized interparticle compression ratio. The single particle crushing zone in the concept would, in that case, correspond to a long parallel chamber outlet with a gradually increasing system stroke. Similarly, the results of *crushing concept IV* can potentially be implemented in both types of crushers, since the system stroke as well as system compression ratio generally increase throughout the obtained crushing sequences.

9 IMPLEMENTATION

The aim of this chapter is to:

- *Present the implemented optimization results for two existing crushing applications for Hydrocone-type crushers*
- *Describe the conceptual chamber designs for Hydrocone-type crushers based on the obtained optimization results*
- *Analyze the full scale test results of the manufactured prototypes in comparison to reference applications*

In order to determine the extent to which existing cone crushers can be improved by practically implementing theoretical optimization results, an implementation study of two crushing applications (one aggregate and one mining) was conducted. An overview of this work process is depicted in Figure 37. As can be seen, the gneissic rock material, which was to be used in the full scale experiments, was initially characterized in laboratory crushing tests. The obtained mathematical models, describing the compressive breakage behavior of the material, were then applied to theoretically optimize the crushing processes of the studied applications. By subsequently translating the optimization results to crushing chamber geometries, the results were implemented in prototypes and tested in full scale experiments. To obtain comparable results, full scale experiments were also performed for the reference applications during the same occasion.

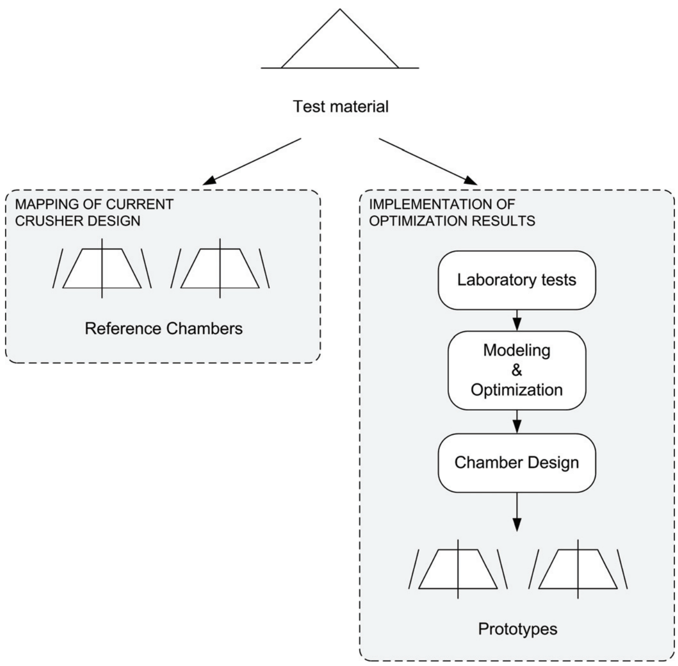

Figure 37. Illustration of the work process in the implementation study.

9.1 AGGREGATE APPLICATION

The objective of the studied aggregate application is to produce several different products with different economical values as shown in Table 12. This production situation, where the objective is to maximize the balanced product yield with respect to different product values, is described by the fitness function for balanced product yield in Eq.(19) (cf. Table 6).

Table 12. Assumed market situation for the studied aggregate application

Product	Assumed market value v_i
11.2- 16 mm	90 SEK/unit
8-11.2 mm	90 SEK/unit
5.6-8 mm	110 SEK/unit
2-5.6 mm	130 SEK/unit
0-2 mm	30 SEK/unit

$$\varphi_{\substack{Balanced\\yield}} = \frac{[\text{Capacity, i.e. rel. amount of 0-16 mm}] \times [\text{Rel. values to 0-2 mm} \times \text{ rel. amounts of desired products}]}{[\text{Rel. amount of 0-2 mm by-product}]} \quad (19)$$

The application is assumed to be fed with a 13-50 mm size fraction of the characterized gneissic rock material from a quarry in Southern Sweden. The assumed feed size distribution, which is shown in Figure 38, was calculated as a measured average of samples taken from the stockpile of test material put aside for the full scale experiments.

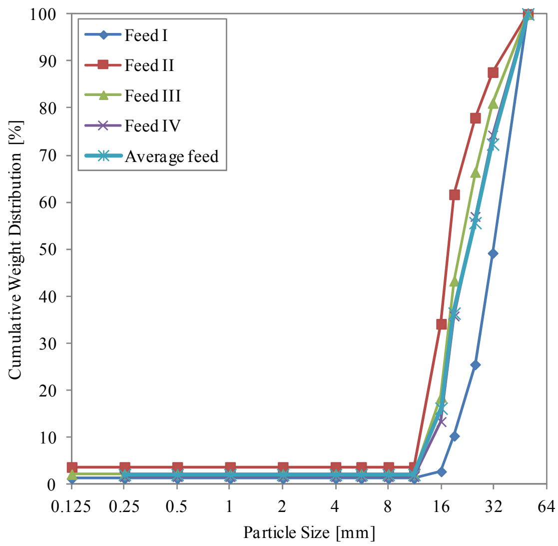

Figure 38. Assumed feed size distribution for the performed optimizations.

OPTIMIZATION RESULTS

Initial optimizations revealed that, with respect to the studied aspects, no interparticle compression should be applied. This is probably due to the larger amounts of fine material generated by interparticle crushing, as well as the better efficiency of single particle crushing in reducing top size. Although not included in the scope of this project, it should be noted that the aggregate industry often measures product quality in terms of particle shape; with a more cubical form considered as better particle shape [7]. Considering that better shaped particles are produced by interparticle crushing [63], the results seem to suggest that the size reduction process in this application should be separated from the particle shaping process.

Having concluded that the optimal crushing process for the studied application should only contain single particle crushing, optimizations of crushing sequences with up to ten single particle compressions and an unlimited system stroke were conducted. The results from these optimizations, seen in Figure 39, show that the optimal crushing sequence only has eight effective single particle compressions. More specifically, the sequence has two large (nearly even) initial system strokes, which become drastically smaller in the third compression before gradually increasing till the last compression. It should, however, be noted that since the system stroke of Hydrocone crushers increases from chamber inlet to chamber outlet, both even strokes and larger initial strokes are difficult to implement. Considering that the optimal crushing sequence only consists of a gradually increasing system stroke if the first two compressions are disregarded, new optimizations were performed for crushing sequences with an increasing system stroke. In practice, this was achieved by forcing the optimization routine to generate one system stroke at a time in each crushing sequence, while requiring each system stroke to be larger than the previous one.

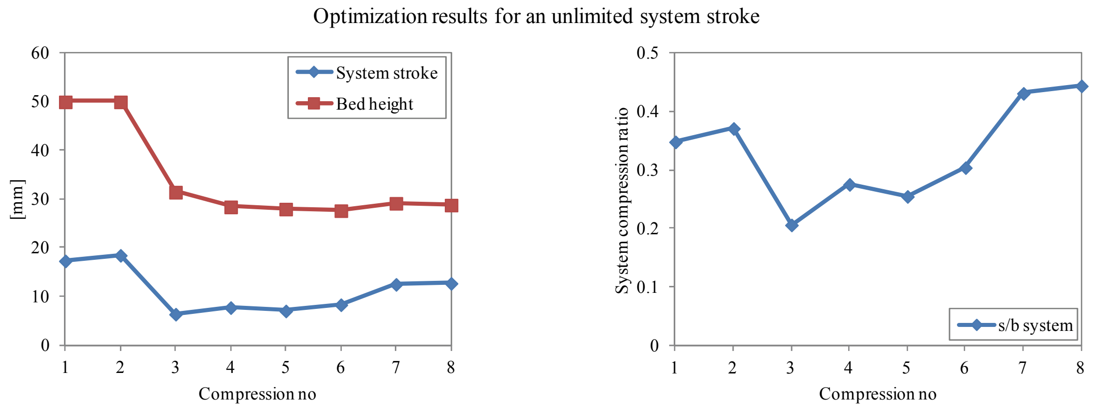

Figure 39. Optimized bed height and system stroke for the studied aggregate application with an unlimited system stroke (to the left), and the corresponding system compression ratio (to the right).

Figure 40 shows the corresponding optimization results for an increasing system stroke. As can be seen, the crushing sequence consists of nine effective single particle compressions with a gradually increasing system stroke from 17 to 36 mm. Similarly, the system compression ratio also increases progressively, which can be compared to the varying bed height that is explained by the system stroke not increasing at the same rate as the system compression ratio.

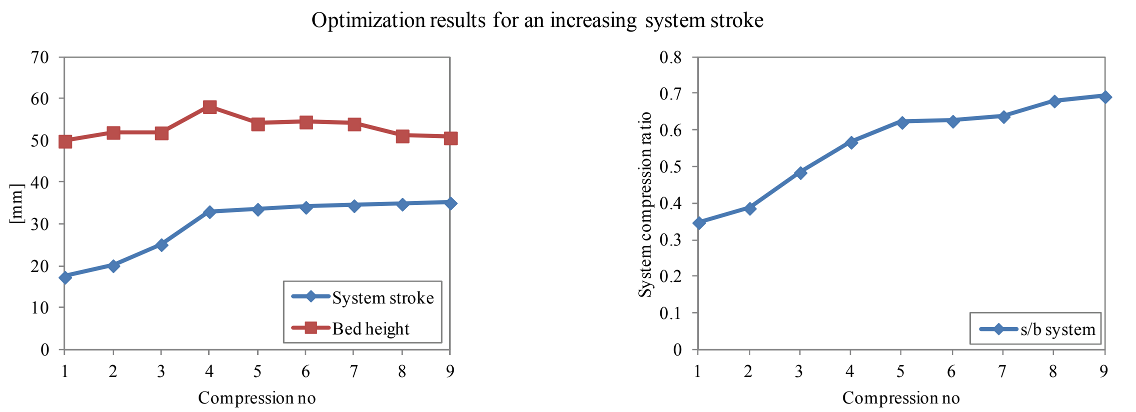

Figure 40. Optimized bed height and system stroke for the studied aggregate application when the system stroke must gradually increase (to the left), and the corresponding system compression ratio (to the right).

Comparison between the optimization results with an unlimited system stroke and those of an increasing system stroke shows that despite differences in e.g. system stroke and system compression ratio, the single particles are in fact compressed with similar single particle compressions. As a result, only a marginal difference of around 1 % can be found between the balanced product yields of the different optimized outputs. This indicates that the difficult-to-implement optimal crushing sequence with an unlimited system stroke can be replaced by the considerably-easier-to-implement optimal crushing sequence with an increasing system stroke.

CONCEPTUAL CHAMBER DESIGN

A fine crushing chamber was chosen as the reference crushing chamber for the aggregate application. As such, the geometry of the chamber was used to develop a prototype based on the obtained optimization results. Comparison between these geometries in Figure 41 shows that the chamber outlet is altered in the proposed chamber. The altered outlet should result in more cautious crushing and a reduced size reduction. Analysis of the cross sectional area of the crushing chambers also indicates that the amount of single particle breakage should increase (at the cost of interparticle breakage) as suggested by the optimization results.

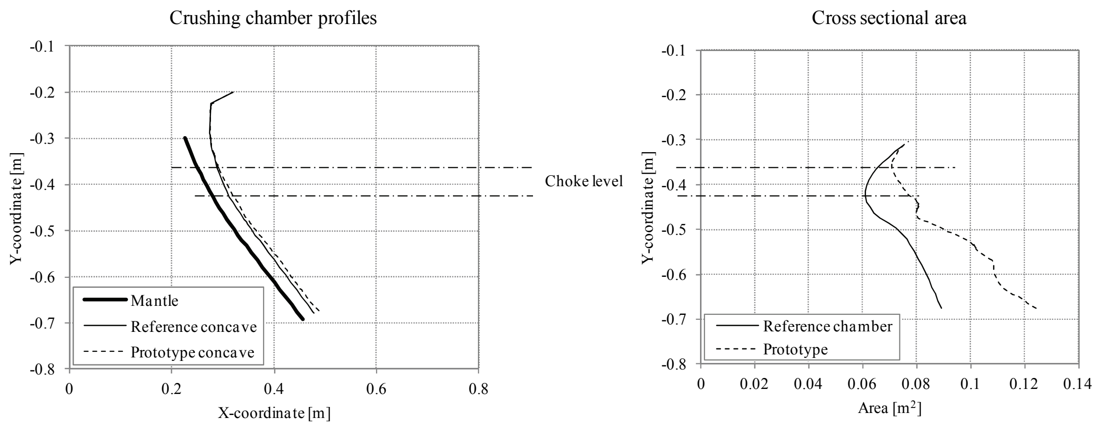

Figure 41. Illustration of the chamber geometries of the reference crushing chamber and the prototype (to the left) along with their corresponding cross sectional areas (to the right).

RESULTS OF FULL SCALE EXPERIMENTS

Full scale experiments were conducted for the prototype as well as the reference using a CH430 cone crusher in the Sandvik test facility in Dalby, Southern Sweden. Tests were carried out for five different eccentric speeds; the standard eccentric speed of 360 rpm ± 10 and ± 20 %, in CSS range of 6-16 mm. Power draw and capacity were measured throughout these tests during which test samples were taken through belt cuts. All samples were then dried in an oven before being sieve analyzed.

By using the measured outputs, the balanced product yields of the different crushing chambers could be determined as shown in Figure 42. As can be seen, the highest product yield is obtained for the prototype run at 288 rpm at a CSS of 14 mm, whereas the highest product yield for the reference chamber is obtained for an eccentric speed of 432 rpm at a CSS of 14 mm. The comparison between these product yield values shows that the product yield of the prototype is more than 5 % larger than that of the reference. The figure also shows a comparison of crusher capacity at the eccentric speed of 288 rpm. This comparison at the same eccentric speed for both the reference and the prototype was conducted to obtain a fair evaluation as different eccentric speeds imply different numbers of crushing zones. The comparison indicates that the prototype has roughly the same total capacity as the reference, but a smaller relative amount of +16 mm material. In other words, a higher balanced yield is obtained for the prototype, which has roughly the same total capacity as the reference.

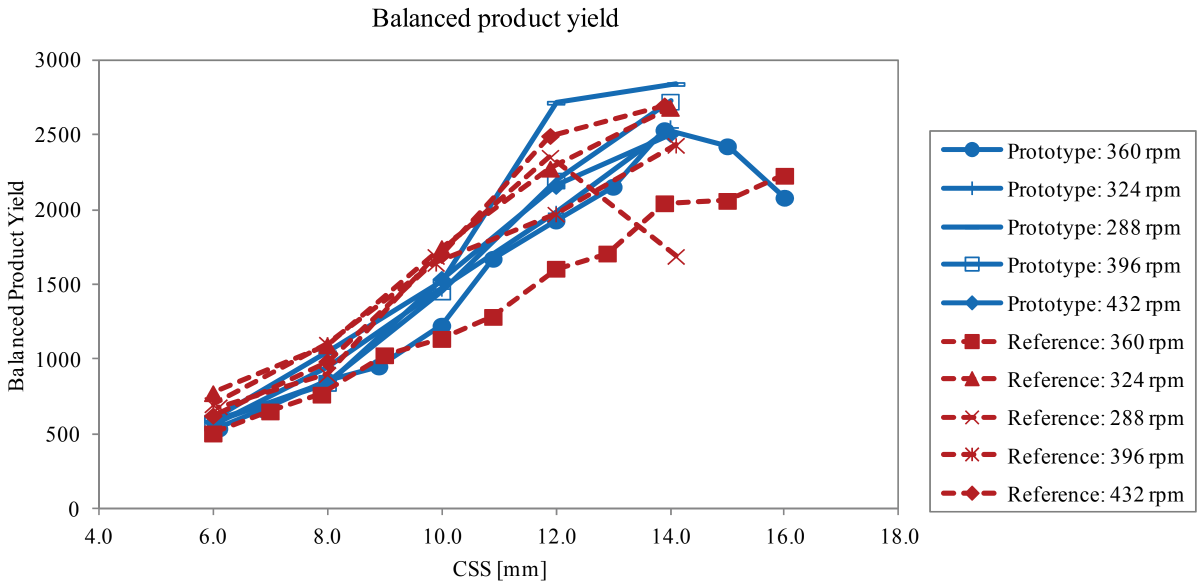

(a)

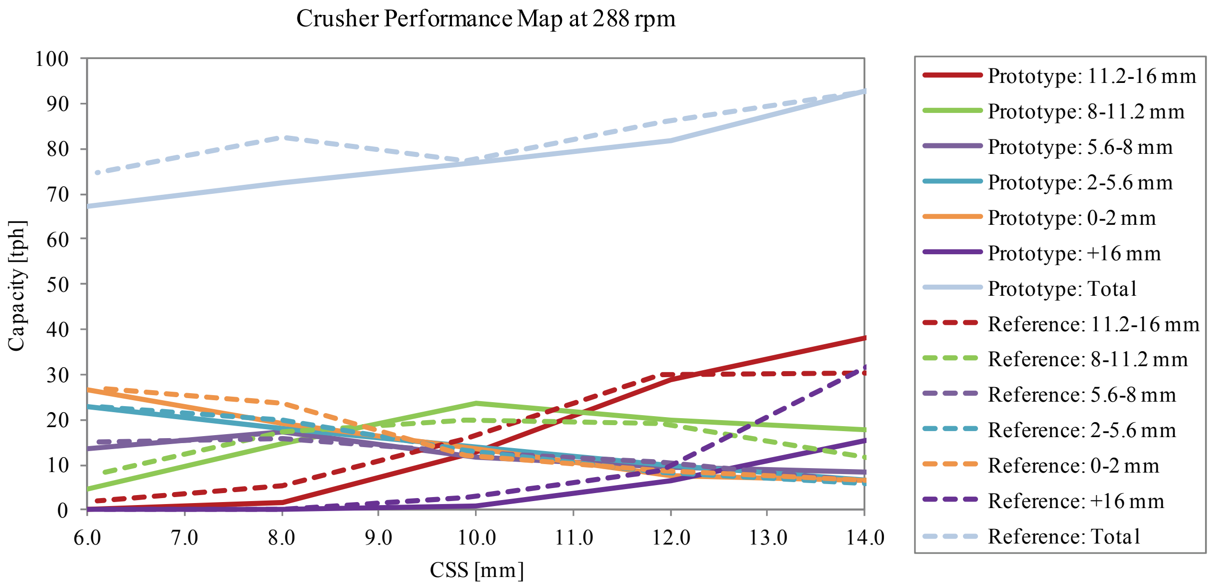

(b)

Figure 42(a). Balanced product yield for both the aggregate reference chamber and its prototype. (b). Crusher performance map comparing the reference and the prototype at 288 rpm.

9.2 MINING APPLICATION

Contrary to the studied aggregate application, the studied mining application only produces one product, namely 0-4 mm material. In other words, the optimization objective of this application is to maximize the production of 0-4 mm material, which can be formulated as in Eq.(20) (cf. Table 6).

$$\varphi_{\text{Product}} = \left[\text{Rel. amount of 0-4 mm}\right] \tag{20}$$

The application is assumed to be fed with the same feed size distribution of the 13-50 mm material shown in Figure 38.

OPTIMIZATION RESULTS

Initial optimizations indicated that both interparticle and single particle compressions should be used for the studied mining application. The use of both breakage modes is believed to be explained by the larger amounts of fine material generated by interparticle crushing, as well as the larger efficiency of single particle crushing in reducing top size. Optimizations were therefore conducted for crushing sequences consisting of four interparticle compressions and six single particle compressions. This proportion of breakage modes was chosen as it roughly corresponds to the proportions determined by Evertsson [4] at different crusher settings. The results from the optimizations, seen in Figure 43, indicate that a constant system stroke as well as constant interparticle compressions should be applied in terms of the studied aspects. However, while the constant interparticle compressions are achievable, as interparticle crushing only considers the applied compression ratio, the constant system stroke for the single particle compressions cannot easily be implemented in a Hydrocone-type construction. As a consequence, another approach was taken – optimizations with a reduced proportion of interparticle crushing were performed. This approach was motivated by the fact that the overall design aspects of a cone crusher imply a cross sectional area, which normally increases towards the outlet for fine crushing chambers. As particle beds cannot easily be formed at a gradually increasing cross sectional area, interparticle crushing is not likely to occur. Thus, by reducing the proportion of interparticle crushing, one is actually raising the choke level of a virtual crushing chamber.

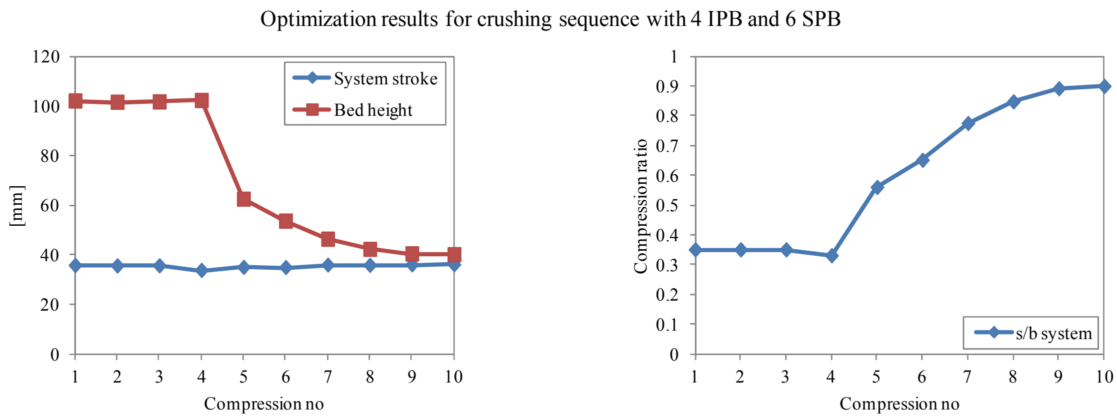

Figure 43. Optimized bed height and system stroke for the studied mining application with an assumed proportion of 4 IPB and 6 SPB (to the left), and the corresponding system compression ratio (to the right).

Reducing the proportion of interparticle crushing while maintaining the length of the crushing sequence resulted in optimizations of crushing sequences with three interparticle compressions and seven single particle compressions. Figure 44 shows the output from the best crushing sequence of the optimization results, whereas Figure 45 presents the optimized bed height and system stroke, as well as the crushing sequence itself. As can be seen, the sequence only contains eight effective compressions; one of which is interparticle, whereas the remaining seven compressions are single particle. Further analysis of the results in Figure 44 reveals that the final single particle compression is almost negligible in terms of the production of 0-4 mm material and could be disregarded without a significant deterioration in fitness value (~1 %). The benefit of disregarding this final compression is that the system stroke of the crushing sequence would then generally increase throughout the sequence as shown in Figure 45.

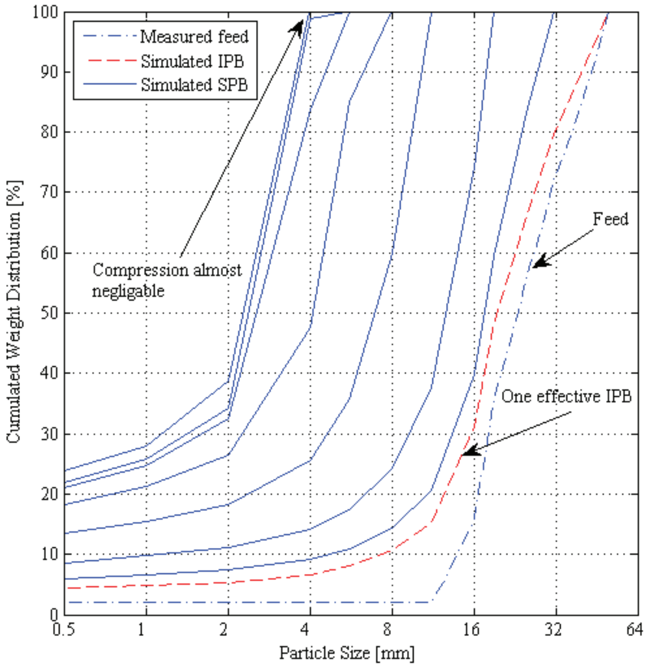

Figure 44. Output from each compression in the best crushing sequence containing 3 IPB and 7 SPB.

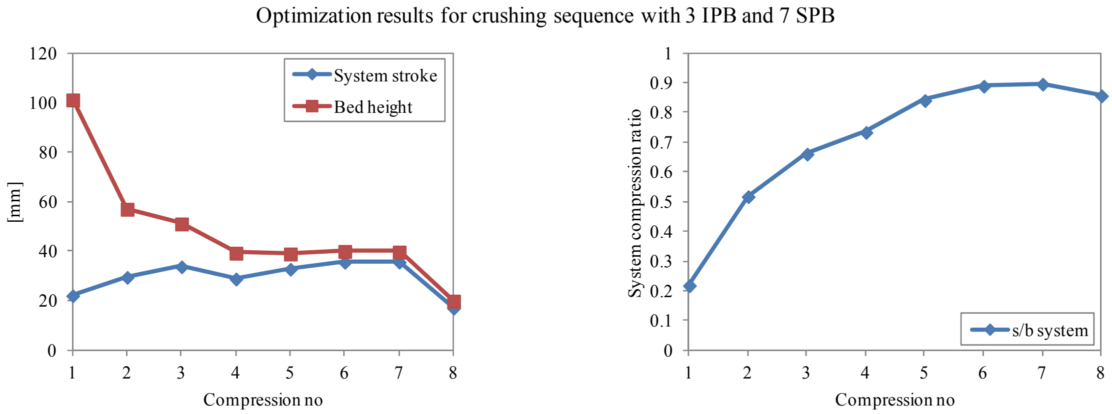

Figure 45. Optimized bed height and system stroke for the studied mining application with an assumed proportion of 3 IPB and 7 SPB (to the left), and the corresponding system compression ratio (to the right). Note only 8 compressions are effective as a result of a single effective interparticle compression.

The comparison between the optimizations with different proportions of breakage modes in Table 13 indicates that better results are obtained by crushing sequences with a larger proportion of single particle crushing. However, by removing the last compression in the crushing sequence with a larger proportion of single particle crushing, the results change in favor of the optimal crushing sequence with a smaller proportion of single particle crushing.

Surprisingly enough, the difference in fitness value is a mere 0.6 %. This can be explained by the fitness function, which only considers the produced amount of 0-4 mm material and not the p_{80}, which is lower for the crushing sequence with the larger proportion of interparticle compressions. Further comparison between the results in Table 13 also shows considerably lower energy consumption for the crushing sequences with larger proportions of single particle crushing. The explanation for this lies in the larger amount of effective interparticle compressions in the sequence shown in Figure 43. In other words, the results indicate that if size reduction is to be maximized, while energy consumption is to be kept to a minimum, a larger proportion of single particle crushing is to be applied. The easier implemented and modified crushing sequence with a larger proportion of single particle crushing was therefore chosen for implementation.

Table 13. Results of the different crushing sequences with different proportions of breakage modes.

	Relative amount of 0-4 mm	**p_{80}**	**Rel. energy consumption (ref: 4 IPB & 6 SPB)**
Sequence with 4 IPB & 6 SPB (see Figure 43)	99.4	~3.1 mm	1
Sequence with 3 IPB & 7 SPB (see Figure 45)	100	~3.2 mm	0.29
Modified sequence of Figure 45 (i.e. last SPB removed)	98.8	~3.25 mm	0.28

CONCEPTUAL CHAMBER DESIGN

The chosen existing mining reference chamber was a crushing chamber classified as extra fine (EF). Similar to the implementation in the aggregate application, the geometry of this chamber was used to develop a prototype based on the obtained optimization results. Comparisons between this reference crushing chamber and the prototype in Figure 46 show that the prototype has both a larger inlet and a smaller outlet than the original chamber. Thus, in order to determine the effects of each alteration, two prototypes were manufactured for the mining application. The difference between the reference chamber and the two prototypes (i.e. mining prototype 1 and mining prototype 2) can be summarized as in Table 14.

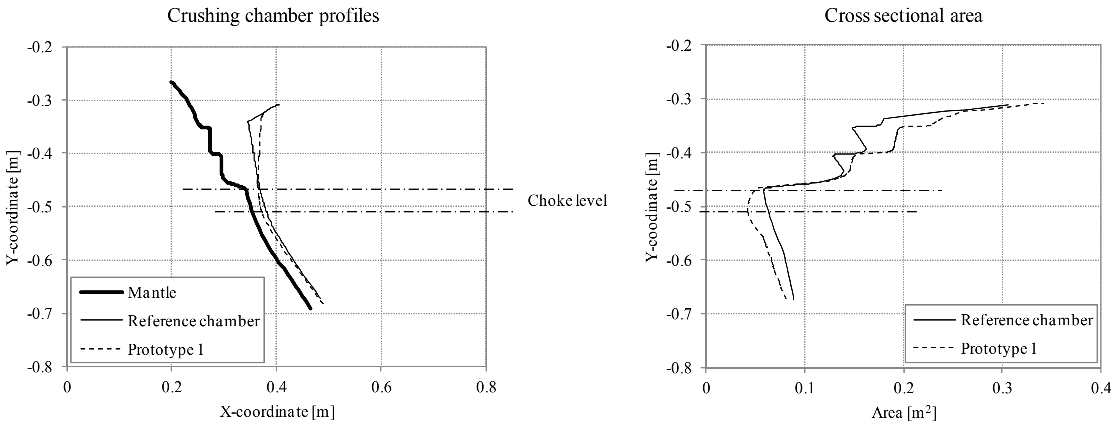

Figure 46. Illustration of the reference crushing chamber and prototype 1(to the left) along with their corresponding cross sectional areas (to the right).

Table 14. Test parameters of the mining crushing chambers.

	Changed inlet – Parameter A	**Changed outlet – Parameter B**
Mining prototype 1	X	X
Mining prototype 2		X
Reference		

Table 14 shows that the effect of parameter A (i.e. the inlet) will manifest itself as the difference between the results of mining prototype 1 and 2 as both prototypes have the same outlet. Similarly, the effect of parameter B (i.e. the outlet) can be determined by comparing the results of mining prototype 2 and the reference as both chambers have the same outlet. Finally, comparisons between mining prototype 1 and the reference chamber will show the effects of a changed inlet as well as a changed outlet.

RESULTS OF FULL SCALE EXPERIMENTS

Both the manufactured prototypes and the reference chamber were tested in full scale experiments using a CH430 cone crusher in the Sandvik test facility in Dalby, Southern Sweden. The crushing chambers were tested for five different eccentric speeds; the standard eccentric speed of 360 rpm ± 10 and ± 20 %. During these tests, parameters such as the CSS, power draw and capacity were continuously measured. Test samples were also periodically taken through belt cuts after which they were dried in an oven before being sieve analyzed.

Figure 47 and Figure 48 present the different productions of 0-4 mm material in the prototypes and the reference crushing chamber. As can be seen, the relative amount of 0-4 mm product is significantly larger in mining prototype 1 than in the reference (i.e. around 20 % larger), whereas roughly the same relative amount of 0-4 mm material is produced in mining prototype 2 and the reference. Considering that more single particle crushing occurs in mining prototype 1 than in the reference and mining prototype 2, the results thus successfully affirm the optimization results indicating that more single particle crushing should be applied if the size reduction is to be maximized.

In terms of power draw, it is shown that, in comparison to the reference chamber, a significantly larger relative amount of 0-4 mm material can be achieved in mining prototype 1 at a lower power draw. Similarly, roughly the same relative amount of 0-4 mm product can be obtained in mining prototype 2 as in the reference chamber, but at a lower power draw. These comparisons between the prototypes and the reference in Figure 47 and Figure 48 clearly indicate that the reference has a power or pressure limit preventing it from being pushed further as opposed to the prototypes. However, further studies reveal that the reference chamber actually has a higher 0-4 mm capacity in terms of tons per hour due to a large drop in the total capacity of both mining prototypes (see Figure 49). This decrease in total capacity can be partly explained by the smaller cross sectional areas of the prototypes, which in turn imply smaller crusher capacities. Also, it is conceivable that the altered chamber profiles could have induced boundary conditions affecting the capacity. Figure 49 further shows that the drop in total capacity is smaller for mining prototype 2 than for mining prototype 1, which explains the larger 0-4 mm capacity for prototype 2 despite its smaller relative amount of 0-4 mm material. It would thus seem that the reference chamber is optimized towards throughput, whereas mining prototype 1 is optimized with respect to size reduction as the aspect of throughput was omitted in the performed optimizations.

Finally, the larger difference in capacity between the prototypes (i.e. different inlet, but the same outlet) than between the reference and mining prototype 2 (i.e. the same inlet, but different outlet) indicates that the inlet affects the capacity of the crusher.

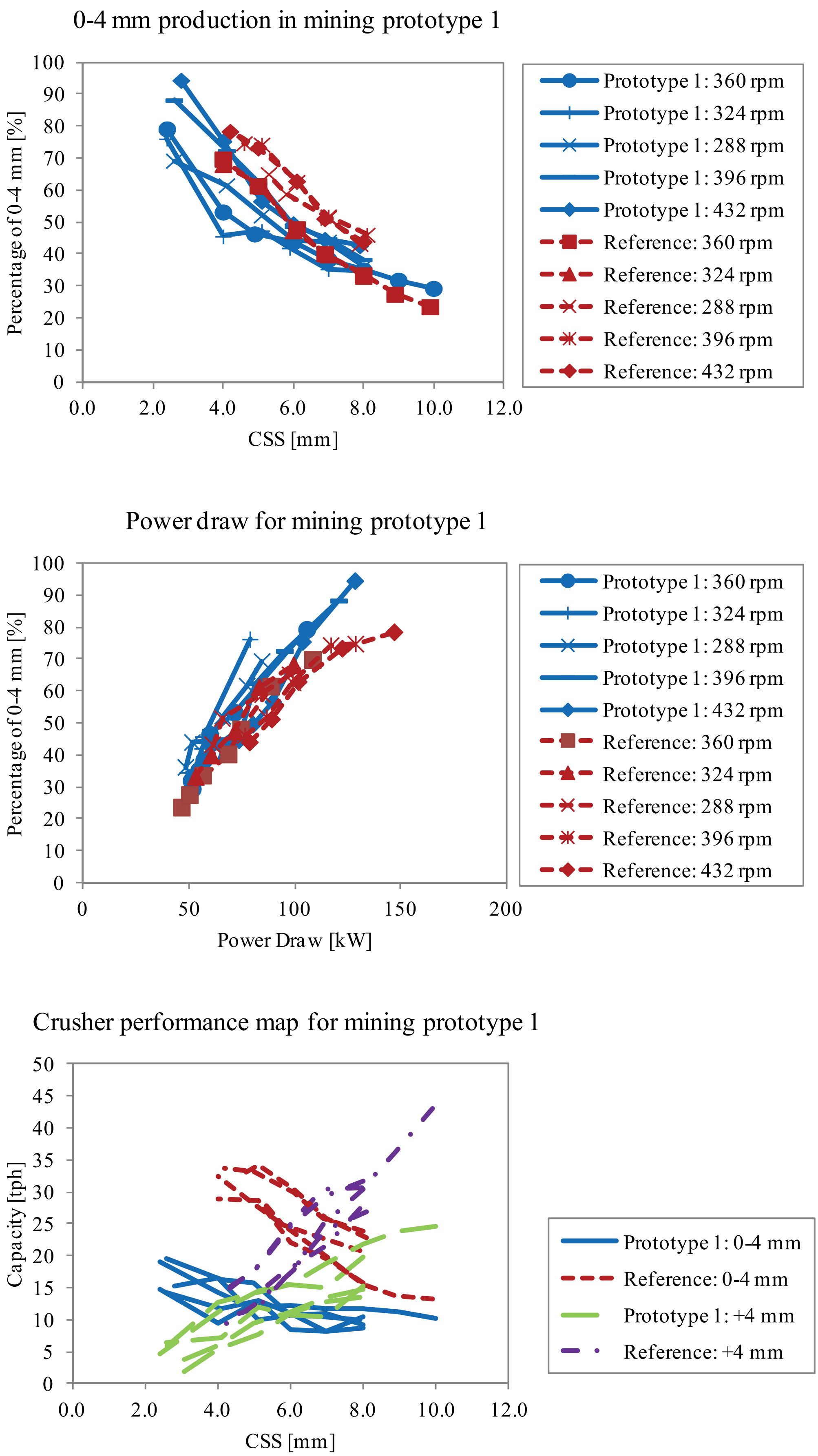

Figure 47. Comparisons between the mining reference chamber and mining prototype 1 in terms of the production of 0-4 mm material, power draw, and crusher performance.

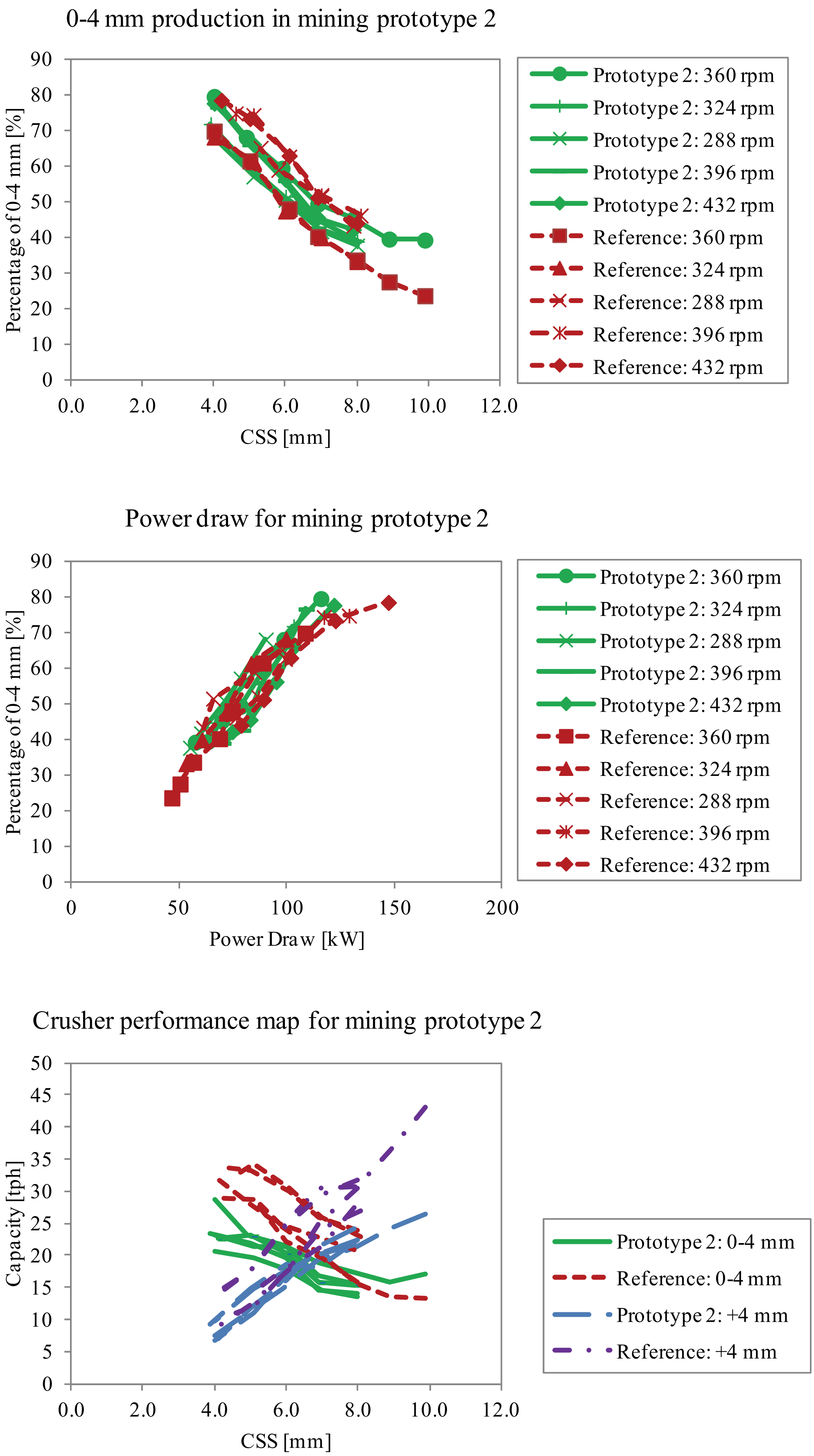

Figure 48. Comparisons between the mining reference chamber and mining prototype 2 in terms of the production of 0-4 mm material, power draw, and crusher performance.

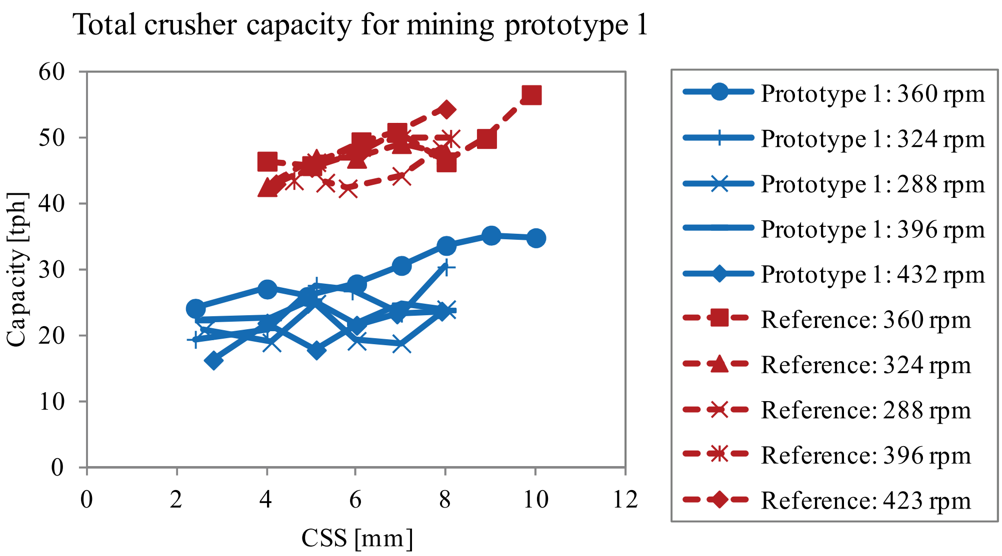

(a)

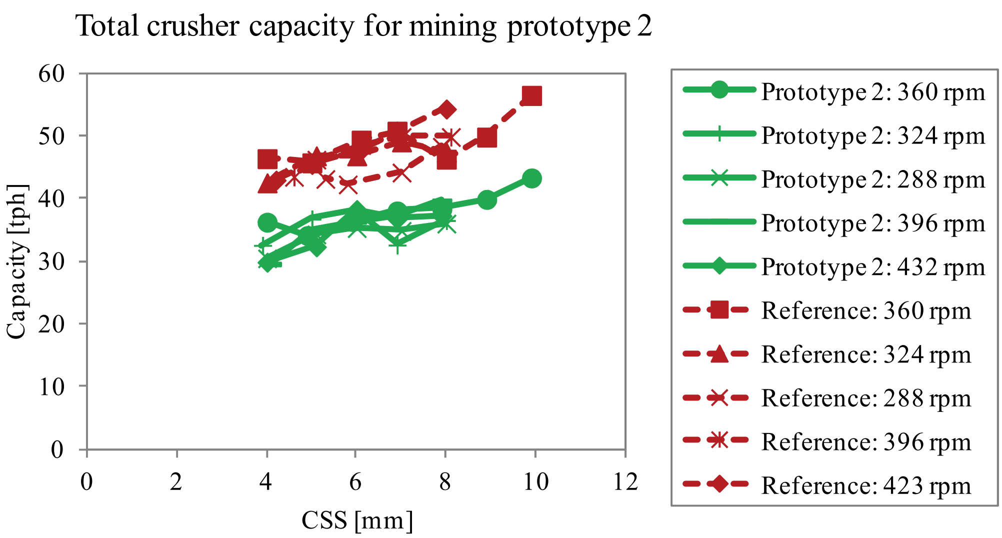

(b)

Figure 49. Comparisons between the mining reference chamber and mining prototype 1 (a), and the mining reference chamber and mining prototype 2 (b) in terms of the total crusher capacity.

10 DISCUSSION

The aim of this chapter is to:

- *Summarize and discuss the results from previous chapters*
- *Discuss, in more general terms, how the knowledge gained in this research project may affect the design and operation of compression crushers*

In this thesis, the complex compressive breakage behaviors of different rock materials were modeled using population balance models and simplifying assumptions regarding influencing parameters. Considering the level of complexity of these assumptions, the applied models have been shown to work well in predicting the output from one compression, as well as series of consecutive compressions (Chapter 5 & 7).

To experimentally study the compressive breakage behavior of different rock materials, form conditioned piston and die tests were conducted (Chapter 5). As suggested by the results, and in contrast to single particle breakage, a minimum compression ratio must be applied in order for interparticle breakage to occur. This threshold in compression ratio is believed to be caused by the optimal bulk volume and packing not being attained in laboratory particle beds. This would mean that the applied strokes in crushing tests are not only used for crushing, but also to push out surpluses of air and to rearrange particles in particle beds. The hypothesis is supported by the work of Mütze and Husemann [64], who described friction losses caused by the rearrangement of particles during the first stage of bed compression. Put into a context such as optimal fragmentation, this implies that small interparticle compressions with low size reduction efficiencies should be avoided. It also means that small compressions with low energy efficiencies should be minimized. These implications can be compared with the fact that if the objective is to lower fines generation, large compressions should be avoided.

In order to further understand how different rock materials should be crushed compressively, an optimization routine based on a genetic algorithm was developed (Chapter 6). Interparticle optimization results for product yield were then successfully validated by the correlation between experimentally measured outputs and corresponding model predictions (Chapter 7). To summarize, obtained optimization results indicated that optimal compressive crushing differs depending on the application and optimization objective (Chapters 7-9). In other words, different types of crushing applications, such aggregate and mining, should not be operated in the same way. Similarly, crushing applications with different optimization objectives, e.g. the same type of application but different production situations, should not be run identically. This concludes that every application has its own optimal output, and that the performance of the application depends on how well the applied crushing matches the corresponding optimal crushing process.

Comparisons between measured outputs from real applications and corresponding optimization results showed that existing cone crushers and crushing applications are not operating optimally. In fact, with the defined theoretical performance efficiencies of 30-40 %, great improvement potential was indicated for the studied aggregate applications in spite of possible mechanical and practical restraints (Chapter 7). The results particularly suggested that rock materials are currently being over-crushed, and that the size reduction process should be separated from the process of particle shaping in aggregate applications (Chapters 7&9). The latter statement was based on results indicating that interparticle crushing should be kept to a minimum in typical aggregate applications, despite its ability to generate better shaped particles than single particle crushing [63]. Thus, to maintain a certain level of product quality (often measured in particle shape in the aggregate industry [7]), additional particle shaping might be necessary if the obtained optimization results were to be implemented.

In terms of mining applications, optimizations results indicated that a larger amount of size reduction should be performed by single particle crushing, if the overall size reduction of the process is to be maximized and the energy consumption is to be kept to a minimum (Chapter 9). This was implemented by designing a larger chamber inlet and a smaller chamber outlet. In comparison, the implementation of optimization results for the previously mentioned aggregate application was achieved by moving the choke level upwards and increasing the designed outlet of the crushing chamber. The results of the subsequent full scale tests showed that the balanced yield of the aggregate application could be improved by at least 5 % while maintaining the throughput. This can be compared to the mining application for which a possible 20 % increase of the relative production of 0-4 mm material was shown. However, due to a decreased total capacity, a larger 0-4 mm capacity was measured for the reference. Further analyses showed that the crusher capacity is affected by the inlet.

Theoretical optimizations of different crushing concepts showed that different crushing approaches can achieve the same results (Chapter 8). However, the implementation of these crushing concepts can be more or less difficult depending on the type of crusher. For instance, crushing concepts with a constant system stroke and a decreasing bed height are more easily implemented in crushers without suspended top bearing, whereas crushing concepts with a constant bed height and an increasing system stroke can be implemented in Hydrocone-type crushers if the correct design adjustments are made. Thus, current crusher designs already have features, resulting from over 100 years of development, which are similar to parts of these optimal crushing concepts. This is very positive as it facilitates the implementation of optimization results, thereby enhancing the improvement potential of existing cone crushers.

The performance of existing crushing applications can also be improved by adjusting operational parameters [18]. This was indicated in the full scale experiments described in Chapter 7, where it was suggested that an optimum of product yield existed at different eccentric speeds depending on the CSS. The shifting optimum can be explained by the correlation of eccentric speed and number of crushing zones in a cone crusher. As the number of crushing zones increases with the eccentric speed [4], the amount of size reduction also increases. Therefore, in order to maintain a balance of size reduction, a larger CSS might have to be applied. However, since the proportion of breakage modes as well as the applied compression ratios change with an altered eccentric speed [4], it is not always evident which combination of eccentric speed and CSS would be optimal. The right choice of operational settings is further complicated by the parameter stroke. As suggested by the presented results, crusher dynamics might be affected by the applied stroke, which would make the effects of an altered stroke more difficult to predict. This is believed to be the explanation as to why, contrary to intuitive knowledge, the increased stroke in the tests did not result in an increased size reduction. Considering the variability of the feed material, both in size distribution and properties, it is believed that a truly optimal performance of a crushing application must be based on an optimized crusher design as well as a continuously optimized crusher operation.

11 CONCLUSIONS

The aim of this chapter is to:

- *Present the most important conclusions drawn in this thesis.*
- *Answer the research questions stated in Chapter 2.*
- *Discuss what has been found important for future work.*

The main hypothesis of this research was that better crushing machines can be achieved by first optimizing a given crushing process theoretically, and then designing the actual crusher. The conducted research can therefore be divided into five main stages, namely rock material characterization, modeling, optimization, evaluation, and implementation. Each of these stages has been covered in this thesis leading to this final chapter, which is intended to bring together the conclusions of the work performed, the objective of this research, and recommendations for future work.

11.1 GENERAL

The crushing process in a compression crusher has been modeled and theoretically optimized in this thesis. More specifically, simulations and theoretical optimizations using different optimization objectives have been performed to study the compressive crushing of different rock materials. The subsequent comparison of optimization results and measured data from existing crushers has in turn made it possible to evaluate the performances of existing crushing applications. These analyses show that existing cone crushers are not optimal in terms of the studied aspects. In fact, the defined performance efficiencies indicate great improvement potential for the examined crushing applications. This is believed to be due to a crusher design, which has remained much the same since the introduction of cone crushers in the early 1900s.

Moreover, the results from the performed parameter study suggest that there is an optimum product yield at different eccentric speeds depending on the CSS. This indicates that the performance of an existing crushing application can be improved by adjusting operational parameters [18].

11.2 ANSWERS TO RESEARCH QUESTIONS

The research questions posed in Chapter 2 are presented below along with their respective answers, which have become evident during the course of this research project.

RQ1: How can the compressive breakage behavior of a given rock material be modeled?

Due to the inherent heterogeneous qualities of rock materials as naturally occurring solid aggregates of minerals, modeling the compressive breakage behavior of a rock material is difficult. However, previous research has shown that the breakage characteristics of rock materials can be modeled by a breakage function and a selection function [4],[30],[31], which use statistics as well as assumptions of homogeneity among the particles.

As the objective is to develop the existing knowledge and approaches to compressive crushing of rock materials, the compressive breakage behavior of a given rock material should be modeled with respect to general and non-machine specific parameters. The objective to give advice for crusher design further argues that parameters such as the number of compressions and the applied compression ratio should be used rather than the variable of applied energy. This is because of the current focus on compression crushers in which size reduction is form conditioned, i.e. energy is considered as a secondary effect and not as an input variable.

To conclude, the compressive breakage behaviors of different rock materials have been modeled by using a breakage function (describing the resulting particle size distribution) and a selection function (describing the breakage probability). These population balance models, which differ depending on the breakage mode (i.e. interparticle or single particle breakage, see Figure 50), are assumed to be only dependent on the applied compression ratio and the initial particle size/feed size distribution.

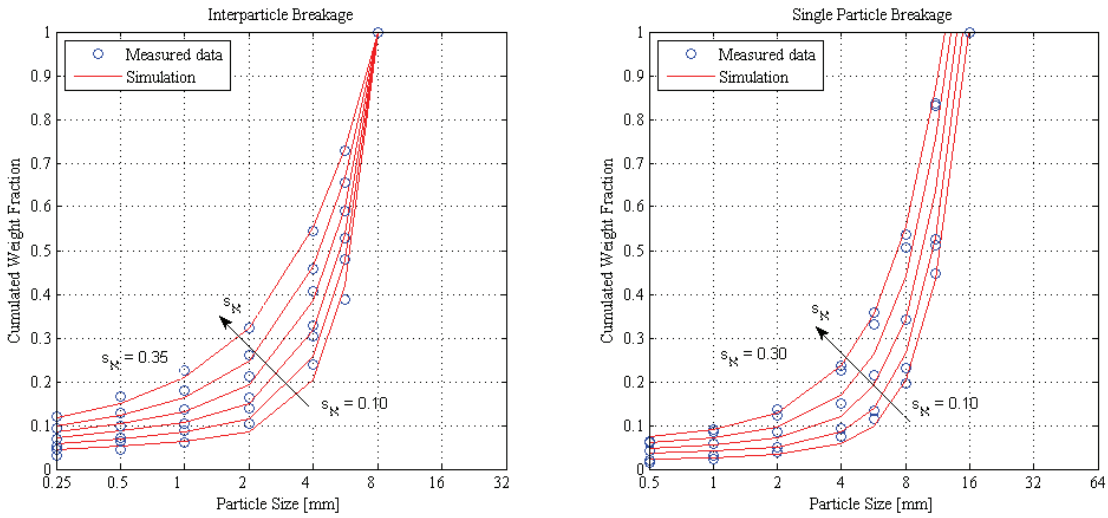

Figure 50. Normalized breakage behavior of the examined gneiss for interparticle breakage (left) and single particle breakage (right).

RQ2: How can the compressive crushing of a given rock material be optimized?

In this project, the compressive crushing of rock materials has been modeled as series of discrete consecutive compressions using discrete complex non-linear compressive breakage models. This means that the optimization of compressive crushing can only be carried out using discrete optimization methods [17]. Genetic algorithms (GA), which is one method among several discrete optimization methods, were therefore chosen for the task. The advantages of GAs are that they do not require the function being optimized to be differentiable or continuous [51], they often find solutions close to the global optimum thanks to their random initiation, and they are robust in terms of their performances [50]. The robustness of the obtained optimization results was also satisfactorily tested by slightly altering optimization conditions and examining the ensuing effects.

RQ3: How should the outcome from optimizations of compressive crushing be evaluated?

Evaluation of results can be performed in a variety of different ways. Visual evaluation, analytical evaluation, and evaluation based on previous practical knowledge are just a few examples of different approaches. What is in common for these approaches is a defined basis or notion for what is good/better and what is bad/worse. However, in spite of this basis for determination, results from optimizations as well as simulations can sometimes be difficult to evaluate. For instance, visual evaluation can be tedious in situations, where only small visible differences are present. The obvious question, which then arises, is how to conduct an objective evaluation, which is also repeatable irrespective of the person or device performing it. This is a concern, which is also present in evaluations based on previous practical knowledge. Therefore, in order to ensure some kind of consistency and objectivity, the basis for evaluation must be analytically defined. One way to go about this is to define a mathematical function, which impartially ranks different solutions according to the optimization objective. This user-defined function is called the *fitness function*.

The formulation of the fitness function is of crucial importance. By formulating the fitness function in one way or another, the optimization can be steered in one direction or another. In other words, the fitness function more or less dictates what the optimization is going to optimize (see Table 15). This means that the obtained optimal solutions can never be better than what is specified in the fitness function, nor are they truly optimal in any other circumstances. An optimal solution is therefore only true for the fitness function, which has been applied during optimization.

Table 15. Examples of fitness functions in the aggregate and mining industries.

Optimization objective	Fitness function	Comment
Maximize *product yield*	$\varphi_{\text{Yield}} = \frac{\sum_{i=1}^{m-1} p_i \cdot \sum_{i=2}^{m-1} p_i}{p_1} = \frac{[\text{Capacity}]\times[\text{Product}]}{[\text{By-product}]}$	Typical *aggregate application*; to maximize the production of a certain product as well as the throughput, while minimizing the by-product.
Maximize *balanced product yield*	$\varphi_{\text{Balanced yield}} = \frac{\sum_{i=1}^{m-1} p_i \cdot \sum_{i=2}^{m-1} \frac{v_i}{v_1} \cdot p_i}{p_1} = \frac{[\text{Capacity}]\times[\text{Relative values } \times \text{ desired products}]}{[\text{By-product}]}$	Similar to the example above (i.e. a typical *aggregate application*), but now with several products of different economical values v_i to maximize.
Minimize *energy consumption*	$\varphi_{\text{Energy}} = \frac{\sum_{i=1}^{m-1} p_i \cdot \sum_{i=2}^{m-1} p_i}{\sum_{j=1}^{M} W_j} = \frac{[\text{Capacity}]\times[\text{Product}]}{[\text{Energy}]}$ $\varphi_{\text{Energy\_mining}} = \frac{\left(\sum_{i=1}^{m-1} p_i\right)^2}{\sum_{j=1}^{M} W_j} = \frac{[\text{Capacity}]\times[\text{Product}]}{[\text{Energy}]}$	The objective here is to attain as much production and process capacity as possible, while minimizing the energy consumption. Please note that the expression for *mining applications* (in which the fine material is the product) can be considered as a special case of the expression for *aggregate applications.*
Maximize *product*	$\varphi_{\text{Product}} = \sum_{i=1}^{m-1} p_i = [\text{Product}]$	Typical *mining application* in which only one product exists to be maximized.

RQ4: How should a given rock material be crushed by means of compressive crushing if e.g. product yield or energy consumption is to be theoretically optimized?

The results have shown that in terms of the defined product yield or balanced product (like in aggregate production), interparticle crushing should be kept to a minimum in the studied applications. This implies that the main part of size reduction should be accomplished by single particle crushing, which is considered to generate worse shaped particles than interparticle crushing. It should, however, be noted that the aspect of particle shape was not included in the scope of this research, which explains these results. Nevertheless, according to optimization results, the single particle compressions should, from a system perspective, generally increase along crushing sequence from ~0.33-0.76 in effective system compression ratio. This can be achieved by increasing the applied stroke, decreasing the applied bed height, or altering both parameters. The same results can thus be accomplished through different approaches.

In terms of the studied energy consumption, it has been indicated that interparticle crushing should be carried out with small initial constant compression ratios at 0.10 before a slightly larger compression (0.11-0.12 in size) prior to the transition to single particle crushing. The subsequent single particle compressions should then be conducted with a generally increasing effective system compression ratio at ~0.44-0.78 depending on the rock material. Despite the larger system compression ratio, the applied single particle crushing is actually similar to that of the crushing sequences from corresponding product yield optimizations. Comparable results are therefore achieved by the different optimal crushing sequences.

RQ5: What are the main differences between current cone crushers and comparable theoretically optimal crushing units?

For aggregate applications, the results have shown that rock materials are currently being over-crushed and that interparticle crushing should be kept to a minimum if product yield is to be optimized. This indicates that a smaller size reduction should be applied and that the process of size reduction should be separated from the process of particle shaping. In practice, the smaller size reduction can be achieved by designing a larger crushing chamber outlet, whereas the decrease of interparticle crushing can be achieved by an upward movement of the choke level.

Regarding mining applications, the analyses have shown that more size reduction should be applied in the single particle crushing zone, if the overall size reduction of the process is to be maximized and the energy consumption is to be kept to a minimum. This can be achieved by designing a smaller crushing chamber outlet.

RQ6: How much can the performance of today's cone crushers be improved by practically implementing research results from this project?

By implementing a reduced proportion of interparticle crushing (in favor of a larger proportion of single particle crushing) and a reduced fines generation of the single particle crushing, the performance of an aggregate prototype crushing chamber has been shown to be superior to that of its corresponding reference crushing chamber. More specifically, analysis of the results from the full scale experiments indicates that the balanced product of the reference chamber can be improved by at least 5 %, while maintaining the throughput capacity.

In comparison, it has been demonstrated that the relative production of 0-4 mm material in the existing mining reference can be improved by 20 %, which affirms the optimization results. However, due to drops in the total capacities of the mining prototypes, the reference crushing chamber actually has a larger 0-4 mm capacity than the prototypes. These decreases of total capacity can, nevertheless, be partly explained by the smaller cross sectional areas of the prototypes and can therefore be compensated.

11.3 FUTURE WORK

As suggested by optimization results, interparticle crushing should be minimized if the defined product yield is to be optimized (like for example in aggregate production). This implies that the process of size reduction should be separated from the process of particle shaping, since interparticle crushing is considered to generate better shaped particles than single particle crushing [63]. However, this may be a consequence of excluding the aspect of particle shape from the scope of this research project. Studies of how such a separation would affect product quality (i.e. particle shape), and how the process should be adjusted to allow for particle shaping are thus highly relevant. It is also recommended that the aspect of particle shape should be included in future optimization studies.

The indicated possible increase of size reduction in mining applications suggests that the work efficiency in the downstream ball mills can be increased. Similarly, a reduced top size of the material from cone crushers can also improve the performance of subsequent HPGRs in mineral processing. It would be interesting to further investigate the impact of such an improved cone crusher on a comminution process as a whole. Another interesting topic would also be to study the optimal setup of cone crushers and HPGRs in terms of particle size distributions generated in cone crushers and subsequently fed to HPGRs.

Furthermore, the results of the conducted parameter study indicate that crusher dynamics are affected by changes of the stroke. In order to understand how an altered stroke affects the crushing process in a cone crusher, dynamic simulations should be made. One way of going about this is to use Discrete Element Method (DEM) simulations, which has been gaining ground in comminution research in the last decades [65],[66],[67]. In DEM, each simulated particle corresponds to a studied entity as opposed to the continuum perspective in Computational Fluid Dynamics (CFD) or Finite Element Method (FEM). This means that particle motion as well as particle interaction (e.g. particle-particle or particle-boundary) can be tracked [66],[68]. By doing so, the dynamic effects of crusher parameters and chamber design can be examined [69].

REFERENCES

[1]. *Berg för byggande - Om bergmaterialindustrin* 2007, Stockholm, Sweden: Sveriges Bergmaterialindustri.

[2]. Marshak, S., *Earth - Portrait of a planet*. 2nd ed, 2005, New York, USA: W.W. Norton & Company, Inc.

[3]. Tarbuck, E. and Lutgens, F.K., *The Earth - An Introduction to Physical Geology*, 1993, New York, USA: Macmillian Publishing Company.

[4]. Evertsson, C.M., *Cone Crusher Performance*. Dept. of Machine and Vehicle Design. PhD Thesis, 2000, Göteborg: Chalmers University of Technology.

[5]. Wills, B.A. and Napier-Munn, T., *Comminution*, in *Wills' Mineral Processing Technology (Seventh Edition)*, 2005, Butterworth-Heinemann: Oxford. p. 108-117.

[6]. King, R.P., *Modelling & simulation of mineral processing stsems*, 2001, Oxford, Great Britain: Butterworth-Heinemann.

[7]. Bengtsson, M., *Quality-Driven Production of Aggregates in Crushing Plants*. Dept. of Product and production Development. PhD Thesis, 2009, Gothenburg, Sweden: Chalmers University of Technology.

[8]. Wills, B.A. and Napier-Munn, T., *Crushers*, in *Wills' Mineral Processing Technology (Seventh Edition)*, 2005, Butterworth-Heinemann: Oxford. p. 118-145.

[9]. Donovan, J.G., *Fracture Toughness Based Modelc for the Prediction of Power Consumption, Product Size, and Capacity of Jaw Crushers*. PhD Thesis, 2003, Blacksburg, Virginia, USA: Virginia Polytechnic Institute and State University.

[10]. Daniel, M.J., *HPGR model verification and scale-up*. Julius Kruttschnitt Mineral Research Centre. Msc Thesis, 2002, Indooroopilly, Australia: University of Queensland.

[11]. *Grus, sand och krossberg, Produktion och tillgångar 2009 (Aggregates, Production and resources 2010)*, 2010: Sveriges geologiska undersökning (SGU).

[12]. *Annual Review 2010-2011*, 2011, Brussels, Belgium: European Aggregate Association (UEPG).

[13]. *Bergverksstatistik 2010 (Statistics of the Swedish Mining Industry 2010)*, 2011: Sveriges geologiska undersökning (SGU).

[14]. Lindstedt, P. and Burenius, J., *The Value Model: How to Master Product Development and Create Unrivalled Customer Value*, 2006: Nimba AB.

[15]. Soldinger Stafhammar, M., *Screening of Crushed Rock Material*. Dept. of Machine and Vehicle Systems. PhD Thesis, 2002, Göteborg, Sweden: Chalmers University of Technology.

[16]. Lindqvist, M., *Wear in cone crusher chambers*. Dept. of Applied Mechanics. PhD thesis, 2006, Göteborg: Chalmers University of Technology. 170.

[17]. Svedensten, P., *Crushing Plant Performance*. Dept. of Applied Mechanics. PhD Thesis, 2007, Göteborg, Sweden: Chalmers University of Technology.

[18]. Hulthén, E., *Real-Time Optimization of Cone Crushers*. Dep. of Product and Production Development. PhD Thesis, 2010, Göteborg: Chalmers University of Technology.

[19]. Allwood, C.M., et al., *Vetenskapsteori för psykologi och andra samhällsvetenskaper*, 1999, Lund, Sweden: Studentlitteratur.

[20]. *Plato*. Wikipedia [Internet] 2012-02-23 [cited 2012 03-06]; Available from: http://en.wikipedia.org/wiki/Plato.

[21]. Åsberg, R., *Det finns inga kvalitativa metoder - och inga kvantitativa metoder heller för den delen*. Pedagogisk Forskning i Sverige 2001. 4. 2001.

[22]. Svensson, L., et al., *Interaktiv forskning - för utveckling av teori och praktik*, 2002, Stockholm, Sweden: Arbetslivsinstitutet.

[23]. Jacob, M., Lundqvist, M., and Hellsmark, H., *Entrepreneurial transformations in the Swedish University system: the case of Chalmers University of Technology*. 32. 2003, Göteborg, Sweden.

[24]. Almefelt, L., *Requirements-Driven Product Innovation. Methods and Tools Reflecting Industrial Needs*. Dept. of Product and Production Development. PhD Thesis, 2005, Göteborg, Sweden: Chalmers University of Technology.

[25]. Mägi, M. and Melkersson, K., *Lärobok i Maskinelement*, 2007, Göteborg, Sweden: EcoDev International AB.

[26]. Lynch, A.J., *Mineral Crushing and Grinding Circuits: Their Simulation, Optimisation, Design and Control*, 1977, Amsterdam, The Netherlands: Elsevier Scientific Publishing Company.

[27]. Evertsson, C.M. *Prediction of Size Distributions from Compressing Crusher Machines*. in *EXPLO conference*. 1995. Brisbane, Australia.

[28]. Morrell, S., *An alternative energy–size relationship to that proposed by Bond for the design and optimisation of grinding circuits.* International Journal of Mineral Processing, 2004. 74(1–4): p. 133-141.

[29]. Lindqvist, M., *Energy considerations in compressive and impact crushing of rock.* Minerals Engineering, 2008. 21: p. 631-641.

[30]. Schönert, K. and Müller, F., *Representation of Breakage Fraction and Breakage Function of Inter-Particle Stressing.* Aufbereitungs-technik, 1990. 31(5): p. 248-256.

[31]. Liu, J. and Schönert, K., *Modelling of interparticle breakage.* International Journal of Mineral Processing, 1996. 44–45(0): p. 101-115.

[32]. Schönert, K., Vogel, L., and Peukert, W., *Separation of the Influences of Material and Machine in Impact Comminution - Modelling with Population Balances.* Aufbereitungs Technik, 2002. 43(8): p. 19-30.

[33]. Vogel, L. and Peukert, W., *Breakage behaviour of different materials—construction of a mastercurve for the breakage probability.* Powder Technology, 2003. 129(1–3): p. 101-110.

[34]. Vogel, L. and Peukert, W., *Determination of material properties relevant to grinding by practicable labscale milling tests.* International Journal of Mineral Processing, 2004. 74: p. 329-338.

[35]. Liu, H., et al., *Microscope Rock Texture Characterization and Simulation of Rock Aggregate Properties*, Sweden, G.S.o., Editor 2005.

[36]. Bearman, R.A., Briggs, C.A., and Kojovic, T., *The applications of rock mechanics parameters to the prediction of comminution behaviour.* Minerals Engineering, 1997. 10(3): p. 255-264.

[37]. Shi, F., et al., *Development of a rapid particle breakage characterisation device – The JKRBT.* Minerals Engineering, 2009. 22(7–8): p. 602-612.

[38]. Napier-Munn, T.J., et al., *Mineral Comminution Circuits: Their Operation and Optimisation*, 1996, Indooroopilly, Australia: Julius Kruttschnitt Mineral Research Centre.

[39]. Jørck, M., Sym, R., and Powell, W.R., *A Study of Mechanical Tests of Aggregates*1994.

[40]. Bengtsson, M., Svedensten, P., and Evertsson, C.M. *Characterization of Compressive Breakage Behaviour*. in *XXIII International Mineral Processing Congress*. 2006. Istanbul, Turkey: Promed Advertising Agency.

[41]. Schönert, K., *The influence of particle bed configurations and confinements on particle breakage.* International Journal of Mineral Processing, 1996. 44–45(0): p. 1-16.

[42]. Aziz, J.-K. and Schönert, K., *Einzelkornzerkleinerung und Gutbettbeanspruchung von Zementklinker-Fraktionen.* Zement Kalk Gips, 1980(5): p. 213-218.

[43]. Fuerstenau, D.W., Gutsche, O., and Kapur, P.C., *Confined particle bed comminution under compressive loads.* International Journal of Mineral Processing, 1996. 44–45(0): p. 521-537.

[44]. Gutsche, O. and Fuerstenau, D.W., *Fracture kinetics of particle bed comminution — ramifications for fines production and mill optimization.* Powder Technology, 1999. 105(1–3): p. 113-118.

[45]. Benzer, H., Aydogan, N.A., and Dündar, H., *Investigation of the breakage of hard and soft components under high compression: HPGR application.* Minerals Engineering, 2011. 24(3–4): p. 303-307.

[46]. Unland, G. and Szczelina, P., *Coarse crushing of brittle rocks by compression.* International Journal of Mineral Processing, 2004. 74(0): p. S209-S217.

[47]. Tondo, L.A., *Phenomenological Modelling of Size Reduction Performed by High Pressure Roll Mill*. Julius Kruttschnitt Mineral Research Centre. MSc Thesis, 1997, Indooroopilly, Australia: University of Queensland.

[48]. Andréasson, N., Evgrafov, A., and Patriksson, M., *An Introduction to Continuous Optimization*, 2005, Lund: Studentlitteratur.

[49]. Lundgren, J., Rönnqvist, M., and Värbrand, P., *Optimization*, 2010, Malmö, Sweden: Studentlitteratur

[50]. Yagiura, M. and Ibaraki, T., *On Metaheuristic Algorithms for Combinatorial Optimization Probelms.* Systems and Computers in Japan, 2001. 32(3): p. 33-55.

[51]. Wahde, M., *An Introduction of Adaptive Algoritms and Intelligent Machines*. 5th ed, 2006, Göteborg, Sweden: Chalmers University of Technology.

[52]. Hulthén, E., Svedensten, P., and Evertsson, C.M. *Theoretical optimal crushing*. in *XXIII International Minerals Processing Congress*. 2006. Istanbul, Turkey: Promed Advertising Agency.

[53]. While, L., et al., *A multi-objective evolutionary algorithm approach for crusher optimisation and flowsheet design.* Minerals Engineering, 2004. 17(11–12): p. 1063-1074.

[54]. Lööf, J., *Managing Geometrical Variation through Optimization and Visualization*. Dept. of Product and Production Development. PhD Thesis, 2010, Göteborg, Sweden: Chalmers University of Technology.

[55]. Magnusson, A., *Evolutionary Optimisation of Morphological Image Processor for Embedded Systems*. Dept. of Applied Mechanics. PhD Thesis, 2008, Göteborg, Sweden: Chalmers University of Technology.

[56]. Narayana Naik, G., Gopalakrishnan, S., and Ganguli, R., *Design optimization of composites using genetic algorithms and failure mechanism based failure criterion.* Composite Structures, 2008. 83(4): p. 354-367.

[57]. Gang, D., Xiumin, F., and Dongming, H., *Analysis and optimization of cone crusher performance.* Minerals Engineering, 2009. 22(12): p. 1091-1093.

[58]. Gang, D., Dongming, H., and Xiumin, F., *Cone crusher chamber optimization using multiple constraints.* International Journal of Mineral Processing, 2009. 93(2): p. 204-208.

[59]. Huang, D., et al., *Multi-objective planning of cone crusher chamber, output and size reduction.* Minerals Engineering, 2007. 20(2): p. 163-172.

[60]. Eloranta, J., *Influence of Crushing Process Variables on the Product Quality of Crushed Rock*. PhD Thesis, 1995, Tampere: Tampere University of Technology.

[61]. Srinivas, M. and Patnaik, L.M., *Adaptive Probabilities of Crossover and Mutation in Genetic Algorithms.* IEEE Transactions on Systems, Man and Cybernetics, 1994. 24(4): p. 656-667.

[62]. Onnela, T. and Eloranta, J. *Improved Aggregates Production by Crusher Cavity Simulation*. in *European Symposium of Comminution and Classisfication (ESCC)*. 2009. Espoo, Finland: ESCC.

[63]. Briggs, C. and Evertsson, C.M., *Shape Potential Of Rock.* Minerals Engineering, 1998. 11(2): p. 125-132.

[64]. Mütze, T. and Husemann, K., *Compressive stress: Effect of stress velocity on confined particle bed comminution.* Chemical Engineering Research and Design, 2008. 86(4): p. 379-383.

[65]. Powell, M.S. and Morrison, R.D., *The future of comminution modelling.* International Journal of Mineral Processing, 2007. 84: p. 228-239.

[66]. Herbst, J.A. and Potapov, A.V., *Making a Discrete Grain Breakage model practical for comminution equipment performance simulation.* Powder Technology, 2004. 143-144: p. 144-150.

[67]. Lichter, J., et al., *New developments in cone crusher performance optimization.* Minerals Engineering, 2009. 22(7-8): p. 613-617.

[68]. Khanal, M., Schubert, W., and Tomas, J., *Discrete element method simulation of bed comminution.* Minerals Engineering, 2007. 20(2): p. 179-187.

[69]. Quist, J. and Evertsson, C.M. *Simulating Capacity and Breakage in Cone Crushers using DEM*. in *Comminution '10*. 2010. Cape Town, South Africa.